ABSTRACT

BOYLE, MICHAEL CHRISTOPHER. Deletion of the Chromatin Remodeling Factor Brg1 Leads to Genomic Instability During Development, and Confers Sensitivity to Adult-onset Doxorubicin Cardiotoxicity in Mice. (Under the direction of Trevor K. Archer, Brian R. Berridge, J. Mac Law, and David E. Malarkey).

Cardiovascular disease is the number one killer of adults in the United States. Paradoxically, a certain subtype of the most prevalent morbidity and mortality factor (heart disease) is due to treatment for the second most prevalent morbidity and mortality factor (cancer): this is the case for doxorubicin cardiotoxicity. Doxorubicin continues to be an efficacious treatment for a variety of solid and hematopoietic liquid tumors, and as such receives continued clinical use. Cardiac toxicity is an under-recognized side effect of several biopharmaceutical and environmental chemical agents. The degree of toxicity may be mediated by epigenetic events, such as chromatin remodeling. It is known the chromatin remodeling factor Brg1, a catalytic subunit of the SWI/SNF ATPase chromatin remodeling complex, is required in cardiovascular development and pathologic cardiac hypertrophy. However, BRG1 necessity during development beyond certain embryonic stages has not been fully investigated, nor has its potential role in doxorubicin cardiotoxicity. Due to the known chromatin remodeling activities of BRG1, the requirement of Brg1 during early embryonic development and its role in the response to cardiotoxicity caused by doxorubicin was investigated. BRG1 ablation beginning at E6.5 results in arrested growth and embryonic death by E9.5 due to developmental defects. Microarray analysis revealed BRG1's role in maintaining genomic integrity, without which there is aberrant expression of cell cycle, proliferation, and apoptosis pathways leading to the observed pathologic phenotype. This demonstrates that BRG1's role in genomic surveillance is essential for survival after the pre-

implantation period for normal cellular proliferation and differentiation. Adult Brg1 WT and Brg1 KO mice were subjected to a doxorubicin regimen with repeated dosing over several weeks, analogous to repeat-dose paradigms used in the human clinical setting. Analyses of tissues including protein and RNA biochemistry, microarray analysis, serum biochemistry, and light and electronic microscopic analyses confirmed the presence of doxorubicin-associated lesions in treated mice; however, morphologically-similar lesions were also observed at a lesser incidence and severity in untreated Brg1 KO mice. Microarray analysis revealed significant differentially expressed genes with common clustering between both the treated groups and the Brg1 KO groups, suggesting both common and dissimilar molecular mechanisms between Brg1 KO-induced cardiomyocyte lesions and those induced by doxorubicin treatment. This analysis additionally identified differentially expressed genes previously unreported to be associated with doxorubicin cardiotoxicity. The work in this dissertation has revealed that not only is Brg1 required for the maintenance of normal cardiomyocyte homeostasis during development, but found that despite previous reports it is required in adulthood as well. Furthermore, its absence has common and dissimilar mechanisms to that suffered from treatment with doxorubicin, suggesting mechanisms unique to Brg1 knockout irrespective of treatment may reveal new pathways for therapeutic targeting in patients at risk for doxorubicin cardiotoxicity.

Deletion of the Chromatin Remodeling Factor Brg1 Leads to Genomic Instability During Development, and Confers Sensitivity to Adult-onset Doxorubicin Cardiotoxicity in Mice

by
Michael Christopher Boyle

A dissertation or thesis submitted to the Graduate Faculty of
North Carolina State University
in partial fulfillment of the
requirements for the degree of
Doctor of Philosophy

Comparative Biomedical Sciences

Raleigh, North Carolina

2014

APPROVED BY:

_____	_____
Dr. J. Mac Law Committee Chair	Dr. Trevor K. Archer
_____	_____
Dr. Brian R. Berridge	Dr. David E. Malarkey

DEDICATION

To my wife, Molly Hope Boyle, without whom none of this would have been possible, to my children, who provide my True North, and to my father, Stephen Robert Boyle, who would be even more proud of this work than I.

BIOGRAPHY

Michael C. Boyle is a veterinary anatomic pathologist with research interests in cardiovascular diseases and cardiac toxicity caused by biopharmaceuticals. His interest in cardiology began in veterinary school at the College of Veterinary Medicine, Michigan State University, under the tutelage of renowned veterinary cardiologists Drs. Bari Olivier and George Eyster. His first research project was in the lab of Dr. Ron Erskine, studying mastitis in dairy herds. His exposure to the safety evaluation of medicines came during an Anatomic and Toxicologic Veterinary Pathology Residency program partnership between Michigan State University and MPI Research, Inc. under the tutelage of Drs. Daniel Patrick and Marlon Rebellato. He was a National Toxicology Program Postdoctoral Fellow, where he assisted in the NTP pathology peer-review program, in addition to serving as a Comparative Anatomic Pathologist for the researchers in the Division of Intramural Research at the National Institute of Environmental Health Sciences. He is currently a Principal Pathologist at Amgen, Inc.

ACKNOWLEDGMENTS

I would like to express my warm appreciation to the following:

The members of my thesis committee: Drs. Trevor Archer, Brian Berridge, Mac Law, and David Malarkey. These individuals challenged and inspired me, while allowing me to blaze my own trail.

The National Toxicology Program, for supporting my training in toxicologic pathology and my independent research leading to the construction of this thesis.

The National Institute of Environmental Health Sciences, for providing a wonderful training ground and family of individuals who have been a joy to work with and learn from. In particular, I would like to acknowledge Jackson Hoffman, Ajeet Singh, Beth Mahler, Eli Ney, Julie Foley, and Natasha Clayton.

My mentors through veterinary school and beyond: The MSU CVM group (Drs. Ron Erskine, Bari Olivier), the DCPAH group (Drs. Scott Fitzgerald, Kurt Williams, Jon Patterson, Thomas Mullaney, Dalen Agnew, and Barbara Steficek), the MPI Research group (Drs. Dan Patrick, Marlon Rebellato, Keith Nelson, Kapil Vashisht) and from my new home at NTP, Dr. Abraham Nyska.

TABLE OF CONTENTS

LIST OF TABLES

LIST OF FIGURES

(B, C) and E9.5 (D). ROSA-cre/ERT2 ROSA-stop stain strongly positive (indigo staining, A-D); ROSA-stop embryos lack staining (44). ROSA-cre/ERT2 ROSA-stop embryos from E7.5 (A), E8.5 (B) and E9.5 shows Cre-ER expression in almost all tissues including extraembryonic ectoderm, epiblast, allantois, and yolk sac.

Figure 2.3: Deletion of BRG1 in BRG1$^{d/d}$ embryos. (A) Genomic PCR of floxed BRG1 (387bp), floxed-out BRG1 (313bp) and Cre (100bp). (B) qPCR of significant downregulation of BRG1 mRNA BRG1$^{d/d}$ versus BRG1 fl/fl embryos. (C to D) BRG1 fl/fl embryo demonstrates strong immunostaining for BRG1 (C) while BRG1$^{d/d}$ demonstrates markedly reduced immunostaining (D). DAB counterstain.

Figure 2.4: BRG1 mutant embryos reveal growth retardation. Substantial growth retardation of BRG1$^{d/d}$ embryos compared to Cre-BRG1 fl/fl embryos from the same litter at E8.5 (A through C). Anatomic structures (EpC, ectoplacental cone; Reichert's membrane, head, heart, allantois) are present in all embryos. E9.5 embryos demonstrate further retardation (D through G).

Figure 2.5: Histologic analysis of Cre-BRG1 fl/fl and BRG1$^{d/d}$ embryos at E9.5. Frontal section of Cre-BRG1 fl/fl (A) shows normal embryo morphology, including neural fold (NF) and developing heart (H). Frontal section of BRG1$^{d/d}$ embryo (B) shows abnormal histomorphology, neural fold deformity (NF), and lack of normal cardiac structures. Higher magnification of Cre-BRG1 fl/fl in (A) reveals normal cardiac structures (C) and normal

neural fold formation (E). Higher magnification of BRG1$^{d/d}$ in (I) reveals necrotic cardiac (D) and neural fold (F) histomorphology.

Figure 2.6: Cell death marker immunohistochemistry of Cre-BRG1 fl/fl and BRG1$^{d/d}$ embryos at E9.5. TUNEL immunolabeling is infrequent in Cre-BRG1 fl/fl embryos (A, higher magnification in C). TUNEL immunolabeling widespread in BRG1$^{d/d}$ embryo (B); higher magnification demonstrates strong nuclear and necrotic cell staining (D). Cleaved caspase-3 (CC3) immunostaining present in both Cre-BRG1 fl/fl (E) and BRG1$^{d/d}$ (F) embryos; however higher magnification of (E) and (F) reveals stronger and more widespread immunopositivity of CC3 in BRG1$^{d/d}$ (H) than Cre-BRG1 fl/fl (G) embryos.

Figure 2.7: Proliferation marker immunohistochemistry of Cre-BRG1 fl/fl and BRG1$^{d/d}$ embryos at E9.5. Cyclin D1 (CCND1) immunolabeling is frequent in Cre-BRG1 fl/fl embryos (A, higher magnification in C). CCND1 immunolabeling less widespread and weaker in BRG1$^{d/d}$ embryo (B); higher magnification demonstrates substantially less immunolabeling (D). Ki67 immunostaining present in both Cre-BRG1 fl/fl (E) and BRG1$^{d/d}$ (F) embryos; however higher magnification of (E) and (F) reveal stronger and more widespread immunopositivity of Ki67 in Cre-BRG1 fl/fl (G) than BRG1$^{d/d}$ (H) embryos.

Figure 2.8: Vascular endothelial immunohistochemistry of Cre-BRG1 fl/fl and BRG1$^{d/d}$ embryos at E9.5. Platelet-endothelial cell adhesion marker (PECAM, CD31)

Figure 3.2: X-gal staining of induced embryos and adults. Lack of staining is present in control embryonic day 9.5 (E9.5) whole embryos (A), E15.5 heart (C) whole mounts, and 9 week-old mouse heart frozen sections (E). Positive indigo staining is present in Cre-ROSA E9.5 whole embryo (B), E15.5 heart (D) whole mounts, and 9 week-old mouse heart frozen sections (F). X-gal stained section without nuclear fast counterstain (G). Nuclear fast red counterstain (E, F). A-D, original dissecting microscope magnification objective 5x. E-G, original brightfield microscope magnification objective 20x.

Figure 3.3: Brg1 knockout evaluation. Genomic PCR revealed a >60% recombination efficiency (A). rt-PCR of Brg1 mRNA revealed a significant decrease in Brg1 mRNA expression in Brg1 KO mice with or without doxorubicin treatment (B). Western blotting for Brg1 protein revealed a decreased protein expression in Brg1 KO mice with or without doxorubicin treatment (C).

Figure 3.4: Body and heart weights. Brg1 KO stunts growth upon recombination (1-2 weeks); doxorubicin treatment accelerated weight loss (4 weeks) (A). Percent body weight gains were negligible with Brg1 KO, but decreased with doxorubicin treatment with or without Brg1 KO (B). Heart weights were significantly increased in Brg1 KO mice, with or without doxorubicin treatment (C).

Figure 3.5: Histologic lesion incidence. Incidence of degeneration/necrosis, cardiomyocyte (A). Brg1 knockout and doxorubicin treatment significantly increased lesion severity grade relative to respective controls (B).

Figure 3.6: Cardiac histopathology. Cardiac histology of Brg1 WT (A), Brg1 KO (B), Brg1 WT+Dox (C), and Brg1 KO+Dox (D) mice. Sarcoplasmic vacuolation (arrows) and fragmentation/degeneration was observed (arrowheads).

Figure 3.7: Cardiac electron microscopy. Brg1 KO+Dox animals (D-F). Normal mitochondrial morphology (arrow) and Z bands in register (arrowhead) in a Brg1 WT+Dox mouse (A). Increased size (arrow) and presence of numerous fission/fusion events (arrowhead) in Brg1 KO mice (B). Mitochondrial myelin figures (arrow) and T-tubule dilation (arrowhead) in a Brg1 WT+Dox mice (C). T-tubule dilation and disruption (arrow) in a Brg1 KO+Dox mouse (E). Mitochondrial degeneration and christolysis (arrowhead) and fusion (arrow) in a Brg1 KO+Dox mouse (F). Magnification of 7A-F: 11,500x, 13,000x, 9,300x, 4,800x, 30,000x, and 18,500x, respectively.

Figure 3.8: Cardiac biomarker analysis. Serum fatty acid binding protein 3 (FABP3) (A) and myosin light chain 3 (Myl3) (B) levels. Weak correlation was observed between relative Brg1 mRNA and FABP3 (C) or Myl3 (D), respectively, in Brg1 WT+Dox animals. Strong correlation is observed between relative Brg1 mRNA and FABP3 (E) or Myl3 (F), respectively, in Brg1 KO+Dox animals.

Figure 4.1: Microarray analysis. Pairwise comparisons (A) and the genes sets yielded based on comparisons (B). Gene signature gradation correlation from loss of Brg1 to treatment with doxorubicin (C). Doxorubicin-induced changes that require Brg1 ("A not C"), doxorubicin-induced changes blocked by Brg1 ("C not A"), and doxorubicin-induced changes independent of Brg1 ("A and C") (D).

Figure 4.2: rt-PCR of select validation genes. Pairwise comparisons (A) and the validation of the relative fold change of Brg1 (B) and S100a9 (C) in those comparisons between rt-PCR and microarray analysis.

Figure 4.3: Enriched networks for doxorubicin-dependent gene expression changes in both wild-type and Brg1 deletion mice. Cardiac gene expression changes induced by doxorubicin treatment independent of Brg1 gene deletion.

Figure 4.4: Enriched networks for doxorubicin-induced or Brg1 deletion-induced gene expression changes. Canonical cell-signaling pathways are enriched either by doxorubicin treatment or by Brg1 deletion.

Figure 4.5: Enriched networks for doxorubicin-induced gene expression changes blocked by Brg1 expression. Brg1 expression prevents differential expression of pathways associated with heart disease (A), and ubiquitin-mediated proteolysis (B).

LIST OF ABBREVIATIONS AND ACRONYMS

AAALAC, Association for Assessment and Accreditation of Laboratory Animal Care International

ARAC, animal research advisory council

Brg1, brahma-related gene 1

Brg1 fl/fl, B6;128S2-Smarca4^{tm1Pcn}/Mmnc

CAG-Cre, CMV immediate-early enhancer coupled with a chicken β-actin/rabbit β-globulin hybrid promoter.

Cre-Brg1 fl/fl, B6.Cg-Tg(CAG-cre/Esr1*)5Amc/J Tg B6;128S2-Smarca4^{tm1Pcn}/Mmnc

CO_2, carbon dioxide

cTnI, cardiac troponin I

cTnT, cardiac troponin T

DEG, differentially expressed genes

DNA, deoxyribonucleic acid

EM, electron microscopy

FABP3, fatty acid binding protein 3

Floxed, flanked by loxP sites

H&E, hematoxylin and eosin

IP, intraperitoneal

KO, knockout

LOAEL, lowest observed adverse effect level

Myl3, myosin light chain 3

NIEHS, National Institute of Environmental Health Sciences

NIH, National Institutes of Health

NOAEL, no observed adverse effect level

PBS, phosphate-buffered saline

PMSF, phenylmethanesulfonyl fluoride

PCR, polymerase chain reaction

RNA, ribonucleic acid

rt-PCR, real-time polymerase chain reaction

ROS, reactive oxygen species

WT, wild-type

SMARCA4, SWI/SNF-related, matrix-associated, actin-dependent, regulator of chromatin, subfamily A, group 4

SWI/SNF, isotype switching, sucrose non-fermenting

CHAPTER 1

Background, Hypothesis, and Specific Aims

General Introduction

The intersection of research into epigenetics and cardiovascular disease is an exciting investigative junction. The field of epigenetics has grown exponentially in the past decade; PubMed citation searches using the search term "epigenetics" yields approximately 700, 1000, 1600, 2500, and 3200 hits from each of the respective years of 2007 through 2011, demonstrating the amazing growth in the field (PubMed.gov). There are thousands of published reviews of epigenetic mechanisms concerning topics ranging from respiratory disease, cancer, cardiovascular disease, and development (Jakopovic et al. 2013, Karmaus et al. 2013, and Ronan et al. 2013). Adding the search term "cardiovascular" to the search yields 7, 17, 42, 77, and 90 hits over the same periods, revealing the opportunity for novel investigation in this important field.

Cardiovascular disease is the number one killer of adults in the United States; heart disease and cancer account for approximately 50% of mortalities in the United States (Siegel et al. 2013). Paradoxically, a certain subtype of the most prevalent morbidity and mortality factor (heart disease) is due to treatment for the second most prevalent morbidity and mortality factor (cancer): this is the case for doxorubicin cardiotoxicity (Sawyer DB 2013). Several therapies for cancer and other diseases have been implicated in cardiovascular toxicity, and numerous others have failed to make it to the market due to cardiovascular complications (Slordal and Spigset 2006, Laverty *et al*. 2011, Cheng and Force 2010). The

following chapters seek to elucidate the probable role of Brg1, a master genome regulator, in doxorubicin-induced cardiotoxicity.

Cardiac Structure and Function

The heart is a four chambered structure, composed of two atria at its base and two ventricles at its apex, responsible for delivering oxygen and nutrients to all tissues of the body, removing carbon dioxide and other waste products, trafficking hormones, interleukins and other cell-signaling molecules, and moving leukocytes to and from their effector sites (Kumar et al. 2007). The heart is composed of several different cell types, including working cardiomyocytes (heart muscle cells), fibroblasts, endothelial cells, smooth muscle cells, Purkinje fibers, nodal or pacemaker cells, and epicardial cells. Despite their relative majority contribution to cardiac mass, working cardiomyocytes represent only approximately 25-50% of cells by number that compose the myocardium, depending upon species (Kumar et al. 2006). The remaining mass is composed of the nonworking cardiomyocytes, including nodal cells and Purkinje fibers, and the mesenchymal (fibroblast, endothelial) support network of the myocardium (Katz 2011). The critical functions of the heart are possible when this functional syncytium of various cell types coordinates through release and uptake of calcium ions through intercalated discs, specialized cardiac cell-to-cell junctions, to generate action potentials, convey those action potentials in series, and contract in a progressive manner to allow proper directional pressure (Topol 2007). The efficiency of this contraction is further enhanced by the oblique to circumferential orientation of the myofibrils from the base of the ventricles to their apex (Stohr et al. 2013, Katz 2011). This action potential is further

efficiently distributed through specialized cardiomyocyte structures, discussed later. The cardiac functional syncytium is sensitive to regional, global, or organismal losses in function and fractionally adjusts accordingly to maintain normal homeostasis (Stohr et al. 2013). Coronary artery disease, deleterious genetic mutations, and medicines (cardiac and non-cardiac) can perturb this homeostasis. The primary cell type responsible for proper contractile cardiac function is the cardiomyocyte, which has several subcellular targets for injury.

Cardiomyocyte Structure

Elongated cardiomyocytes contain numerous myofibrils, which are cross-striated microscopically due to the presence of Z and M lines, present within I and A bands, respectively, of the cells' contractile apparatus. Z lines bisect I bands, the latter of which are composed primarily of monomers of the thin filament actin, but also the regulatory proteins tropomyosin and cardiac troponins C, I, and T (Topol 2007). M lines are present within the middle of the sarcomere, bisecting A bands, which are composed primarily of the thick filament actin (Sarantitis et al. 2012). Numerous other proteins are present which modulate the interactions and relative positioning of the thick and thin filaments, including titin, S100, tropomodulin, desmin, and ankyrin (Kho et al. 2012, Clark et al. 2002). The cardiomyocyte has a specialized endoplasmic or sarcoplasmic reticulum, which as a part of the sarcotubular network transports and stores calcium ions for immediate access for generation of action potentials and binding to contractile elements (Katz 2006).

An important component of this sarcotubular network is the transverse tubule (T-tubule) system, which encircle myofibrils and is continuous with both the plasma and sarcotubular network membranes (Guo 2013, Smolich 1995). Damage to any aspect of this specialized network will prevent sufficient trafficking of calcium thereby potentially leading to contractile dysfunction or downstream effects of excess intracellular calcium including mitochondrial dysfunction or apoptosis, and has been shown to undergo considerable remodeling in cardiac disease (Dorn 2013, Guo 2013).

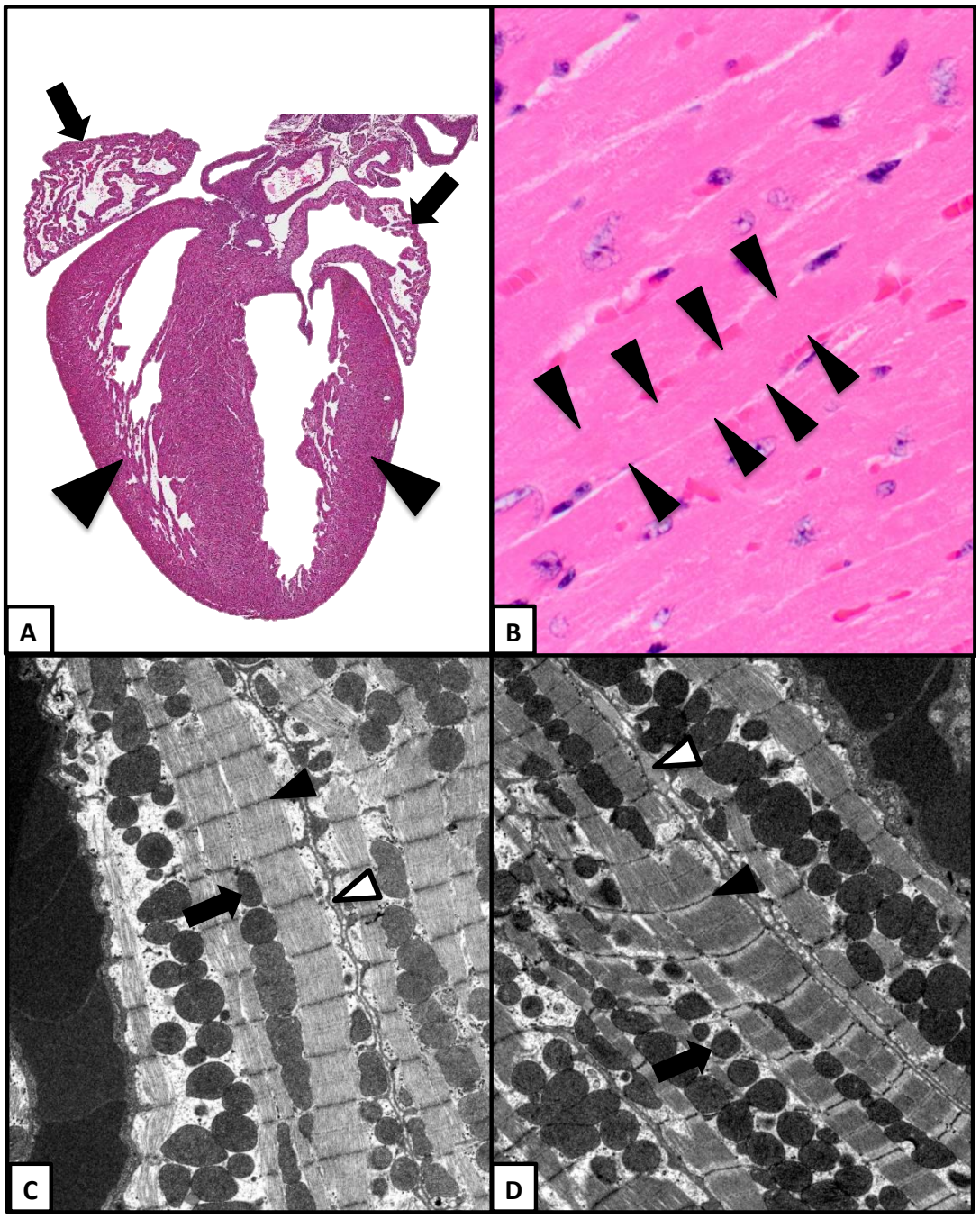

Figure 1.1: Normal mouse myocardial microscopy. Histology of normal mouse heart; cross section demonstrates atria (arrows) and ventricles (arrowheads)(postnatal day 7) (A). Histology of normal murine left ventricle; an individual cardiomyocyte is delineated (arrowheads) (6 month old) (B). Electron microscopy of normal murine left ventricle (C, D); mitochondria (arrows), Z-lines (arrowheads), and the intercellular spaces continuous with the sarcolemmal network (open arrowheads) are evident. A, original magnification objective 2x. B, original magnification objective 60x (B). C, D, original magnification 4,800x.

Cardiovascular Disease

Cardiovascular disease is the leading cause of death in developed countries. Heart failure is a global pandemic that results in increasingly significant health care costs as the general population ages and life expectancy increases, and is the leading cause of hospitalizations in patients of 65 years old. Heart failure treatment is estimated to cost approximately $39 billion dollars a year in the United States (Kazi and Mark 2013), with approximately 550,000 new cases reported each year (Octavia 2012b).

Medicines and Cardiotoxicity

Cardiotoxicity is the number one cause of preclinical failures of medicines to reach the market or late-stage clinical trials. The number one cause of withdrawal of new chemical entities is also the incidence of adverse cardiac events associated with their use. Entire classes of effective medicines for a variety of conditions including cancers, pain, diabetes, and Parkinson's disease have a variety of deleterious cardiac effects associated with their use (Pai and Nahata 2000, Slordal and Spigset 2006). Anthracyclines are the most well-known cardiotoxic class of anticancer medicines, though medicines of other classes, such as the vinca alkaloids (vincristine, vinblastine), alkylating agents (cisplatin, carmustine, cyclophosphamide), paclitaxel, etoposide, and monoclonal antibodies are known to cause cardiotoxicity through a variety of mechanisms (Slordal and Spigset 2006, Pai and Nahata 2000). Some medicines, such as trastuzumab, have an additive toxic effect to the myocardium when used in conjunction with radiation therapy or other chemotherapies such as doxorubicin or paclitaxel (Kalam and Marwick 2013, Pai and Nahata 2000).

Doxorubicin Cardiotoxicity

Doxorubicin cardiotoxicity is one of the most well-studied medicine-induced cardiotoxicity syndromes (Chatterjee 2010). Approximately 40% of all PubMed citation searches for the term "cardiotoxicity" are associated with doxorubicin. Doxorubicin (trade name Adriamycin) is an anthracycline antibiotic isolated from the bacterium *Streptomyces peucetius caesius* (Roca-Alonso *et al*. 2012, Carvalho *et al.* 2013). It is used as a cancer therapeutic for a wide range of epithelial, mesenchymal, and round cell neoplasms, including breast cancer, Kaposi sarcoma, and Hodgkin's lymphoma (Volkova and Russel 2011, Geiger *et al*. 2010, Chatterjee *et al*. 2010). In some instances, doxorubicin serves as the primary or only line of treatment for particular types of cancer, such as certain sarcomas (Ray-Coquard and Le Cesne 2012).

Doxorubicin's efficacy against tumor cells is mostly attributed to its ability to intercalate DNA. However, its quinone-like structure lends itself to accept a donated electron, subsequently undergo oxidation, and generate free radicals through Fenton chemistry (Octavia 2012b, Casarett and Doull 2008). Induction of apoptosis, growth arrest, and DNA helicase and topoisomerase disruption are also potential contributors (Carvalho *et al*. 2013, Octavia *et al*. 2012a, Tacar *et al*. 2013). These effects are not only felt by the target cancer cells, but by the off-target cardiomyocytes. Cardiac off-target effects include myelosuppression, gastrointestinal upset, and a rare myocarditis-pericarditis syndrome (Singal and Iliskovic 1998). Other acute syndromes include transient ECG changes which may affect up to 30% of patients, though typically with no clinical consequence (Gharib and Burnett 2002). However the risk of heart failure in treated patients, which may not become

clinical for several years to decades upon cessation of therapy, continues to be the main concerning side effect in clinical doxorubicin chemotherapy (Octavia et al. 2012b). This treated population pool, or susceptible population, contains patients with few to no comorbidities suffering adolescent-onset cancers to adults with comorbidities undergoing concomitant treatment, to the elderly.

Due to the wide-ranging indications for doxorubicin, and continued use in susceptible populations, much investigation is underway into adjuvant therapies, such as dexrazoxane, to decreased toxicity (Schunke et al. 2013, Jin et al. 2013, Chen et al. 2007, Wang et al. 2013). These investigations were born out of necessity due to the increasing clinical cardiotoxicity observed, as is the case with HER2 positive breast cancer patients co-administered trastuzumab and doxorubicin (Cheng and Force 2010, Klein and Dybdal 2003). Currently, mechanism-based solutions are the most promising hope for decreasing morbidity in a population that is continually gaining remission time and consequently, more susceptibility to the hazardous sequela of some of the most effective chemotherapies. In fact, the discipline of cardio-oncology is partly the result of unmet needs in this investigative area (Moslehi and Cheng 2013).

The Brg1 Chromatin Remodeling Complex

Chromatin, or the assembly of DNA-wrapped nucleosomes into secondary and tertiary structures, is a mechanism required to compact approximately 1.7 meters of DNA into a nucleus (Kornberg 1975). Despite the seemingly compact nature of this arrangement, significant portions of the genome require accessibility for the initiation or elongation of

transcription. This accessibility requirement is met by chromatin remodeling complexes, which hydrolyze ATP to alter the chromatin landscape in a way to allow or prevent access to the basal transcriptional machinery (Trotter and Archer 2004). The SWI/SNF, CHD, ISWI, and INO80 chromatin remodeling families are delineated based on the structure of their ATPase domain. The SWI/SNF (switching isotype/sucrose non-fermenting) chromatin remodeling complexes were first discovered in *Saccharomyces cerevisiae* mutations, and appropriately named for their phenotype in that system (Sudarsanam and Winston 2000, Chen et al. 2006). The murine catalytic subunit of the SWI/SNF complex is Brahma-related gene 1, or Brg1, named for its human paralog with which it has high sequence similarity (Trotter and Archer 2008). The HSA, ATPase, and AT-hook domains modulate protein binding and catalytic activity (Fan et al. 2005, Trotter and Archer 2008). Various transcriptional requirements for the activity of Brg1 have been described, including activation of genes including GR, BRCA1, and p53, and repression of RB and HP1 (Trotter and Archer 2008). Brg1 also partners with other chromatin modifying enzymes to regulate transcription, including the WINAC, NCoR, NUMAC, and mSin3A/HDAC complexes. The BAF complex, is composed of Brg1 ATPase and Brg1-associated factors (BAFs), including BAF250a, and BAF155. The BAF composition of these complexes does impart tissue specificity in some instances, as in the presence of BAF60c in cardiac progenitor cell BAF complexes and BAF60a and BAF60b in post-mitotic neuronal BAF complexes (Lickert et al. 2004, Ho and Crabtree 2010). The unique composition of these complexes determines their functional significance, central to which is the ability to hydrolyze ATP to remodel nucleosome assembly (Simone 2006, Trotter and Archer 2008). Current data suggests

chromatin remodeling complexes are recruited to their effector sites by a combination of Transcription factors, chromatin modifications and promoter regulatory regions, but it is as yet undetermined precisely what controls the construct of these complexes to impart tissue specificity and differentiation (Cairns 2009, Ho and Crabtree 2010, Sudarsanam and Winston 2000).

Recent analysis of promoter binding in Brg1-silenced cell systems suggests that on a global genome scale, the complex promotes transcriptional repression and nucleosome immobilization (Tolstorukov et al. 2013). Brg1 has been demonstrated as an important gene in several cancers including malignant rhabdoid tumors, and lung and mammary carcinomas (Romero and Sanchez-Cespedes 2013). Indeed, Brg1 acts as a tumor suppressor regulating growth arrest and senescence through pathways including RB, p53, c-Myc, and BRCA1 (Euskirchen et al. 2012, Kang et al. 2004, Romero and Sanchez-Cespedes 2013). Brg1 has also been implicated in E2F6-directed RB silencing (Leung and Nevins 2013).

Heart Development

The differentiation of mammalian mesodermal cell to cardiac lineage is primarily under the control of the transcription factors Nkx2-5, Tbx5, and Gata4, and the regulator Baf60c (Takeuchi and Bruneau, 2009) Genome regulation by SWI/SNF complexes (Brg1), chromodomains (CHD7), HDACs (Jumonji), HMTs (MLL2), and PRCs (Rae28) organize the concurrent expression of transcription factors to coordinate differentiation of cardiomyocytes, smooth muscle cells, and endothelial cells (Chang and Bruneau, 2012; Wamstad et al, 2012). Under the influence of Notch, BMP, and TGF-β signaling, progenitor

cells undergo epithelial to mesenchymal transition within the primitive streak to form the first and second heart fields of the lateral plate mesoderm at embryonic day 9 (E9), forming the cardiac crescent (Chang and Bruneau, 2012; Marcela et al, 2012; Garside et al, 2013). At E9.5, under the regulation of Baf60c, the rudimentary heart tube undergoes left to right looping from the initial C-shaped structure to an S-shaped structure during E9.5-E11.5 (Takeuchi *et al*, 2007; Marcela *et al*, 2012). During chamber development, the myocardium is composed of an outer myocardial cell layer, an inner endocardial cell layer, and the intervening cardiac jelly, a matrix with limited trabeculation. Trabeculation in the chambers matures due to Adamts1 expression under the influence of Brg1 chromatin remodeling (Chang and Bruneau, 2012). From E12.5-E14.5, under the control of Jarid2 and Jmjd6, the looped structure exhibits chamber formation and orientation, and the outflow tracts begin separation due to Rae28-directed gene silencing (Chang and Bruneau, 2012; Marcela *et al*, 2012). During heart looping and outflow tract formation and separation, the four cardiac valves are being formed as part of the cardiac septation process. The atrioventricular valves are formed from the atrioventricular canal (AVC), and the semilunar or outflow tract valves formed from the ventricular outflow tract (OFT), respectively (Garside *et al*, 2013). Valve formation begins as an endocardial to mesenchymal transition of endocardial cells in the AVC and OFT, which invade the underlying cardiac jelly, proliferation, and formation of the cardiac cushions (Kruithof *et al*, 2012). The outflow tracts are closed by E15.5 and the mature heart formed by E16.5 (Marcela *et al*, 2012). Valve maturation continues from E15.5 until the postnatal period (Garside *et al*, 2013). Not all septation is completed due to cushion formation and septation, as the foramen ovale remains patent at birth. Specialized

nonworking myocardial cells develop into the well-defined conduction system. The atrioventricular node is the first to develop as a medial subendocardial thickening in the primitive left atrium. This develops into the atrioventricular fasciculus that distributes impulses in the ventricular walls through the Purkinje fibers. The sinoatrial node develops subepicardially at the future opening of the vena cava caudalis.

Brg1 in Development and Cardiovascular Disease

The "return to the fetal genome" paradigm is relevant to many disease processes, including cardiovascular disease (Degenhardt et al. 2013, Oka et al. 2007, Rajabi et al. 2007). As master regulators of the genome, chromatin remodelers are at the heart of many of these epigenetic effects (Mymryk et al. 1995, Hargreaves and Crabtree 2011, Mohrmann and Verrijzer 2005, Hansen 2002, Horn and Peterson 2002). Chromatin modifications and chromatin remodelers have been linked to both hypertrophic and failing myocardial phenotypes (Mahmoud and Poizat 2013). In mouse models of increased cardiac preload, the requirement of Brg1 for the prevention of adult-onset cardiovascular disease suggests that Brg1 is required during critical cardiovascular developmental time points, for the maintenance of cardiovascular homeostasis, and potentially, for the amelioration or prevention of other cardiovascular diseases (Hang *et al*. 2010). If and when Brg1 is required during the postimplantation period, and if Brg1 plays a role in the response to disease in models other than the increased preload models already described, is yet to be determined (Takeuchi et al. 2007, Li et al. 2013, Xu et al. 2013, Reisman et al. 2009, Indra et al. 2005).

Clearly Brg1 is present in the postnatal period as well as through adulthood in the mouse (Figure 1.2).

There has been within the last decade an impressive amount of research elucidating the molecular mechanisms of Brg1 regulation of developmental and disease processes, and the reader is referred to several excellent reviews (Ho and Crabtree 2010, Hargreaves and Crabtree 2011, Chang and Bruneau 2012). This research has elucidated the Brg1 chromatin remodeling complex is required for cardiovascular lineage development, in particular the requirements of Brg1 and BAF60c for normal cardiomyocyte development and left-right symmetry morphogenesis, Brg1 and BAF180 for coronary vessel development and differentiation, and that Brg1 and BAFs are critical for expression of cardiac lineage-specific genes Nkx2-5, Tbx20, and Tbx5.

Numerous intriguing possible roles for Brg1 in doxorubicin cardiotoxicity exist within research investigating the mechanisms of doxorubicin or those of Brg1-dependent transcriptional regulation. ROS play a large role in heart failure through activation of a variety of pathways including apoptosis, fibrosis, contractile dysfunction, and hypertrophy (Octavia 2012b). Brg1 is known to modulate ROS by binding to antioxidant promoter regions in specific disease states, such as in Fanconi Anemia patients (Du et al. 2013). Xu et al showed that increasing Brg1 levels in diabetic rats, also increased hemoxygenase-1 (HO-1) levels, which is a critical antioxidant (Xu et al. 2013). Those animals additionally had decreased expression of the proinflammatory genes TNF-a and Il-6. Other groups have shown that the maintenance of stemness, a tenet of the shift to the fetal paradigm, is

instrumental in the cardiac progenitor cell's ability to survive the stress of doxorubicin treatment (De Angelis et al 2010).

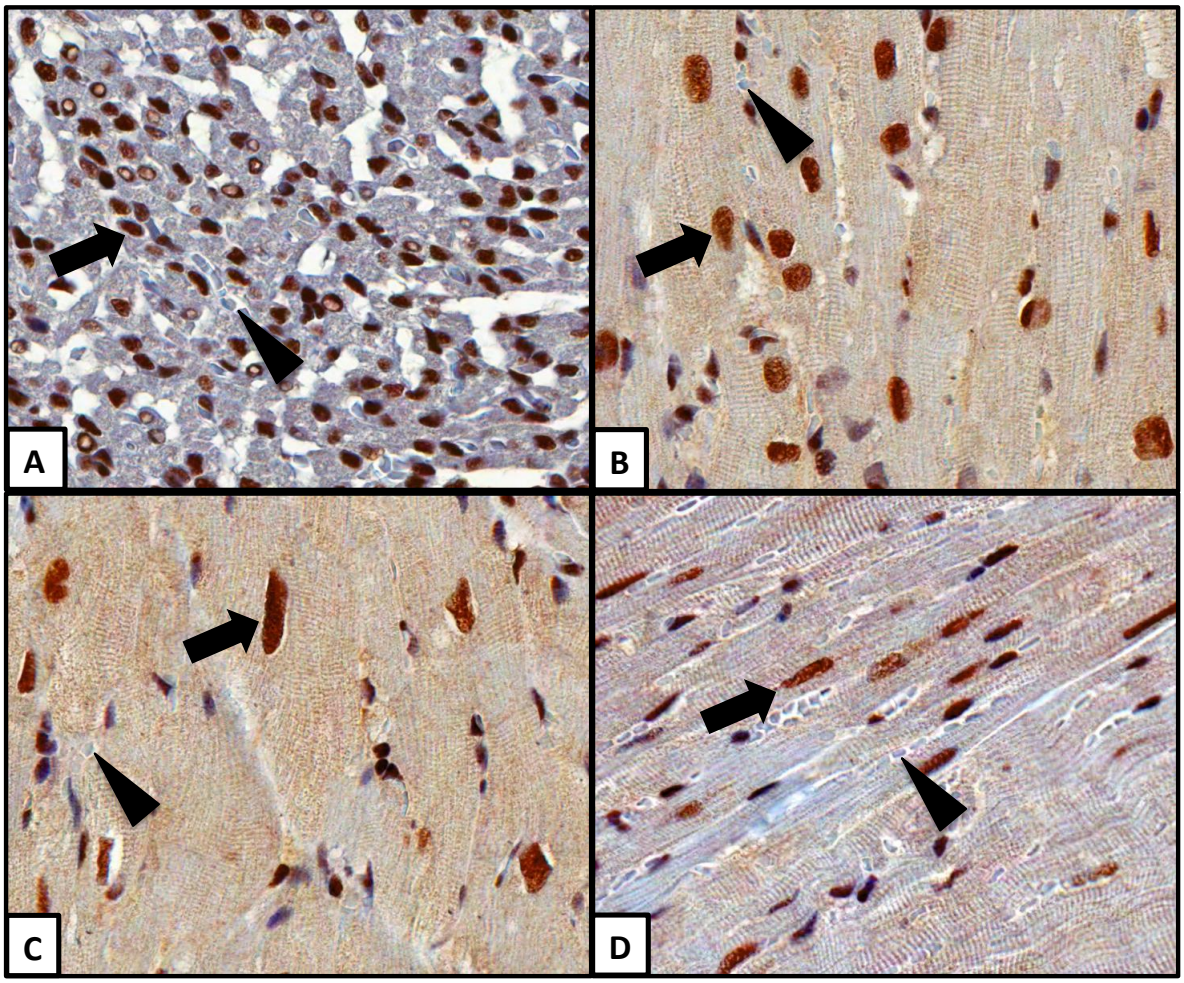

Figure 1.2: Expression of Brg1 in murine myocardium. Heart sections from 1 day (A), 1 month (B) 6 month (C) and 2 year-old (D) CD-1 mice stained with an anti-mouse Brg1 antibody. Arrows indicate positively-staining cardiomyocyte nuclei; arrowheads indicate negatively-staining erythrocytes as internal negative controls. DAB counterstain. Original magnification objective 40x.

Animal Models of Doxorubicin Cardiotoxicity

There are numerous in vitro models to investigate doxorubicin cardiotoxicity, from fresh isolation of neonatal mouse or rat cardiomyocytes, culture of H9c2 cells from cardiomyoblasts, or differentiation of pluripotent stem cells to cardiomyocyte progenitors (Navarrete et al. 2013, Zordoky et al. 2007, Louch et al. 2007). However, work by Branco et al. has shown the differentiation state of the cell system is critical for evaluation of toxic endpoints, and that more differentiated cells exhibit greater toxicity (Branco et al. 2012).

Animal models of doxorubicin cardiotoxicity to date have been designed to create structural or functional deleterious changes in the heart of the test species. Only very recently, as demonstrated by Desai et al., have efforts been made to design rodent studies receiving clinically comparable doses of doxorubicin over clinically comparable timeframes (Desai et al. 2013, Simunek, 2009, Robert 2007). These models, including those in the rat, rabbit, dog, pig, and nonhuman primate, have focused on generating significantly different deviations in echo- or electrocardiographic parameters, or cardiomyocyte degeneration, necrosis, and inflammation as determined by light microscopy (Desai et al. 2013, Wang et al. 2013, Chen et al. 2007, Van Vleet and Ferrans 1980).

Careful evaluation of animal models of human disease facets must be carefully evaluated so the scientist can differentiate the normal from abnormal. Regarding the cardiovascular system, the constellation of lesions comprising the Rodent Progressive Cardiomyopathy syndrome should not be confused with potential test article-related findings. Cardiomyocyte degeneration and necrosis with accompanying inflammatory cell infiltrates, and eventually, fibrosis, occur at a low yet predictable rate in the young laboratory mouse.

Inducible Transgenics and Cre Recombinetics

Gene knockout strategies in mammalian systems have vastly increased the opportunities to design mouse models of human disease mediators. In fact, the designers of these strategies suitably won a Nobel Prize (Mak 2007, Koller and Smithies 1992). These systems utilize a bacteriophage recombinase which specifically recognizes a palindromic sequence in the bacterial DNA, the LoxP site, for targeted cleavage. Cells expressing the Cre enzyme and containing sections of DNA flanked by LoxP sites, or "floxed" sites, will undergo recombination through targeted excision and degradation of the floxed sequence (Rossant and McMahon 1999).

The utility of this system was hugely improved by Zhang et al. through the creation of the tamoxifen-inducible Cre enzyme, constructed of the Cre enzyme bound to a murine estrogen receptor with a mutated hormone-binding domain (Zhang et al. 1996). Inducible knockout models have allowed researchers to study gene perturbations in a temporal and/or tissue-specific manner, which abrogates limitations posed by phenomena such as embryonic lethality from dysregulation of the developmental program. (Sohal et al. 2001, O'Neal and Agah 2007). Additionally, this revolutionary system has allowed comparative biologists to investigate the effect of perturbing their gene or genes of interest at specific time points concurrent with other stimuli.

These advances are not without pitfalls, however, as Koitabashi et al. discovered in their investigations using a tamoxifen-inducible cardiomyocyte-specific Cre construct (Koitabashi et al 2009). Their research revealed that a cardiac phenotype observed in their model was due to toxicity of the Cre construct, and not perturbation of their gene of interest.

Careful evaluation of tissue morphology for Cre toxicity, with manifestations including widespread tissue necrosis and lack of erythroid progenitors in embryos, must be performed in concurrent Cre-positive control animals (Naiche and Papaioannou 2007, Ackerl et al. 2007).

Inducible knockout models have been used to investigate the effects of perturbing Brg1 dependent chromatin remodeling, through deletion of the ATPase domain of Brg1 (Sumi-Ichinose et al. 1997). This construct, after Cre-mediated recombination, produces a truncated Brg1 protein lacking ATPase activity, but retaining binding activity at its HSA and Brk domains.

Hypothesis and Specific Aims

The current work investigates the requirement for Brg1 in a temporal fashion in early embryonic development in the mouse, and for the protective response in the face of doxorubicin cardiotoxicity. Transgenic mice will be used to achieve these aims as no in vitro systems exist which recapitulate the animal heart in its entirety. Additionally, use of in vitro systems to investigate mechanisms of cardiotoxicity has recently been reported to depend on the differentiation state of the system (Branco et al. 2012). These investigations will be performed using an inducible knockout mouse model system developed to temporally delete portions of the genome. One half of the required genetic construct, the Brg1 floxed mouse, has been used by other laboratories to investigate the effects of temporal deletions (Sumi-ichinose *et al*. 1997, Bultman *et al*. 2000). This work is performed in conjunction with the core laboratory facilities at the NIEHS, which have extensive experience with the techniques

needed to evaluate the investigations outlined in the specific aims listed below, including but not limited to: mouse breeding and genetics, necropsy, histology, immunohistochemistry, electron microscopy, , microarray, bioinformatics, and image analysis. The scientists in the Laboratory of Molecular Carcinogenesis, particularly those in the Chromatin and Gene Expression Section, were instrumental in aiding and performing Western blotting and rt-PCR in support of various aspects of this work.

Specific Aim 1: Establish a tamoxifen-inducible mouse model for analyzing the effects of Brg1 deletion during mid-late gestational development and in adulthood, particularly bridging knowledge gaps in the perigastrulation period. Brg1 deletion in this model will cause gene dysregulation during development leading to fetal death. Brg1 deletion during adulthood in this model will lead to no adverse effects.

Specific Aim 2: Establish an in vivo mouse model emulating chronic doxorubicin toxicity in cancer patients. This mouse model will exhibit cardiomyocyte lesions of vacuolation and degeneration observed microscopically in human cases of doxorubicin cardiotoxicity.

Specific Aim 3: Determine the role of Brg1 in doxorubicin cardiotoxicity. Brg1 plays a protective role in cardiovascular development, and under duress of cardiotoxicity. Brg1 deletion will increase cardiotoxicity from doxorubicin through differential expression of a unique set of genes involved in maintenance of cell homeostasis.

Based on preliminary results of experiments in our laboratory, we have determined that Brg1 indeed plays a master regulatory role in our model system (See Chapter 2). The lesions observed in our initial studies suggest Brg1 plays a regulatory role both in maintaining normal cellular growth and proliferation during critical developmental phases, as well as in the cardiotoxic response to chronic doxorubicin administration. The hypothesis is that Brg1 deletion will confer sensitivity to doxorubicin cardiotoxicity. The expectation in the cardiotoxicity study is that a deletional event will be achieved which will render the Cre-Brg1 floxed mice less able to remodel chromatin in a manner needed to "return to the fetal genome." Those mice will be further subjected to the dysregulation observed in our preliminary studies, and thus will have a greater incidence and severity of lesions characteristic of doxorubicin cardiotoxicity. Additionally, mice with a Brg1 deletion in the absence of additional stress variables (i.e. doxorubicin treatment) will not have a significantly increased number of lesions, amount of cardiac damage biomarker free in serum, nor significantly DEGs related to cardiomyocyte damage. Furthermore, there will be no significant differences in the levels of Brg1 mRNA or the levels of Brg1 protein between Brg1 KO animals, irrespective of doxorubicin treatment. The use of this model system will provide the most appropriate translational data for the human condition, as efficacy of biomarkers and identification of molecular targets can be directly pursued in this model. Alternatively, no significant difference may be elucidated between the treated animals with or without Cre activity. Investigation into the level of Brg1 disruption would be necessary to determine if a gene dosage effect is an additional variable.

This thesis investigates a novel link amongst the various pathogeneses of doxorubicin cardiotoxicity involving the Brg1 chromatin remodeling complex. These studies have the potential to reveal mechanistic information regarding mammalian development, as well as indicate new targets for decreasing the toxicity of a widely-used cancer therapy that causes significant morbidity under its current uses.

Chapter 1 References:

Ackerl, R., Walko, G., Fuchs, P., Fischer, I., Schmuth, M., and Wiche, G. (2007). Conditional targeting of plectin in prenatal and adult mouse stratified epithelia causes keratinocyte fragility and lesional epidermal barrier defects. *Journal of cell science* **120**(Pt 14), 2435-43, 10.1242/jcs.004481.

Branco, A. F., Sampaio, S. F., Moreira, A. C., Holy, J., Wallace, K. B., Baldeiras, I., Oliveira, P. J., and Sardao, V. A. (2012). Differentiation-dependent doxorubicin toxicity on H9c2 cardiomyoblasts. *Cardiovascular toxicology* **12**(4), 326-40, 10.1007/s12012-012-9177-8.

Bultman, S., Gebuhr, T., Yee, D., La Mantia, C., Nicholson, J., Gilliam, A., Randazzo, F., Metzger, D., Chambon, P., Crabtree, G., and Magnuson, T. (2000). A Brg1 null mutation in the mouse reveals functional differences among mammalian SWI/SNF complexes. *Molecular cell* **6**(6), 1287-95.

Carvalho, F. S., Burgeiro, A., Garcia, R., Moreno, A. J., Carvalho, R. A., and Oliveira, P. J. (2013). Doxorubicin-Induced Cardiotoxicity: From Bioenergetic Failure and Cell Death to Cardiomyopathy. *Medicinal research reviews*, 10.1002/med.21280.

Casarett, L. J., Doull, J., and Klaassen, C. D. (2008). *Casarett and Doull's toxicology : the basic science of poisons*. 7th ed. McGraw-Hill, New York.

Chatterjee, K., Zhang, J., Honbo, N., and Karliner, J. S. (2010). Doxorubicin cardiomyopathy. *Cardiology* **115**(2), 155-62, 10.1159/000265166.

Chen, B., Peng, X., Pentassuglia, L., Lim, C. C., and Sawyer, D. B. (2007). Molecular and cellular mechanisms of anthracycline cardiotoxicity. *Cardiovascular toxicology* **7**(2), 114-21, 10.1007/s12012-007-0005-5.

Cheng, H., and Force, T. (2010). Molecular mechanisms of cardiovascular toxicity of targeted cancer therapeutics. *Circulation research* **106**(1), 21-34, 10.1161/CIRCRESAHA.109.206920.

Clark, K. A., McElhinny, A. S., Beckerle, M. C., and Gregorio, C. C. (2002). Striated muscle cytoarchitecture: an intricate web of form and function. *Annual review of cell and developmental biology* **18**, 637-706, 10.1146/annurev.cellbio.18.012502.105840.

De Angelis, A., Piegari, E., Cappetta, D., Marino, L., Filippelli, A., Berrino, L., Ferreira-Martins, J., Zheng, H., Hosoda, T., Rota, M., Urbanek, K., Kajstura, J., Leri, A., Rossi, F., and Anversa, P. (2010). Anthracycline cardiomyopathy is mediated by depletion of the

cardiac stem cell pool and is rescued by restoration of progenitor cell function. *Circulation* **121**(2), 276-92, 10.1161/CIRCULATIONAHA.109.895771.

Degenhardt, K., Singh, M. K., and Epstein, J. A. (2013). New approaches under development: cardiovascular embryology applied to heart disease. *The Journal of clinical investigation* **123**(1), 71-4, 10.1172/JCI62884.

Desai, V. G., Herman, E. H., Moland, C. L., Branham, W. S., Lewis, S. M., Davis, K. J., George, N. I., Lee, T., Kerr, S., and Fuscoe, J. C. (2013). Development of doxorubicin-induced chronic cardiotoxicity in the B6C3F1 mouse model. *Toxicology and applied pharmacology* **266**(1), 109-21, 10.1016/j.taap.2012.10.025.

Euskirchen, G., Auerbach, R. K., and Snyder, M. (2012). SWI/SNF chromatin-remodeling factors: multiscale analyses and diverse functions. *The Journal of biological chemistry* **287**(37), 30897-905, 10.1074/jbc.R111.309302.

Fan, H. Y., Trotter, K. W., Archer, T. K., and Kingston, R. E. (2005). Swapping function of two chromatin remodeling complexes. *Molecular cell* **17**(6), 805-15, 10.1016/j.molcel.2005.02.024.

Geiger, S., Lange, V., Suhl, P., Heinemann, V., and Stemmler, H. J. (2010). Anticancer therapy induced cardiotoxicity: review of the literature. *Anti-cancer drugs* **21**(6), 578-90, 10.1097/CAD.0b013e3283394624.

Gharib, M. I., and Burnett, A. K. (2002). Chemotherapy-induced cardiotoxicity: current practice and prospects of prophylaxis. *European journal of heart failure* **4**(3), 235-42.

Hang, C. T., Yang, J., Han, P., Cheng, H. L., Shang, C., Ashley, E., Zhou, B., and Chang, C. P. (2010). Chromatin regulation by Brg1 underlies heart muscle development and disease. *Nature* **466**(7302), 62-7, 10.1038/nature09130.

Hansen, J. C. (2002). Conformational dynamics of the chromatin fiber in solution: determinants, mechanisms, and functions. *Annual review of biophysics and biomolecular structure* **31**, 361-92, 10.1146/annurev.biophys.31.101101.140858.

Hargreaves, D. C., and Crabtree, G. R. (2011). ATP-dependent chromatin remodeling: genetics, genomics and mechanisms. *Cell research* **21**(3), 396-420, 10.1038/cr.2011.32.

Ho, L., and Crabtree, G. R. (2010). Chromatin remodelling during development. *Nature* **463**(7280), 474-84, 10.1038/nature08911.

Horn, P. J., and Peterson, C. L. (2002). Molecular biology. Chromatin higher order folding--wrapping up transcription. *Science* **297**(5588), 1824-7, 10.1126/science.1074200.

Indra, A. K., Dupe, V., Bornert, J. M., Messaddeq, N., Yaniv, M., Mark, M., Chambon, P., and Metzger, D. (2005). Temporally controlled targeted somatic mutagenesis in embryonic surface ectoderm and fetal epidermal keratinocytes unveils two distinct developmental functions of BRG1 in limb morphogenesis and skin barrier formation. *Development* **132**(20), 4533-44, 10.1242/dev.02019.

Jakopovic, M., Thomas, A., Balasubramaniam, S., Schrump, D., Giaccone, G., and Bates, S. E. (2013). Targeting the Epigenome in Lung Cancer: Expanding Approaches to Epigenetic Therapy. *Frontiers in oncology* **3**, 261, 10.3389/fonc.2013.00261.

Jin, Z., Zhang, J., Zhi, H., Hong, B., Zhang, S., Guo, H., and Li, L. (2013). The beneficial effects of tadalafil on left ventricular dysfunction in doxorubicin-induced cardiomyopathy. *Journal of cardiology* **62**(2), 110-6, 10.1016/j.jjcc.2013.03.018.

Kalam, K., and Marwick, T. H. (2013). Role of cardioprotective therapy for prevention of cardiotoxicity with chemotherapy: a systematic review and meta-analysis. *Eur J Cancer* **49**(13), 2900-9, 10.1016/j.ejca.2013.04.030.

Kang, H., Cui, K., and Zhao, K. (2004). BRG1 controls the activity of the retinoblastoma protein via regulation of p21CIP1/WAF1/SDI. *Molecular and cellular biology* **24**(3), 1188-99.

Karmaus, W., Ziyab, A. H., Everson, T., and Holloway, J. W. (2013). Epigenetic mechanisms and models in the origins of asthma. *Current opinion in allergy and clinical immunology* **13**(1), 63-9, 10.1097/ACI.0b013e32835ad0e7.

Katz, A. M. (2011). *Physiology of the heart*. 5th ed. Wolters Kluwer Health/Lippincott Williams & Wilkins Health, Philadelphia, PA.

Kazi, D. S., and Mark, D. B. (2013). The economics of heart failure. *Heart failure clinics* **9**(1), 93-106, 10.1016/j.hfc.2012.09.005.

Kho, A. L., Perera, S., Alexandrovich, A., and Gautel, M. (2012). The sarcomeric cytoskeleton as a target for pharmacological intervention. *Current opinion in pharmacology* **12**(3), 347-54, 10.1016/j.coph.2012.03.007.

Klein, P. M., and Dybdal, N. (2003). Trastuzumab and cardiac dysfunction: update on preclinical studies. *Seminars in oncology* **30**(5 Suppl 16), 49-53.

Koitabashi, N., Bedja, D., Zaiman, A. L., Pinto, Y. M., Zhang, M., Gabrielson, K. L., Takimoto, E., and Kass, D. A. (2009). Avoidance of transient cardiomyopathy in cardiomyocyte-targeted tamoxifen-induced MerCreMer gene deletion models. *Circulation research* **105**(1), 12-5, 10.1161/CIRCRESAHA.109.198416.

Koller, B. H., and Smithies, O. (1992). Altering genes in animals by gene targeting. *Annual review of immunology* **10**, 705-30, 10.1146/annurev.iy.10.040192.003421.

Kornberg, R. D. (1974). Chromatin structure: a repeating unit of histones and DNA. *Science* **184**(4139), 868-71.

Kumar, V., Abbas, A. K., Fausto, N., Robbins, S. L., and Cotran, R. S. (2005). *Robbins and Cotran pathologic basis of disease*. 7th ed. Elsevier Saunders, Philadelphia.

Laverty, H., Benson, C., Cartwright, E., Cross, M., Garland, C., Hammond, T., Holloway, C., McMahon, N., Milligan, J., Park, B., Pirmohamed, M., Pollard, C., Radford, J., Roome, N., Sager, P., Singh, S., Suter, T., Suter, W., Trafford, A., Volders, P., Wallis, R., Weaver, R., York, M., and Valentin, J. (2011). How can we improve our understanding of cardiovascular safety liabilities to develop safer medicines? *British journal of pharmacology* **163**(4), 675-93, 10.1111/j.1476-5381.2011.01255.x.

Leung, J. Y., and Nevins, J. R. (2012). E2F6 associates with BRG1 in transcriptional regulation. *PloS one* **7**(10), e47967, 10.1371/journal.pone.0047967.

Li, L., Liu, D., Bu, D., Chen, S., Wu, J., Tang, C., Du, J., and Jin, H. (2013). Brg1-dependent epigenetic control of vascular smooth muscle cell proliferation by hydrogen sulfide. *Biochimica et biophysica acta* **1833**(6), 1347-55, 10.1016/j.bbamcr.2013.03.002.

Louch, W. E., Sheehan, K. A., and Wolska, B. M. (2011). Methods in cardiomyocyte isolation, culture, and gene transfer. *Journal of molecular and cellular cardiology* **51**(3), 288-98, 10.1016/j.yjmcc.2011.06.012.

Mahmoud, S. A., and Poizat, C. (2013). Epigenetics and chromatin remodeling in adult cardiomyopathy. *The Journal of pathology* **231**(2), 147-57, 10.1002/path.4234.

Mak, T. W. (2007). Gene targeting in embryonic stem cells scores a knockout in Stockholm. *Cell* **131**(6), 1027-31, 10.1016/j.cell.2007.11.033.

Mohrmann, L., and Verrijzer, C. P. (2005). Composition and functional specificity of SWI2/SNF2 class chromatin remodeling complexes. *Biochimica et biophysica acta* **1681**(2-3), 59-73, 10.1016/j.bbaexp.2004.10.005.

Moslehi, J., and Cheng, S. (2013). Cardio-oncology: it takes two to translate. *Science translational medicine* **5**(187), 187fs20, 10.1126/scitranslmed.3006490.

Mymryk, J. S., Zaniewski, E., and Archer, T. K. (1995). Cisplatin inhibits chromatin remodeling, transcription factor binding, and transcription from the mouse mammary tumor

virus promoter in vivo. *Proceedings of the National Academy of Sciences of the United States of America* **92**(6), 2076-80.

Naiche, L. A., and Papaioannou, V. E. (2007). Cre activity causes widespread apoptosis and lethal anemia during embryonic development. *Genesis* **45**(12), 768-75, 10.1002/dvg.20353.

Navarrete, E. G., Liang, P., Lan, F., Sanchez-Freire, V., Simmons, C., Gong, T., Sharma, A., Burridge, P. W., Patlolla, B., Lee, A. S., Wu, H., Beygui, R. E., Wu, S. M., Robbins, R. C., Bers, D. M., and Wu, J. C. (2013). Screening drug-induced arrhythmia events using human induced pluripotent stem cell-derived cardiomyocytes and low-impedance microelectrode arrays. *Circulation* **128**(11 Suppl 1), S3-13, 10.1161/CIRCULATIONAHA.112.000570.

O'Neal, K. R., and Agah, R. (2007). Conditional targeting: inducible deletion by Cre recombinase. *Methods Mol Biol* **366**, 309-20, 10.1007/978-1-59745-030-0_17.

Octavia, Y., Tocchetti, C. G., Gabrielson, K. L., Janssens, S., Crijns, H. J., and Moens, A. L. (2012). Doxorubicin-induced cardiomyopathy: from molecular mechanisms to therapeutic strategies. *Journal of molecular and cellular cardiology* **52**(6), 1213-25, 10.1016/j.yjmcc.2012.03.006.

Oka, T., Xu, J., and Molkentin, J. D. (2007). Re-employment of developmental transcription factors in adult heart disease. *Seminars in cell & developmental biology* **18**(1), 117-31, 10.1016/j.semcdb.2006.11.012.

Pai, V. B., and Nahata, M. C. (2000). Cardiotoxicity of chemotherapeutic agents: incidence, treatment and prevention. *Drug safety : an international journal of medical toxicology and drug experience* **22**(4), 263-302.

Ray-Coquard, I., and Le Cesne, A. (2012). A role for maintenance therapy in managing sarcoma. *Cancer treatment reviews* **38**(5), 368-78, 10.1016/j.ctrv.2011.07.003.

Reisman, D., Glaros, S., and Thompson, E. A. (2009). The SWI/SNF complex and cancer. *Oncogene* **28**(14), 1653-68, 10.1038/onc.2009.4.

Robert, J. (2007). Preclinical assessment of anthracycline cardiotoxicity in laboratory animals: predictiveness and pitfalls. *Cell biology and toxicology* **23**(1), 27-37, 10.1007/s10565-006-0142-9.

Roca-Alonso, L., Pellegrino, L., Castellano, L., and Stebbing, J. (2012). Breast cancer treatment and adverse cardiac events: what are the molecular mechanisms? *Cardiology* **122**(4), 253-9, 10.1159/000339858.

Romero, O. A., and Sanchez-Cespedes, M. (2013). The SWI/SNF genetic blockade: effects in cell differentiation, cancer and developmental diseases. *Oncogene*, 10.1038/onc.2013.227.

Ronan, J. L., Wu, W., and Crabtree, G. R. (2013). From neural development to cognition: unexpected roles for chromatin. *Nature reviews. Genetics* **14**(5), 347-59, 10.1038/nrg3413.

Rossant, J., and McMahon, A. (1999). "Cre"-ating mouse mutants-a meeting review on conditional mouse genetics. *Genes & development* **13**(2), 142-5.

Sarantitis, I., Papanastasopoulos, P., Manousi, M., Baikoussis, N. G., and Apostolakis, E. (2012). The cytoskeleton of the cardiac muscle cell. *Hellenic journal of cardiology : HJC = Hellenike kardiologike epitheorese* **53**(5), 367-79.

Sawyer, D. B. (2013). Anthracyclines and heart failure. *The New England journal of medicine* **368**(12), 1154-6, 10.1056/NEJMcibr1214975.

Schunke, K. J., Coyle, L., Merrill, G. F., and Denhardt, D. T. (2013). Acetaminophen attenuates doxorubicin-induced cardiac fibrosis via osteopontin and GATA4 regulation: Reduction of oxidant levels. *Journal of cellular physiology*, 10.1002/jcp.24367.

Siegel, R., Naishadham, D., and Jemal, A. (2013). Cancer statistics, 2013. *CA: a cancer journal for clinicians* **63**(1), 11-30, 10.3322/caac.21166.

Simone, C. (2006). SWI/SNF: the crossroads where extracellular signaling pathways meet chromatin. *Journal of cellular physiology* **207**(2), 309-14, 10.1002/jcp.20514.

Simunek, T., Sterba, M., Popelova, O., Adamcova, M., Hrdina, R., and Gersl, V. (2009). Anthracycline-induced cardiotoxicity: overview of studies examining the roles of oxidative stress and free cellular iron. *Pharmacological reports : PR* **61**(1), 154-71.

Singal, P. K., and Iliskovic, N. (1998). Doxorubicin-induced cardiomyopathy. *The New England journal of medicine* **339**(13), 900-5, 10.1056/NEJM199809243391307.

Slordal, L., and Spigset, O. (2006). Heart failure induced by non-cardiac drugs. *Drug safety : an international journal of medical toxicology and drug experience* **29**(7), 567-86.

Sohal, D. S., Nghiem, M., Crackower, M. A., Witt, S. A., Kimball, T. R., Tymitz, K. M., Penninger, J. M., and Molkentin, J. D. (2001). Temporally regulated and tissue-specific gene manipulations in the adult and embryonic heart using a tamoxifen-inducible Cre protein. *Circulation research* **89**(1), 20-5.

Stohr, E. J., Gonzalez-Alonso, J., Bezodis, I. N., and Shave, R. E. (2013). Left ventricular energetics: New insight into the plasticity of regional contributions at rest and during

exercise. *American journal of physiology. Heart and circulatory physiology*, 10.1152/ajpheart.00938.2012.

Sudarsanam, P., and Winston, F. (2000). The Swi/Snf family nucleosome-remodeling complexes and transcriptional control. *Trends in genetics : TIG* **16**(8), 345-51.

Sumi-Ichinose, C., Ichinose, H., Metzger, D., and Chambon, P. (1997). SNF2beta-BRG1 is essential for the viability of F9 murine embryonal carcinoma cells. *Molecular and cellular biology* **17**(10), 5976-86.

Tacar, O., Sriamornsak, P., and Dass, C. R. (2013). Doxorubicin: an update on anticancer molecular action, toxicity and novel drug delivery systems. *The Journal of pharmacy and pharmacology* **65**(2), 157-70, 10.1111/j.2042-7158.2012.01567.x.

Takeuchi, J. K., Lickert, H., Bisgrove, B. W., Sun, X., Yamamoto, M., Chawengsaksophak, K., Hamada, H., Yost, H. J., Rossant, J., and Bruneau, B. G. (2007). Baf60c is a nuclear Notch signaling component required for the establishment of left-right asymmetry. *Proceedings of the National Academy of Sciences of the United States of America* **104**(3), 846-51, 10.1073/pnas.0608118104.

Tolstorukov, M. Y., Sansam, C. G., Lu, P., Koellhoffer, E. C., Helming, K. C., Alver, B. H., Tillman, E. J., Evans, J. A., Wilson, B. G., Park, P. J., and Roberts, C. W. (2013). Swi/Snf chromatin remodeling/tumor suppressor complex establishes nucleosome occupancy at target promoters. *Proceedings of the National Academy of Sciences of the United States of America* **110**(25), 10165-70, 10.1073/pnas.1302209110.

Tonomura, Y., Matsushima, S., Kashiwagi, E., Fujisawa, K., Takagi, S., Nishimura, Y., Fukushima, R., Torii, M., and Matsubara, M. (2012). Biomarker panel of cardiac and skeletal muscle troponins, fatty acid binding protein 3 and myosin light chain 3 for the accurate diagnosis of cardiotoxicity and musculoskeletal toxicity in rats. *Toxicology* **302**(2-3), 179-89, 10.1016/j.tox.2012.07.012.

Topol, E. J., and Califf, R. M. (2007). *Textbook of cardiovascular medicine*. 3rd ed. Lippincott Williams & Wilkins, Philadelphia.

Trotter, K. W., and Archer, T. K. (2004). Reconstitution of glucocorticoid receptor-dependent transcription in vivo. *Molecular and cellular biology* **24**(8), 3347-58.

Trotter, K. W., and Archer, T. K. (2008). The BRG1 transcriptional coregulator. *Nuclear receptor signaling* **6**, e004, 10.1621/nrs.06004.

Van Vleet, J. F., and Ferrans, V. J. (1984). Ultrastructural alterations in the atrial myocardium of pigs with acute monensin toxicosis. *The American journal of pathology* **114**(3), 367-79.

Volkova, M., and Russell, R., 3rd (2011). Anthracycline cardiotoxicity: prevalence, pathogenesis and treatment. *Current cardiology reviews* **7**(4), 214-20.

Wang, Y., Zheng, D., Wei, M., Ma, J., Yu, Y., Chen, R., Lacefield, J. C., Xu, H., and Peng, T. (2013). Over-expression of calpastatin aggravates cardiotoxicity induced by doxorubicin. *Cardiovascular research* **98**(3), 381-90, 10.1093/cvr/cvt048.

Wang, Y., Zheng, D., Wei, M., Ma, J., Yu, Y., Chen, R., Lacefield, J. C., Xu, H., and Peng, T. (2013). Over-expression of calpastatin aggravates cardiotoxicity induced by doxorubicin. *Cardiovascular research* **98**(3), 381-90, 10.1093/cvr/cvt048.

Xu, J., Lei, S., Liu, Y., Gao, X., Irwin, M. G., Xia, Z. Y., Hei, Z., Gan, X., Wang, T., and Xia, Z. (2013). Antioxidant N-acetylcysteine attenuates the reduction of brg1 protein expression in the myocardium of type 1 diabetic rats. *Journal of diabetes research* **2013**, 716219, 10.1155/2013/716219.

Zhang, Y., Riesterer, C., Ayrall, A. M., Sablitzky, F., Littlewood, T. D., and Reth, M. (1996). Inducible site-directed recombination in mouse embryonic stem cells. *Nucleic acids research* **24**(4), 543-8.

CHAPTER 2: BRG1 deletion de-represses p53 pathways inducing cell cycle inhibition and apoptosis during peri-gastrulation development of mice

The content of this chapter is in the form required by the American Society of Microbiology for submission to their peer-reviewed publication *Molecular and Cellular Biology*. Michael Boyle, Ajeet P. Singh, and Trevor K. Archer devised the research concept. The animal experiments were designed by Michael C. Boyle, and performed by Michael C. Boyle and Ajeet P. Singh. The molecular biology experiments were performed by Ajeet P. Singh, Michael C. Boyle, and Mark Rubino. The microarray analysis was performed by the Microarray core at NIEHS; validation and interpretation was by Ajeet P. Singh and Michael C. Boyle. The manuscript was written by Michael Boyle, Ajeet Singh, and Trevor K. Archer.

BRG1 deletion de-represses p53 pathways inducing cell cycle inhibition and apoptosis during peri-gastrulation development of mice

Abstract:

BRG1 is a catalytic subunit of the SWI/SNF ATPase chromatin remodeling complex, which plays a vital role in gene regulation and tumorigenesis. Germline SWI/SNF function loss results in early embryonic lethality at approximately E3.5 in the mouse. However, BRG1 necessity during development beyond this embryonic stage has not been described. The myriad temporal genomic changes during development require remodeling of the chromatin to facilitate differential gene expression. Due to chromatin remodeling activities of BRG1, we hypothesized that BRG1 deficiency during post-implantation development may cause anomalies. Here we show that BRG1 ablation beginning at E6.5 results in arrested growth and embryonic death by E9.5. Mutant embryos failed to grow; histologic analysis revealed several developmental defects such as lack of normal cardiac structure and disrupted neural fold architecture. We demonstrate aberrant expression of cell cycle and apoptosis marker proteins in BRG1 mutants, suggesting a role for BRG1 in maintaining genomic integrity. Microarray analysis revealed BRG1 ablation increased expression of cell cycle regulators, particularly within the p53 pathway. Furthermore, BRG1 coordinates with CHD4 to suppress p53 pathways. These results suggest BRG1's role in genomic surveillance is essential for survival after the pre-implantation period for normal cellular proliferation and differentiation.

Introduction:

Mammalian embryogenesis can be defined by three distinct developmental windows: (1) pre-implantation, the source of pluripotent ES cells from which the future fetus will develop; (2) implantation, and (3) post-implantation, including gastrulation, organogenesis and growth. Embryonic cells divide very slowly, with little increase in mass prior to implantation. After implantation, as gastrulation initiates, a massive increase in growth occurs accompanied by a decrease in cell cycle length (1). The implanted epiblast is composed of an estimated 120 cells at embryonic day (E5.5) E5.5 that becomes approximately 660 cells at E6.5 and approximately 8,060 cells at E7.5 (2). Shortening of the cell cycle from approximately 11.5 hours at E5.5 to 4.4 hours by E6.5 accommodates this rapid proliferation of cells. The accelerated cell division during gastrulation and attendant genetic events require a host of DNA surveillance systems. Several DNA repair and genome surveillance genes such as Rad1, Rad21 and Bmi1 are expressed during gastrulation and are required for embryonic survival(3). Ectopic or aberrant expression of these regulators may cause accumulation and progression of genome instability through the cell cycle, leading to slowing or full development arrest.

The functional state of chromatin is fundamental to gene expression regulation. Chromatin remodeling factors can modify the balance between an active or repressive chromatin state, acting as key regulators of gene expression. Transcription factors play several important roles in early embryonic development including during self-renewal, proliferation, and differentiation of stem cells(4). However, these genes must function in the context of DNA arrangement in higher order chromatin structure, which is modulated by

chromatin remodeling factors at the highest hierarchical level(5). Elucidating the molecular mechanisms underlying the roles of chromatin remodeling factors is required to dissect molecular pathways governing the biology of stem cells and early developmental processes. The SWI/SNF (isotype-SWItching/Sucrose Non-Fermenting) chromatin remodeling complex has been shown to be critical for development as well as in disease processes (6). The human SWI/SNF complex contains 10-12 subunits and has been grouped into BAF and PBAF subfamilies (7). SWI/SNF, ATP-dependent chromatin remodeling factors play vital roles ensuring appropriate spatial and temporal gene regulation during development (8). BRG1 has a key role in development and transcriptional regulation by remodeling of chromatin structure at the promoters of target genes to direct cell proliferation and differentiation (8-14). The need for BRG1 containing complexes for cell cycle control, apoptosis and cell differentiation in many biological systems has been demonstrated (9, 15-20). Knockout of the BRG1 gene in mice causes pre-implantation lethality, whereas heterozygotes show increased susceptibility to tumors (9, 21, 22). BRG1 function has been shown to regulate transcription of genes in the differentiation of various cell types including myeloid, erythroid, lymphoid, muscle, neural and adipocyte commitment (9, 15-20).

The SWI/SNF-BRG1 complex acts as a global transcriptional regulator and appears to be essential for development. Targeted deletion of SWI/SNF complex subunits hinders function of the SWI/SNF complex during mammalian development resulting in global gene deficiencies; recent studies have used tissue-specific BRG1 or their constituent subunits' ablation using a Cre-loxP system (8, 10-12). Cre-loxP approaches have been used to demonstrate the involvement of SWI/SNF BRG1 complex in the organogenesis and

formation of the mouse heart. Tissue-specific deletion of BRG1 in the endocardium leads to embryonic lethality at E10.5-E11.5 due to impaired ventricular trabeculation during cardiogenesis (11). Recent studies have shown a role for BRG1 in fetal cardiac growth, differentiation and gene expression regulation (8). Additionally, it has been shown that dosage of BRG1 is critical for mouse and zebrafish cardiogenesis (12). These studies highlight role of the BRG1 in heart development. However, the precise role of BRG1 during early post-implantation development remains uncharacterized.

Due to the complex influence of chromatin remodeling factors on specific gene sets of various biological processes during development and cellular differentiation, we are now just beginning to elucidate the role of BRG1 during early post-implantation development. We used a tamoxifen-inducible system in which Cre recombinase ($CreER^{TM}$) inactivates $BRG1^{floxed/floxed}$ beginning at E6.5 in early developing embryo. We found that BRG1 deficiency beginning at E6.5 causes post-implantation growth arrest resulting in embryonic lethality by E9.5. Histology of the BRG1 mutant embryos revealed multiple defects such as lack of normal cardiac structure and disrupted neural tube formation. Further loss of BRG1 caused apoptotic and necrotic cell death despite continued cellular proliferation. In this article we demonstrate BRG1 elimination results in developmental arrest due to massive programmed and necrotic cell death within the embryo in the face of a developmental proliferative program.

Materials and Methods:

BRG1 gastrulation and organogenesis. C57Bl/6J pregnant dams were obtained. Embryonic staging was determined by standard methods setting E0.5 as the morning on which vaginal plugs were found. Embryos were harvested at E5.5, E6.5, E7.5, E8.5, E9.5 and E10.5; extra-embryonic tissue was used for genotyping. Embryos and their placenta were photographed and fixed in 10% neutral-buffered formalin for 24 hours. Embryos were embedded in paraffin, sectioned at 5um, mounted on glass slides and stained with hematoxylin and eosin for histological examination.

Inducible BRG1 knockout mice. Mice harboring the floxed BRG1 allele (B6;128S2-Smarca4^{tm1Pcn}/Mmnc) were a generous gift from Dr. Terry Magnuson (University of North Carolina, Chapel Hill) (24, 25). The floxed BRG1 allele encodes the wild type BRG1 protein but the deleted BRG1 allele does not produce a functional protein. To generate the inducible Cre-BRG1 fl/fl, BRG1 fl/fl mice were bred with ROSA-cre/ERT2 transgenic mice carrying the Cre-ER^{TM} gene driven by the endogenous mouse *Gt(ROSA)26Sor* promoter (B6.129-Gt(ROSA)26Sor$^{tm1(cre/ERT2)Tyj}$/J). To delete the floxed-BRG1 gene in developing embryos, ROSA-cre/ERT2 (B6;129-Gt(ROSA)26Sor$^{tm1(cre/ERT2)Tyj}$/ floxed BRG1 (Smarca4^{tm1Pcn}) pregnant dams were given 100mg/kg body weight pharmaceutical grade tamoxifen citrate (Sigma) IP at 12pm once daily for one day (E6.5, E7.5, E8.5 stages) or two days (E9.5 and E10.5 stages). Embryonic staging was determined by standard methods setting E0.5 as the morning on which vaginal plugs were found. Embryos were harvested at E6.5, E7.5, E8.5, E9.5 and E10.5; extra-embryonic tissue was used for genotyping. Embryos and their placenta were photographed and fixed in 10% neutral-buffered formalin for 24 hours. Embryos were

embedded in paraffin, sectioned at 5um, mounted on glass slides and stained with hematoxylin and eosin for histological examination. For BRG1 genotyping, three primers were used to amplify wild type (241bp PCR product), floxed (387bp PCR product) and deleted (313bp PCR product) BRG1 alleles; P1- GTCATACTTATGTCATAGCC, P2- GCCTTGTCTCAAACTGATAAG, P3- GATCAGCTCATGCCCTAAGG (23). For Cre genotyping, the forward (5'- GCGGTCTGGCAGTAAAAACTATC-3') and the reverse (5'- GTGAAACAGCATTGCTGTCACTT-3') primer were used for PCR amplification (23, 24). All animal husbandry, handling, and experiments were performed in accordance with NIEHS/NIH guidelines covering the humane care and use of laboratory animals in research.

Tamoxifen dose determination. Tamoxifen for the 100 mg/kg dose was dissolved in ethanol to yield a 100 mg/mL stock, which then diluted with corn oil to achieve a 10 mg/mL tamoxifen formulation (10% ethanol in final tamoxifen formulation). The higher 225 mg/kg and 150 mg/kg doses were prepared from correspondingly higher concentrations of ethanol stocks diluted with corn oil to a 10% ethanol concentration. The initial maximum dose level was 225 mg/kg, with a maximum dose volume of 0.45 ml per animal. Toxicity testing was performed in unmated mice, beginning with a tamoxifen IP dose level of 225-mg/kg body weight. To distinguish potential Cre toxicity from possible tamoxifen toxicity, and to establish a lowest observed adverse effects level (LOAEL) and no observed adverse effect level (NOAEL), unmated adult wild type females (without Cre) were dosed intraperitoneally (IP) with 225, 150 and 100 mg/kg of body weight tamoxifen (10 ml/kg dosing volume). Animals received a total of two injections over two consecutive days. Body weights were

collected prior to dosing and weekly for a total of 3 weeks (the length of time needed for a mother to raise a litter). Animals were observed daily for health effects. Mice receiving the 225 and 150 mg/kg dose levels were either found dead or were euthanized as moribund. Mice tolerated the tamoxifen dose level of 100 mg/kg for two consecutive days well with no evidence of tamoxifen toxicity on weight gain or through histopathologic evaluation of heart, liver, lung, kidneys, or spleen.. TAM-induced toxicity was also assessed in embryos carrying Rosa26-Cre-ERT with no observed aberrant developmental phenotype. Tamoxifen toxicity in embryos was assessed by injecting 100 mg/kg of body weight IP at E6.5 and evaluating gross morphological changes in the embryos at E8.5 and E9.5. 100 mg/kg dose of tamoxifen produced no obvious morphological changes.

LacZ staining. To confirm the Cre recombinase activity, we bred the ROSA-cre/ERT2 mice (B6.129-Gt(ROSA)26Sor$^{tm1(cre/ERT2)Tyj}$/J) with ROSA-stop reporter mice (B6.129S4-Gt(ROSA)26Sor^{tm1Sor}/J) and measuring β-galactosidase activity in the double mutant embryos (B6.129S4-Gt(ROSA)26Sor^{tm1Sor}/J Tg(B6.129-Gt(ROSA)26Sor$^{tm1(cre/ERT2)Tyj}$)) as a measure of Cre recombinase activity. X-gal staining to measure β-galactosidase activity (*lacZ* staining) of whole embryos was performed according to a standard protocol (25).

Histologic analysis and TUNEL assay. Timed mating was conducted using Cre/Cre, BRG1 fl/fl and Cre/Cre, BRG1 fl/fl males with BRG1 fl/fl females to obtain Cre/Cre, BRG1 fl/fl and BRG1 fl/fl embryos. The next day females with vaginal plugs were considered to be at embryonic day 0.5 (E0.5) of gestation. Pregnant females were dosed with Tamoxifen

(100mg/kg body weight) and sacrificed at sequential time points of gestation (E6.5, E7.5, E8.5, E9.5, E10.5), and the embryos were dissected free of maternal tissue, examined, photographed, and genotyped by PCR. For histological preparation, embryos without decidua and in decidua were fixed in 4% paraformaldehyde–PBS or 10% neutral-buffered formalin for 18 hours at 4°C, dehydrated, and embedded in paraffin. Paraffin-embedded tissues were sectioned at 5um, mounted on positively-charged glass slides. For analysis of programmed cell death, the sections were stained based on reactivity determined by terminal deoxynucleotidyltransferase-mediated dUTP-biotin nick end labeling (TUNEL) using the Apop Teg *in situ* apoptosis detection kit (Oncor) according to the manufacturer's instructions.

BrdU labeling and Immunohistochemistry. Pregnant females were administered bromodeoxyuridine (BrdU) following administration of tamoxifen. BrdU in sterile PBS was administered by IP injection to pregnant dams at a dose level of 50 mg/kg and a dosing volume of 5 ml/kg, and the uteri were removed at sequential time points of gestation (E6.5, E7.5, E8.5, E9.5, E10.5). Decidual swellings were fixed in 4% paraformaldehyde at 4°C for 18 hours, dehydrated, and embedded in paraffin. Paraffin-embedded tissues were sectioned at 5um, mounted on positively charged glass slides and processed for anti-BrdU labeling (Accurate Chemical and Scientific Corp. # OBT0030) and BRG1 (Santa Cruz #SC-10768) TUNEL (Millipore #S7101), cleaved Caspase-3 (Biocare Medical #CP229A), Ki67 (Dako #M7249), and CyclinD1 (Cell Marque #241R-15) immunohistochemistry (IHC). For BrdU labeling, formalin fixed, paraffin embedded human tissues were deparaffinized and

rehydrated. Heat and acid denaturation was performed by 20 minute incubation in 2N HCl at 37^{o}C followed by 1 minute in boric acid-borate buffer at 20 ^{o}C. Proteolytic antigen retrieval was performed using 0.01% trypsin at 37^{o}C for 3 minutes (Biocare Medical, Concord, CA). Endogenous peroxidase was blocked with 3% hydrogen peroxide. The sections were incubated with 10% normal rabbit serum (Jackson Immunoresearch Laboratories, Inc., West Grove, PA) for 20 minutes, followed by the Avidin-Biotin Blocking Kit (Vector Laboratories, Burlingame, CA). The sections were incubated with primary (Accurate Chemical and Scientific Corp. # OBT0030) antibody and no negative serum for 30 minutes at 1:2000 dilution. Sections were incubated with a rabbit anti-rat secondary antibody (Accurate Chemical and Scientific Corp. # OBT0030) for 30 minutes at 1:500 dilution. Label incubation was performed using Vector R.T.U. Vectastain Kit (Vector Laboratories, Burlingame, CA) for 30 minutes also. Antigen-antibody complex was visualized using DAB (Dako, Carpinteria, CA) for 6 minutes. The sections were counterstained with hematoxylin, dehydrated, cleared in xylene, and coverslipped. For Brg1 IHC, formalin fixed, paraffin embedded human tissues were deparaffinized and rehydrated. Endogenous peroxidase was blocked with 3% hydrogen peroxide. Antigen retrieval was performed with heat and pressure, using Citrate Buffer (Biocare Medical, Concord, CA). The sections were incubated with 10% Normal Donkey Serum (Jackson Immunoresearch Laboratories, Inc., West Grove, PA) for 20 minutes, followed by the Avidin-Biotin Blocking Kit (Vector Laboratories, Burlingame, CA). The sections were incubated with Brg-1 (5HK, Investigator provided, Durham, NC) antibody and no negative serum for 60 minutes at 1:2000 dilution. Sections were incubated with a Donkey anti-Rabbit secondary antibody (Jackson Immunoresearch

Laboratories, Inc., West Grove, PA) for 30 minutes at 1:1000 dilution. Label incubation was performed using Vector R.T.U. Vectastain Kit (Vector Laboratories, Burlingame, CA) for 30 minutes also. Antigen-antibody complex was visualized using DAB (Dako, Carpinteria, CA) for 6 minutes. The sections were counterstained with hematoxylin, dehydrated, cleared in xylene, and coverslipped. For TUNEL IHC, formalin-fixed, paraffin-embedded tissues were sectioned at 4um and treated according to the manufacturer's recommendations contained within the ApopTag Plus Peroxidase In Situ Apoptosis Detection Kit (Cat# S7101, Millipore, Billerica, MA). Staining was visualized using 3-diaminobenzidine (DAB) chromagen (DakoCytomation, Carpenteria, CA) and counterstained with hematoxylin. The slides were dehydrated through graded ethanol, cleared in xylene, and coverslipped. For cleaved Caspase-3 IHC, formalin-fixed, paraffin-embedded tissues were deparaffinized in xylene and rehydrated through graded ethanol. Endogenous peroxidase was blocked using 3% H_2O_2; after which heat-induced epitope retrieval was performed using a 10mM citrate buffer solution, pH 6.0 (Biocare Medical, Concord, CA) in the Decloaker® pressure chamber for 5 minutes at 120C. Non-specific sites were blocked using 10% normal donkey serum (Jackson Immunoresearch, West Grove, PA) for 20 minutes at room temperature. Next, the sections were incubated with avidin/biotin blocking kit (Vector Laboratories, Burlingame, CA). The sections were then incubated with Caspase-3 (Cleaved) rabbit polyclonal antibody (Biocare Medical, Concord, CA, Catalog #CP229A) at a 1:100 dilution for one hour at room temperature. Secondary incubation was done by using a donkey anti-rabbit IgG antibody (Jackson Immunoresearch, West Grove, PA) at a dilution of 1:500 for 30 minutes at room temperature. Further, the sections were incubated with 4+ Streptavidin AP Label (Biocare

Medical, Concord, CA) for 15 minutes at room temperature. The antigen-antibody complex was visualized using Warp Red Chromogen Kit (Biocare Medical, Concord, CA) for 10 minutes at room temperature. The sections were counterstained with hematoxylin, dehydrated through graded ethanol, cleared in xylene, and coverslipped. For CyclinD1 IHC, formalin-fixed, paraffin-embedded tissues were deparaffinized in xylene and rehydrated through graded ethanol. Endogenous peroxidase was blocked with 3% hydrogen peroxide. Antigen retrieval was performed with heat and pressure, using EDTA buffer (Biocare Medical, Concord, CA). The sections were incubated with 10% normal donkey serum (Jackson Immunoresearch Laboratories, Inc., West Grove, PA) for 20 minutes, followed by the avidin-biotin blocking kit (Vector Laboratories, Burlingame, CA). The sections were incubated with CyclinD1 (Catalog # 241R-15, Cell Marque, Rocklin, CA) antibody for 60 minutes at 1:25 dilution. Negative control was not included. Sections were further incubated with a donkey anti-rabbit secondary antibody (Jackson Immunoresearch Laboratories, Inc., West Grove, PA) for 30 minutes at 1:500 dilution. Label incubation was performed using Vector R.T.U. Vectastain kit (Vector Laboratories, Burlingame, CA) for 30 minutes. Antigen-antibody complex was visualized using DAB (Dako, Carpinteria, CA) for 6 minutes. Finally, the sections were counterstained with hematoxylin, dehydrated, cleared and coverslipped.

Microarray Analysis: Hearts minced and frozen in RNALater (Qiagen) at -80 degrees Celsius at necropsy were thawed on ice and homogenized in Trizol (Invitrogen) using a Tissue Tearor Homogenizer (Biospec Products, Inc.). Trizol-isolated RNA was cleaned-up

using the RNeasy Midi kit (Qiagen) and submitted to the Microarray Group of the NIEHS Molecular Genomics Core. Gene expression analysis was conducted using Agilent Whole Mouse Genome 4x44 multiplex format oligo arrays (014868) (Agilent) following the Agilent 1-color microarray-based gene expression analysis protocol. Starting with 500ng of total RNA, Cy3 labeled cRNA was produced according to manufacturer's protocol. For each sample, 1.65ug of Cy3 labeled cRNAs were fragmented and hybridized for 17 hours in a rotating hybridization oven. Slides were washed and then scanned with an Agilent Scanner. Data was obtained using the Agilent Feature Extraction software (v9.5), using the 1-color defaults for all parameters. The Agilent Feature Extraction Software performed error modeling, adjusting for additive and multiplicative noise. The resulting data were processed using OmicSoft Array Studio (Version 6.0) software.

Results:

BRG1 detected in egg cylinder stage and in subsequent organogenesis

In early embryos, expression of BRG1 appeared to be highly expressed in decidua and extra-embryonic and epiblast cells at E5.5, E6.5 and E7.5 followed by the heart, head and trunk at E8.5, E9.5 and E10.5. At E5.5, implantation has occurred and BRG1 positive cells are present uniformly in the extra-embryonic and embryonic ectoderm (Fig. 2.1A). At E6.5 BRG1 staining remains strongly positive in both tissue types (Fig. 2.1B). At E7.5, the exocoelom begins to divide the epiblast and amniotic cavity. BRG1 is localized to the nuclei of cells comprising the ectodermal layers of the chorion, the ectoplacental canal, the early allantoic bud (mesoderm), and cells of the adjacent amniotic ectoderm (Fig. 2.1C). In

addition, all other tissues, including the greater part of the ectoplacental cone and epiblast and primitive streak itself, are entirely positive.

In embryos examined at E8.5, all the tissues of the embryo and placental tissues exhibit strong immunoreactivity for BRG1, including the covering ectoderm, the mesoderm extending into the root of the allantois, and the endodermal epithelium of the hindgut rudiment.

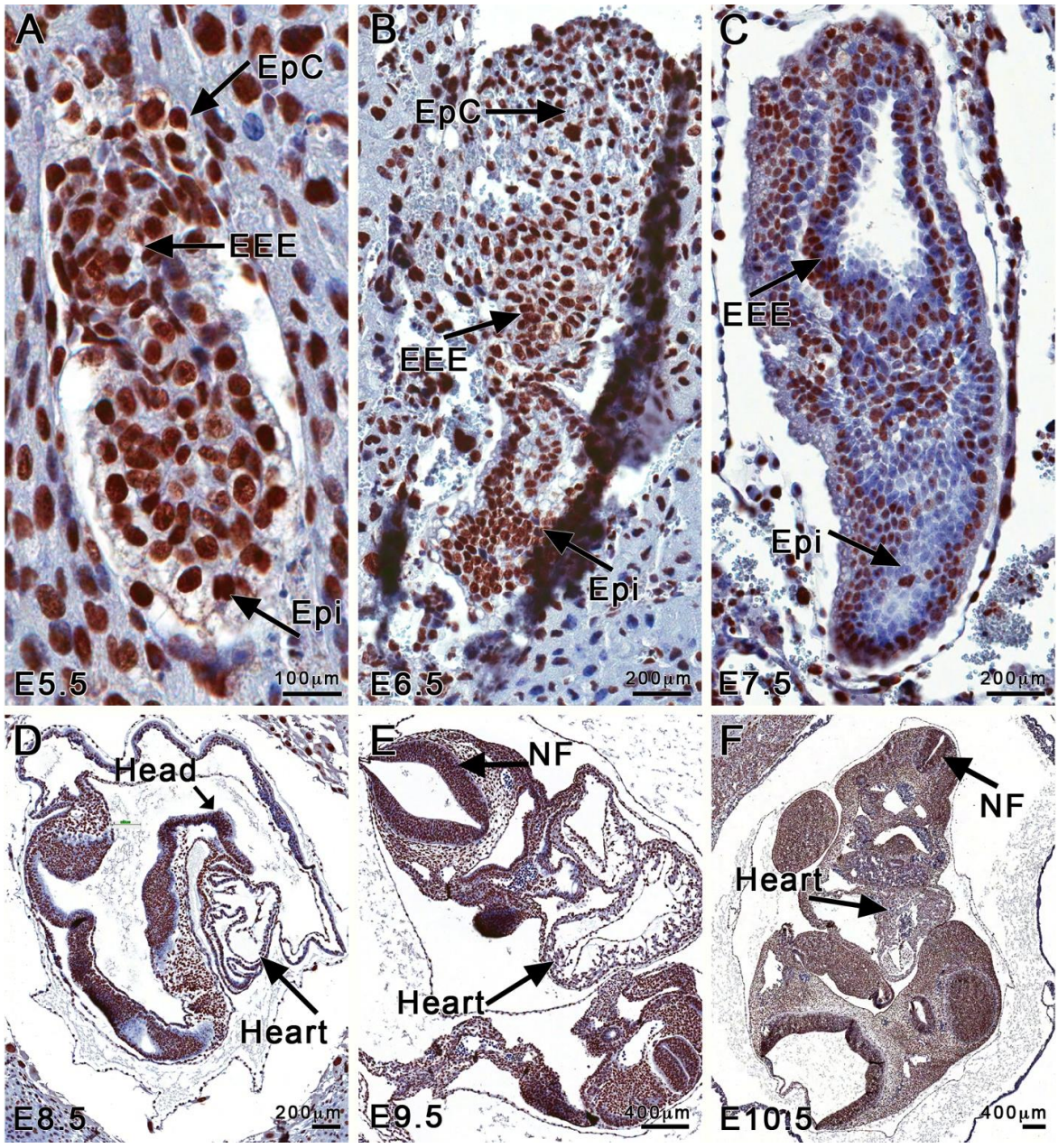

Figure 2.1: Expression of BRG1 during early post-implantation embryonic development in wild-type embryos. Embryos from E5.5 (A), E6.5 (B) and E7.5 (C) show strong BRG1 immunoreactivity in the ectoplacental cone (EpC), extraembryonic ectoderm (EEE) and epiblast (Epi). Embryos from E8.5 (D), E9.5 (E) and E10.5 (F) exhibit strong immunoreactivity in all organs and tissues types visible at these later stages. DAB counterstain.

More anteriorly, immunoreactivity for BRG1 was strongly detected in the neural plate and notochord, optical vesicle, gut, head mesenchyme, future brain, dorsal aorta and somites staining (Fig. 2.1D to F). BRG1 protein was detected in various tissue types of the heart; myocardium, endocardium, epicardium, cardiac cushion, and ventricular trabeculae (Fig. 2.1D to F).

At E9.5 and E10.5, the regressing tail bud is still apparent and all the tissues in this region remain strongly positive. As one passes forward, the neural tube, notochord, and hindgut stain strongly (Fig. 2.1E, F). As in the previous stage, the somites, post-segmental paraxial mesoderm and cardiac structures uniformly stained for BRG1.

At this stage of development, the hemochorial placenta is becoming functional. Strong immunoreactivity for BRG1 is present in the spongy cytotrophoblast lying subjacent to the penetration zone of trophoblastic giant cells, which form the more superficial layer of the fetal placenta (Fig. 2.1). The strong expression of BRG1 required investigation of BRG1 function during perigastrulation development.

ROSA-cre/ERT2 globally excised floxed gene in early development. Toxicity testing was performed in unmated mice, beginning with a tamoxifen IP dose level of 225-mg/kg body weight. To distinguish potential Cre toxicity from possible tamoxifen toxicity, and to establish a lowest observed adverse effects level (LOAEL) and no observed adverse effect level (NOAEL), unmated adult wild type females (without Cre) were dosed intraperitoneally (IP) with 225, 150 and 100 mg/kg of body weight tamoxifen (10 ml/kg dosing volume). Animals received a total of two injections over two consecutive days. Body weights were

collected prior to dosing and weekly for a total of 3 weeks (the length of time needed for a mother to raise a litter). Animals were observed daily for health effects. Mice receiving the 225 and 150 mg/kg dose levels were either found dead or were euthanized as moribund. Mice tolerated the tamoxifen dose level of 100 mg/kg for two consecutive days well with no evidence of tamoxifen toxicity on weight gain or through histopathologic evaluation of heart, liver, lung, kidneys, or spleen.. TAM-induced toxicity was also assessed in embryos carrying Rosa26-Cre-ERT with no observed aberrant developmental phenotype. Therefore, we examined tamoxifen toxicity in embryos by injecting 100 mg/kg of body weight IP at E6.5 and evaluating gross morphological changes in the embryos at E8.5 and E9.5. We found that 100 mg/kg dose of tamoxifen produced no obvious morphological changes. Thus, having determined the LOAEL to be 150 mg/kg, and the NOAEL to be 100mg/kg in this study, we selected 100 mg/kg of body weight tamoxifen as the maximum dose to be used in the study.

Following preliminary toxicity testing to confirm the Cre recombinase activity, we bred the ROSA-cre/ERT2 mice (B6.129-Gt(ROSA)26Sor$^{tm1(cre/ERT2)Tyj}$/J) with ROSA-stop reporter mice (B6.129S4-Gt(ROSA)26Sor^{tm1Sor}/J). Pregnant females were dosed with 100 mg/kg tamoxifen on different embryonic days and fetuses were collected for measuring β-galactosidase activity in the double transgenic embryos (B6.129S4-Gt(ROSA)26Sor^{tm1Sor}/J Tg(B6.129-Gt(ROSA)26Sor$^{tm1(cre/ERT2)Tyj}$) as a measure of Cre recombinase activity. ROSA-cre/ERT2 x ROSA-stop double transgenic embryos exhibited ubiquitous strong positive *lacZ* staining while their ROSA-stop embryo littermates showed negative staining at indicated developmental stages (Fig. 2.2A, B, C, D). Based on these results, we decided to inject 100-mg/kg body weight of tamoxifen into pregnant females to induce cre-mediated excision of

the floxed BRG1 gene.

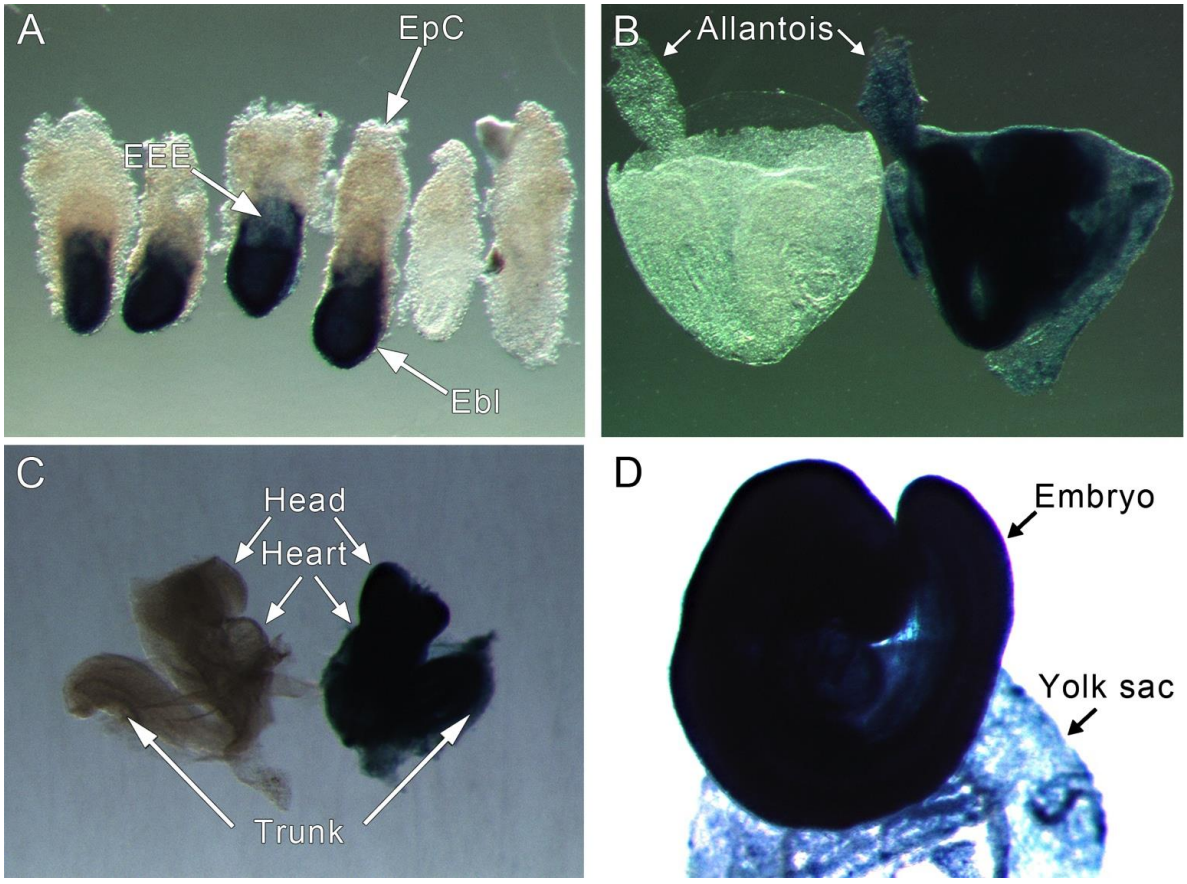

Figure 2.2: Cre activity of ROSA-cre/ERT2. *LacZ* staining of ROSA-stop and ROSA-cre/ERT2 ROSA-stop embryos from a tamoxifen-treated pregnant female at E7.5 (A), E8.5 (B, C) and E9.5 (D). ROSA-cre/ERT2 ROSA-stop stain strongly positive (indigo staining, A-D); ROSA-stop embryos lack staining (44). ROSA-cre/ERT2 ROSA-stop embryos from E7.5 (A), E8.5 (B) and E9.5 shows Cre-ER expression in almost all tissues including extraembryonic ectoderm, epiblast, allantois, and yolk sac.

Tamoxifen induced ROSA-cre/ERT2 excised BRG1 floxed sequence.

We generated tamoxifen inducible Cre-BRG1 fl/fl mice (B6;129-Gt(ROSA)26Sor$^{tm1(cre/ERT2)Tyj}$/J Smarca4^{tm1Pcn}) and crossed them with BRG1-fl/fl female

mice. The cross yielded Cre-BRG1-fl/fl progeny at the expected Mendelian frequency of 50%. Based on the ROSA-cre/ERT2 x ROSA-stop result, tamoxifen treatment was predicted to produce ubiquitously distributed BRG1-inactivated ($BRG1^{d/d}$) cells in the Cre-BRG1 fl/fl embryos. In order to inactivate BRG1 during early development, we injected tamoxifen at a dose of 100mg/kg of body weight into pregnant females at E6.5 and embryos were collected at E7.5 - E9.5. All the $BRG1^{d/d}$ embryos were dying at E9.5, while their littermate controls showed normal development. Embryos in which BRG1 was inactivated were smaller than their littermates and appeared to be more pale. However, all $BRG1^{d/d}$ embryos were alive at E7.5-E8.5, and the litter sizes were normal. The efficient ablation of BRG1 in the whole embryo was confirmed by genotyping of the embryonic tissues. For BRG1 genotyping, three primers were used to amplify wild type (241bp PCR product), floxed sequence (387bp PCR product) and deleted (313bp PCR product) BRG1 alleles (23, 24) (Fig. 2.3A). For Cre genotyping primer sets produced a 102bp PCR product (Fig. 2.3). In agreement with these genotyping PCR results, BRG1 mRNA level was significantly decreased and BRG1 protein was barely detected by immunohistochemistry in E9.5 Cre-Brg1 fl/fl whole embryo (Fig. 2.3B, D). In contrast, BRG1 protein was readily detected in BRG1 fl/fl littermate (Fig. 2.3C). These data demonstrated the successful creation of a BRG1 conditional mouse model to ubiquitously delete BRG1 temporally in early development.

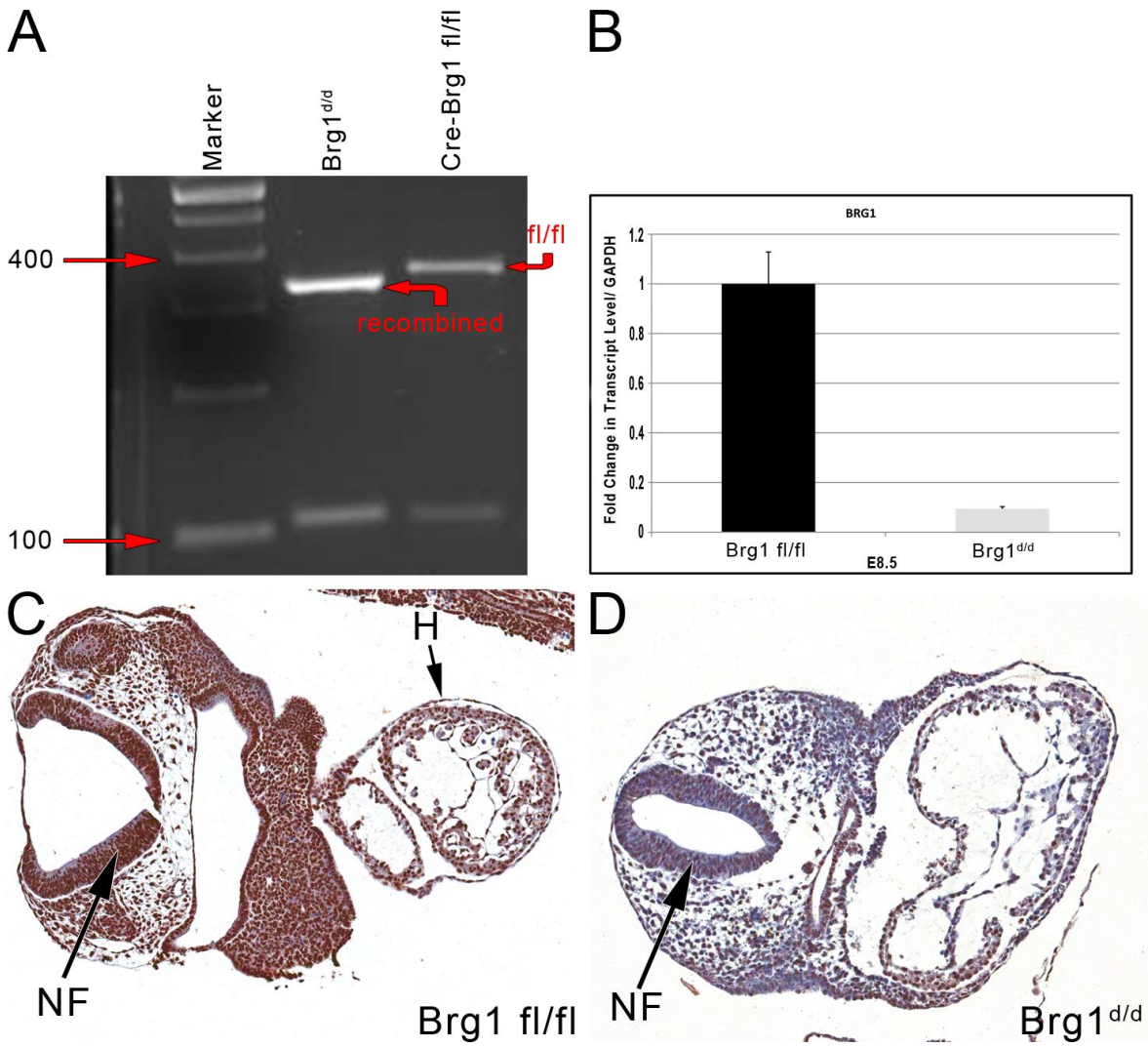

Figure 2.3: Deletion of BRG1 in BRG1$^{d/d}$ embryos. (A) Genomic PCR of floxed BRG1 (387bp), floxed-out BRG1 (313bp) and Cre (100bp). (B) qPCR of significant downregulation of BRG1 mRNA BRG1$^{d/d}$ versus BRG1 fl/fl embryos. (C to D) BRG1 fl/fl embryo demonstrates strong immunostaining for BRG1 (C) while BRG1$^{d/d}$ demonstrates markedly reduced immunostaining (D) embryos. DAB counterstain.

Lack of BRG1 results in developmental arrest, retarded growth, and subsequent death during early gestation. Pregnant dams were dosed at E6.5 and embryos were collected at E7.5, E8.5 and E9.5 for analysis. The genotypes of the dissected embryos were determined

by performing PCR of genomic DNA obtained from the yolk sacs of each embryo. BRG1$^{d/d}$ embryos were detected from E7.5 to E9.5. Even at E7.5, BRG1$^{d/d}$ embryos were slightly smaller than wild types (not shown). This retardation was more obvious by E8.5 and E9.5 (Fig. 2.4A to G), and an increased number of resorbed and empty conceptuses were observed. E8.5 BRG1$^{d/d}$ embryos had 2 to 6 somites and were approximately two-thirds of the size of their wild-type littermates, which had 8 to 12 somites (Fig. 2.4C to E).

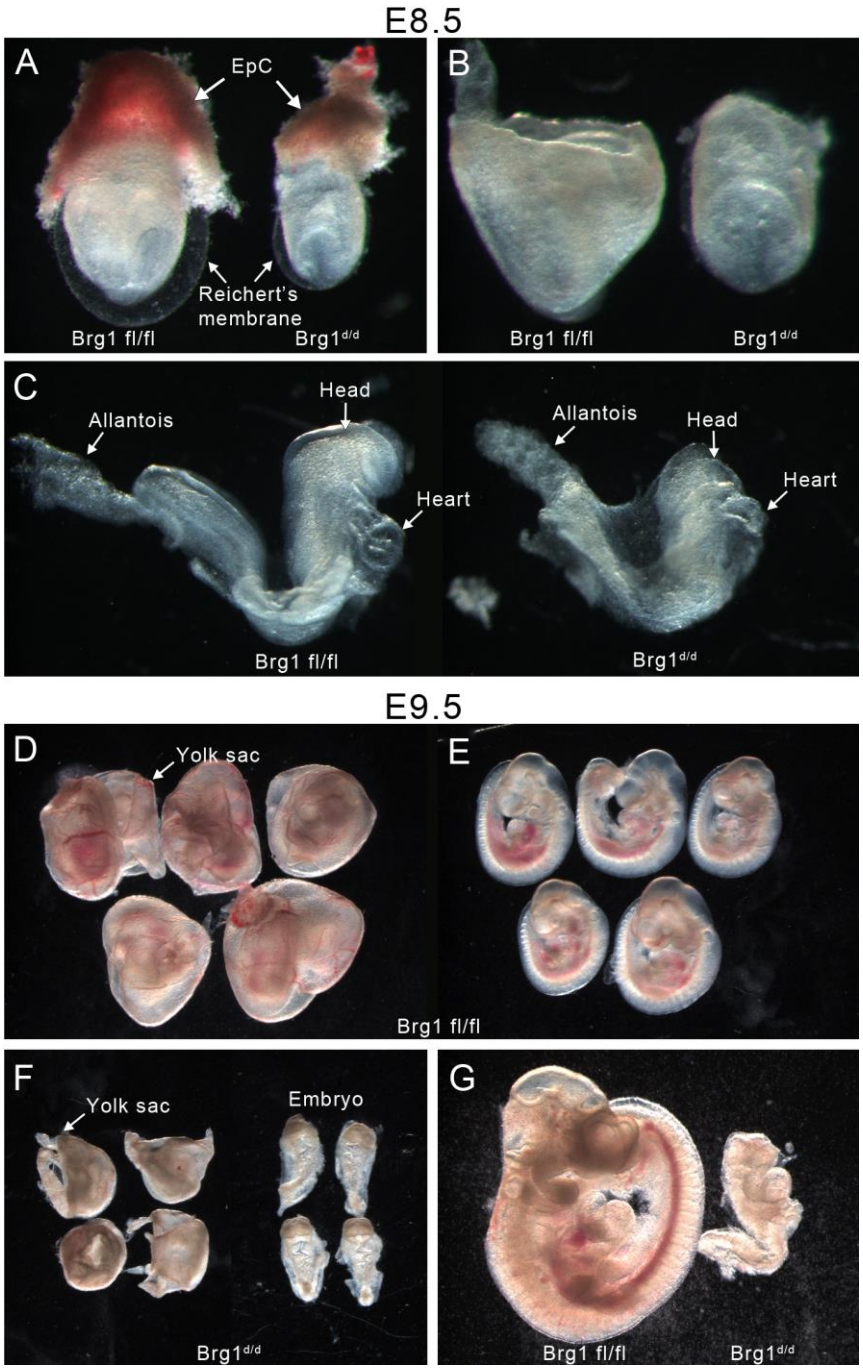

Figure 2.4: BRG1 mutant embryos reveal growth retardation. Substantial growth retardation of BRG1$^{d/d}$ embryos compared to Cre-BRG1 fl/fl embryos from the same litter at E8.5 (A through C). Anatomic structures (EpC, ectoplacental cone; Reichert's membrane, head, heart, allantois) are present in all embryos. E9.5 embryos demonstrate further retardation (D through G).

All BRG1$^{d/d}$ embryos exhibited severe developmental defects and were dying by E9.5. Surviving BRG1 mutant embryos at E8.5 and E9.5 could be easily distinguished from their littermates by their much smaller size, pale color, enlarged pericardium, and incomplete process of turning. The most severely affected embryos were approximately one third the size of normal E9.5 embryos, were undergoing resorption, and also exhibited rotational defects and developmental growth arrest (Fig. 2.4C; right image, F and G). Mutant embryos could not be isolated at E10.5, likely due to advanced resorption. A summary of morphologic observations is present in Table 2.1.

Table 2.1: Brg1 deletion effect		
Stage	BRG1d/d	BRG1 fl/fl
E8.5	Normal (10/28)	Normal (24/24)
E8.5	Small/abnormal (18/28)	-
E9.5	abnormal/dead (23/23)	normal (31/31)

Histologic sections of *BRG1*$^{fl/fl}$ embryos exhibited normal embryonic structures, including heart and neural fold formation (Fig. 2.5A, C, E). In contrast, histologic sections of E9.5 BRG1$^{d/d}$ embryo revealed several developmental defects including disrupted neural tube and cardiac formations (Fig. 2.5B, D, F). Histologic sections revealed that E8.5 and E9.5 BRG1$^{d/d}$ embryos contained apoptotic and oncotic necrotic lesions. Despite these defects, all the BRG1$^{d/d}$ embryos maintained yolk sacs. The severity of BRG1 mutant phenotype at E9.5 was consistent with our inability to recover these embryos at later stages and suggest that lethality occurs during E9 and E10. As BRG1 is expressed broadly in the embryo, these

results confirm BRG1 plays a critical role in early mammalian embryonic development.

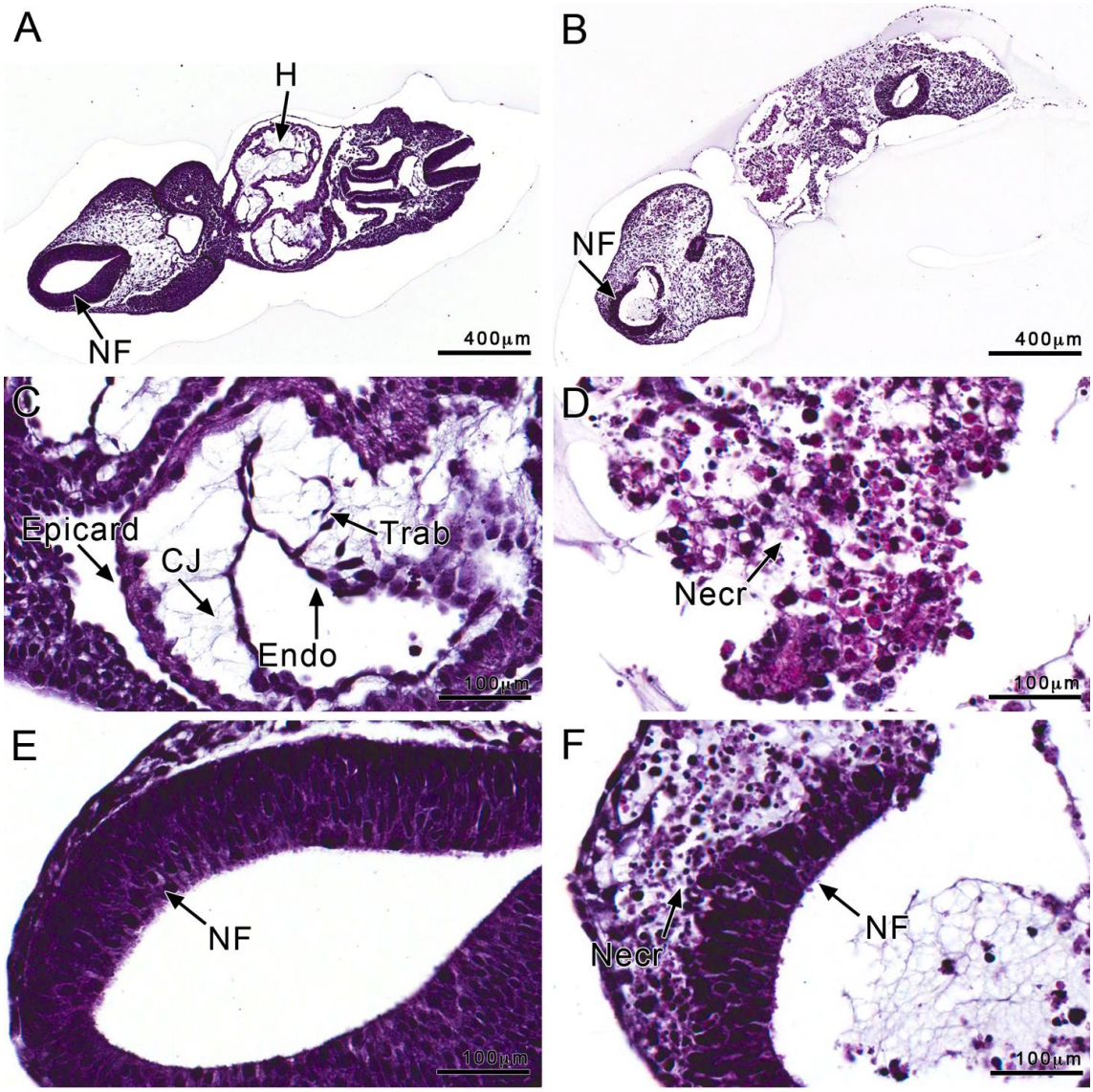

Figure 2.5: Histologic analysis of Cre-BRG1 fl/fl and BRG1$^{d/d}$ embryos at E9.5. Frontal section of Cre-BRG1 fl/fl (A) shows normal embryo morphology, including neural fold (NF) and developing heart (H). Frontal section of BRG1$^{d/d}$ embryo (B) shows abnormal histomorphology, neural fold deformity (NF), and lack of normal cardiac structures. Higher magnification of Cre-BRG1 fl/fl in (A) reveals normal cardiac structures (C) and normal neural fold formation (E). Higher magnification of BRG1$^{d/d}$ in (B) reveals necrotic cardiac (D) and neural fold (F) histomorphology.

Increased apoptotic cell death in BRG1$^{d/d}$ embryos. Gross morphologic analysis revealed defects consistent with insufficient cellular proliferation, increased apoptosis, necrosis, or a combination thereof. To determine whether the frequent pyknosis and growth failure of BRG1 mutant embryos were associated with increased programmed cell death, we analyzed TUNEL immunoreactivity of sagittal sections of E9.5 BRG1$^{d/d}$ and BRG1 fl/fl embryos. As programmed cell death naturally occurs during early development (27), TUNEL-positive cells were expected in sections of BRG1 fl/fl embryos. In these embryos, TUNEL staining was mostly observed in inner ear epithelium and gut (Fig. 2.6A, C). In contrast, TUNEL staining is widely distributed throughout BRG1$^{d/d}$ embryo bodies including neural fold, head mesenchyme, and heart (Fig. 2.6B, D), suggesting that the increases in cell death were correlated with the deletion of BRG1, and resultant embryonic mortality.

To confirm the apoptotic phenotype of BRG1$^{d/d}$ embryos, we analyzed another apoptosis marker, cleaved caspase-3. Cleaved caspase-3 immunostaining was detectable in the sections of Brg1 fl/fl embryos (Fig. 2.6E, G). However, cleaved caspase-3 immunoreactivity was greater in the number of cells with positively-staining nuclei in the sections of BRG1$^{d/d}$ embryos, particularly in the regions of the head mesenchyme, heart, gut and neural fold (Fig. 2.6F, H) consistent with the massive cell death observed in these tissues. Change in the expression of DNA damage response proteins suggests that loss of BRG1 chromatin remodeling function may cause genomic instability leading to cell death, which retards growth and ultimately causes embryonic death.

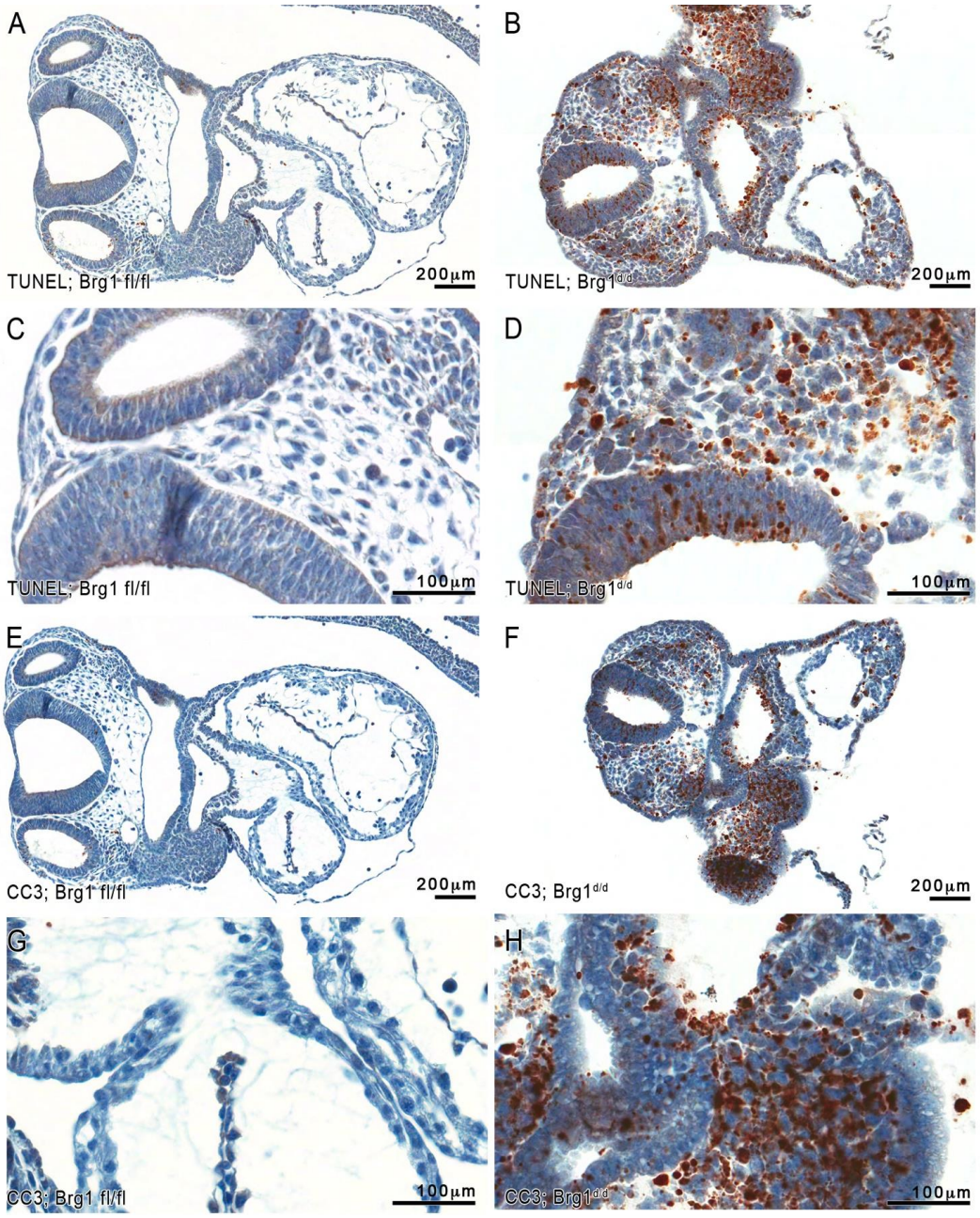

Figure 2.6: Cell death marker immunohistochemistry of Cre-BRG1 fl/fl and BRG1$^{d/d}$ embryos at E9.5. TUNEL immunolabeling is infrequent in Cre-BRG1 fl/fl embryos (A, higher magnification in C). TUNEL immunolabeling widespread in BRG1$^{d/d}$ embryo (B); higher magnification demonstrates strong nuclear and necrotic cell staining (D). Cleaved caspase-3 (CC3) immunostaining present in both Cre-BRG1 fl/fl (E) and BRG1$^{d/d}$ (F) embryos; however higher magnification of (E) and (F) reveals stronger and more widespread immunopositivity of CC3 in BRG1$^{d/d}$ (H) than Cre-BRG1 fl/fl (G) embryos.

Decreased cell proliferation rates in BRG1$^{d/d}$ mutant mice. A second possibility to explain the developmental arrest and reduced embryonic growth of the BRG1$^{d/d}$ embryos could be an alteration in cellular proliferation due to changes in cell cycle progression, or decreased self-renewal. Therefore we analyzed the expression of several proliferation markers using histologic sections of the BRG1$^{d/d}$ and Brg1 fl/fl embryos. Cyclin D1 (CCND1) is part of the core cell cycle machinery, and is frequently over-expressed in human cancers (28, 29). CCND1 functions as a regulatory protein for the G1-S cell cycle phase transition, and for transcriptional control of mammalian cells in the regulation of proliferation and differentiation. We observed a striking difference in the Cyclin D1 (CCND1) staining in BRG1 fl/fl versus BRG1$^{d/d}$ embryos. CCND1 immunostaining was observed in the neural fold and head mesenchyme of the BRG1 fl/fl embryo sections (Fig. 2.7A, C). In contrast, CCND1 staining was greatly reduced in BRG1$^{d/d}$ embryo sections (Fig. 2.7B, D). Tissue homeostasis is needed to maintain the proper balance of proliferation and differentiation in normal tissues, but can be altered in premalignant and malignant conditions. Deregulated CCND1 promotes genetic instability *in vitro* and tumorigenesis *in vivo* (30-32). CCND1 gene alteration and/or protein deregulation has been widely observed in human malignant and premalignant tissues. Thus, deregulation of CCND1 in BRG1$^{d/d}$ embryos might promote genetic instability and developmental arrest.

To examine further the cellular proliferation rate in BRG1$^{d/d}$ embryos, we evaluated the expression of the nuclear antigen Ki67, which detects the nuclei of all proliferating cells. Immunohistochemical analysis showed punctate and diffused Ki67 staining in BRG1$^{d/d}$ embryos sections (Fig. 2.7E, G), which was strikingly different from that in the BRG1 fl/fl

littermate sections (Fig. 2.7F, H). These observations strongly suggest that at this early stage of development BRG1 function is required for proper cell proliferation and survival.

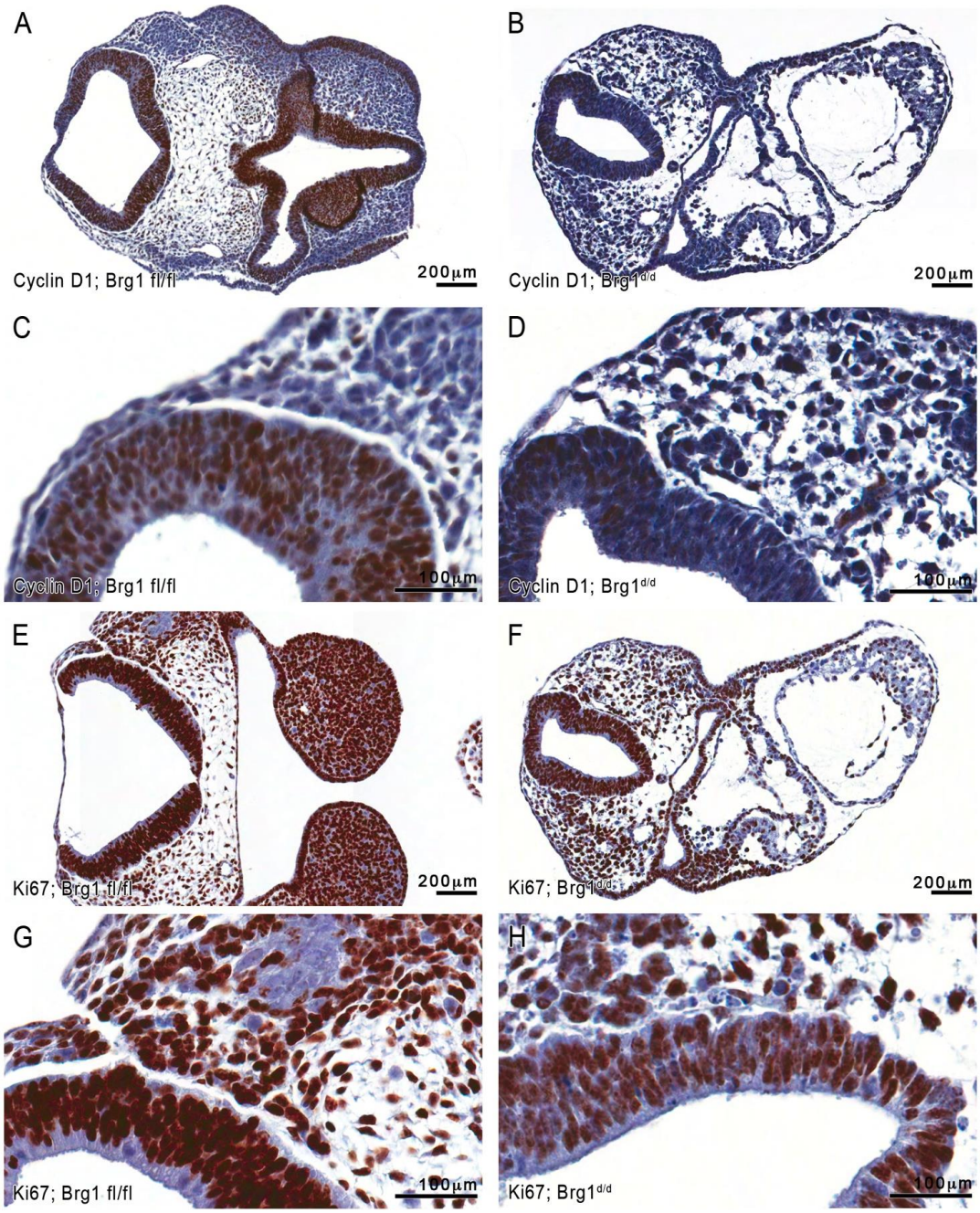

Figure 2.7: Proliferation marker immunohistochemistry of Cre-BRG1 fl/fl and BRG1$^{d/d}$ embryos at E9.5. Cyclin D1 (CCND1) immunolabeling is frequent in Cre-BRG1 fl/fl embryos (A, higher magnification in C). CCND1 immunolabeling less widespread and weaker in BRG1$^{d/d}$ embryo (B); higher magnification demonstrates substantially less immunolabeling (D). Ki67 immunostaining present in both Cre-BRG1 fl/fl (E) and BRG1$^{d/d}$ (F) embryos; however higher magnification of (E) and (F) reveal stronger and more widespread immunopositivity of Ki67 in Cre-BRG1 fl/fl (G) than BRG1$^{d/d}$ (H) embryos.

Finally, we examined vascular structures in the BRG1$^{d/d}$ versus BRG1 fl/fl embryos. Hematopoiesis is required for embryonic growth and survival (33). Hematopoiesis in the mouse embryo first occurs in the extraembryonic yolk sac; this yolk sac subsequently fuses with the embryonic vasculature becoming the primary source of embryonic red blood cells. Mesodermal cells of the yolk sac proliferate and differentiate into blood islands. Anastomosing networks of blood islands produce nucleated red blood cells. BRG1$^{d/d}$ embryos, though smaller than Cre-BRG1 fl/fl embryos, had all hallmarks of early yolk sac development, including blood islands (Fig. 2.4A). We examined whether platelet-endothelial cell adhesion marker (PECAM, CD31) expression, a marker of mesoderm-derived endothelial cells, was altered in BRG1$^{d/d}$ versus Cre-BRG1 fl/fl embryos (Figs. 2.8A-D). Strong immunopositivity is detected in multiple vessels of both BRG1$^{d/d}$ and Cre-BRG1 fl/fl embryos. Additionally, no irregularities are observed in the structure and continuum of endothelium in the BRG1$^{d/d}$ embryos. These data suggest the gross differences in vascularization of the embryos (Fig. 2.4) may not be due to intrinsic ability of endothelial cells to organize and form vascular channels (Fig. 2.8A-D), but to a lack of proliferation of functional vascular progenitor cells and/or stability of said vascular progenitor cells' genomes.

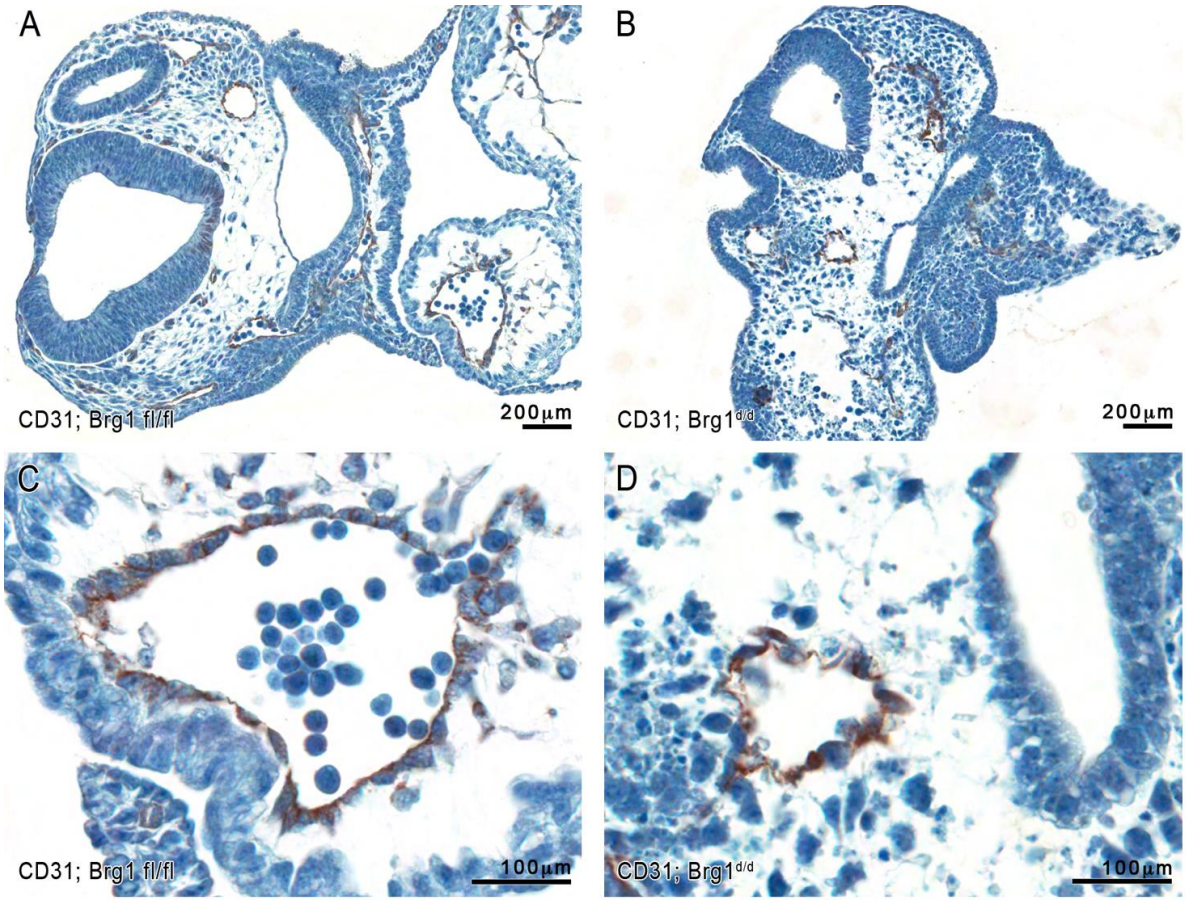

Figure 2.8: Vascular endothelial immunohistochemistry of Cre-BRG1 fl/fl and BRG1$^{d/d}$ embryos at E9.5. Platelet-endothelial cell adhesion marker (PECAM, CD31) immunostaining reveals comparable intensity and integrity of vascular structure immunolabeling between Cre-BRG1 fl/fl and BRG1$^{d/d}$ embryos.

Identification of genes regulated by BRG1 in early development. To gain molecular insight in early developmental growth arrest in BRG1 mutant embryos we performed global gene expression analysis. From comparative microarray analyses of mRNA from untreated and tamoxifen-treated Cre-BRG1 fl/fl E8.5 mice, statistical analysis identified 4,819 probes as differentially expressed genes (DEGs) between the treated and untreated E8.5 mice, which were not significantly differentially expressed or clustered at E7.5 (Fig 2.9).

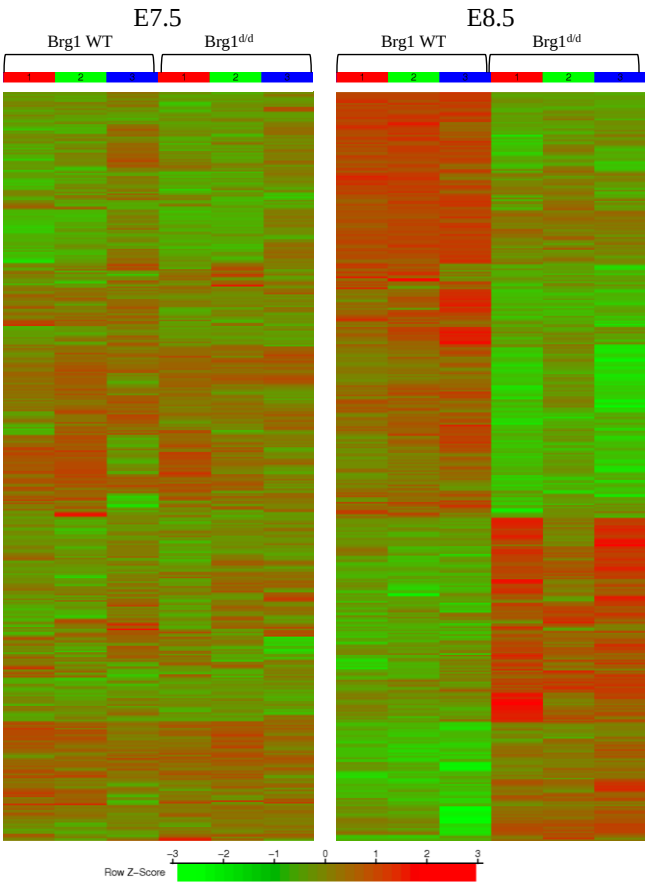

Figure 2.9: **Gene expression profile in BRG1 mutants.** Induced genes are indicated in shades of red, and repressed genes are indicated in shades of green (A). DEG clusters unapparent at E7.5; prominent clustering at E8.5.

As expected, BRG1 was significantly downregulated in treated ($BRG1^{d/d}$) embryos. To further evaluate DEGs, we used abs (fold change) >=2 and nominal p-value <= 0.05 to define DEGs. We found 476 DEGs, of which 206 genes were upregulated and 269 genes were down-regulated. Additional pathway analysis of up-regulated genes revealed networks associated with cell cycle regulation, cell death and survival, cell-to-cell signaling, cellular, tissue, and embryonic development. In contrast, top networks of down-regulated genes are associated with DNA replication, recombination and repair, developmental disorder, and

cardiovascular system development. This further supports that BRG1 is a critical molecule of molecular pathways control genomic stability and developmental processes and confirms the temporal BRG1 deletion event.

BRG1 deletion altered senescence responsive genes. To explore the molecular basis of the BRG1 ablated embryo phenotype we performed ingenuity pathways analysis of DEGs in BRG1 E8.5 mutant embryos. We found that several genes associated with cell cycle regulation, proliferation, apoptosis, and cell adhesion were misregulated in $BRG1^{d/d}$ embryos and associated with top functional networks (Fig. 2.10).

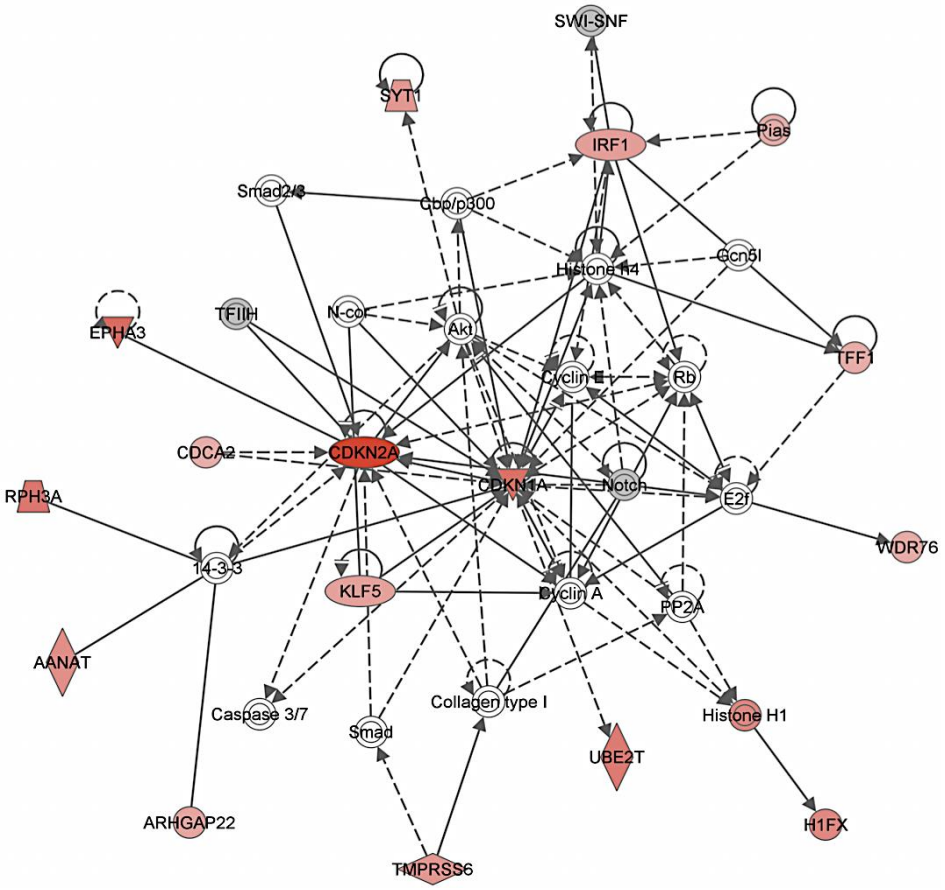

Figure 2.10: Pathway analysis in E8.5 Brg1 mutants. Induced genes are indicated in shades of red. Functional networks correlated with BRG1 ("SWI-SNF").

The p53 pathway is a key regulator of cell cycle arrest and apoptosis, which was the most upregulated pathway in BRG1 mutants (Fig 2.11). This result suggests that the phenotype of BRG1$^{d/d}$ early embryos may be due to altered expression of senescence response pathway genes, which trigger BRG1-related biological effects.

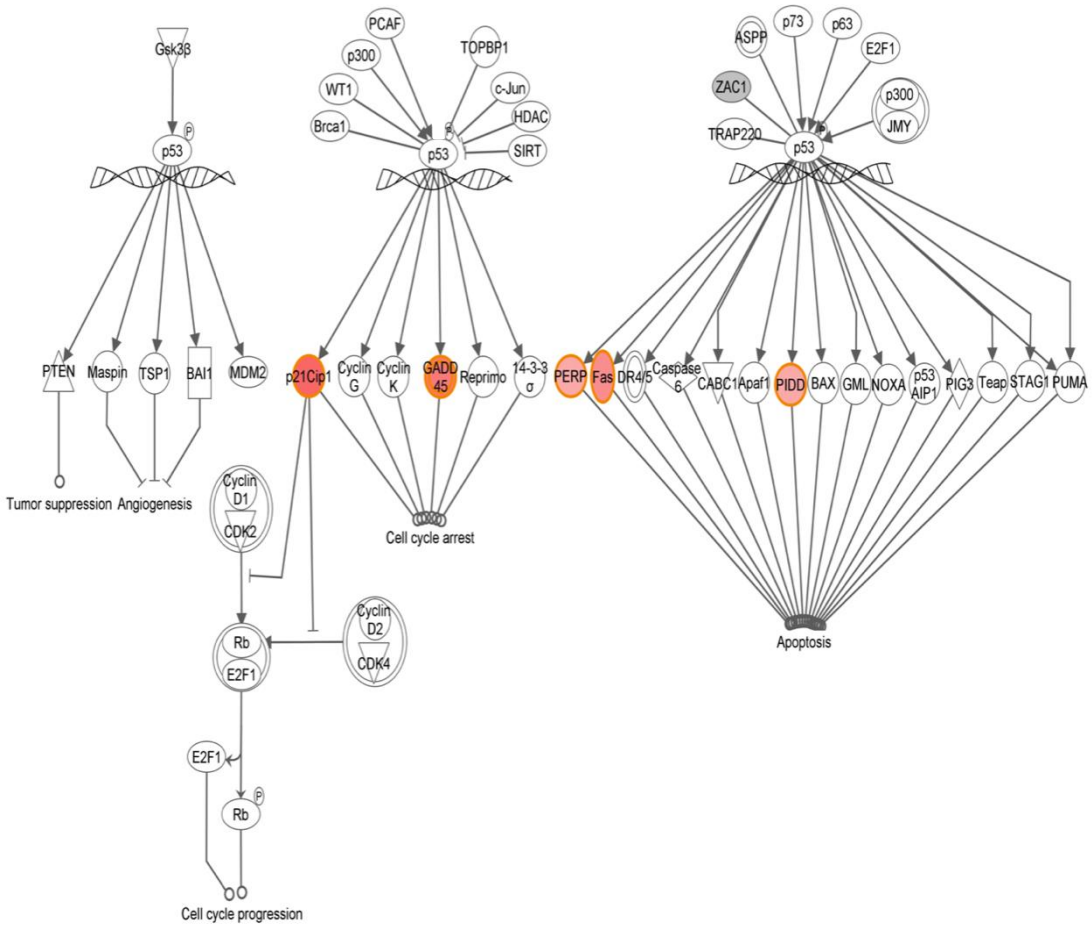

Figure 2.11: Pathway analysis in E8.5 Brg1 mutants. Individual genes within cell arrest or death pathways, particularly those enriched for p53, are upregulated.

While cellular senescence is induced by a wide variety of condition, we chose to analyze the genes required for cell adhesion, cytoskeleton, the DNA damage response, cell cycle regulation, apoptosis and those that contribute to the senescence response pathway, specifically, TP53 (+2.01), Cdkn1a (+4.04), Gadd45b (+3.2), Pidd (+2.01), Perp (+2.01), Fas (+2.9), Cdkn2a (+5.6), Clo1a1 (-3.45), Rad51 (+2), Rad18 (-1.8), Chek2 (+2.4), Cdk17 (+2.3), Cdkn2b (+8.7), and Cdk20 (+3) that have shown to be significantly altered in

BRG1$^{d/d}$ embryos by microarray analysis. A complementary quantitative RT-PCR was used to validate expression of the senescence responsive genes in BRG1$^{d/d}$ vs. Cre-BRG1 fl/fl embryos. The expression of p53, Cdkn1a, Cdk20, Cdkn2b, Chek2, Rad1, Gadd45b, Pidd, Perp, and Fas were elevated while Rad21, and Col1a1 is attenuated in BRG1$^{d/d}$ embryos compared to Cre-BRG1 fl/fl embryos (Fig. 2.12). These results further suggest that the phenotype of E9.5 BRG1$^{d/d}$ embryos is due to altered expression of senescence response pathway genes leading to developmental growth arrest.

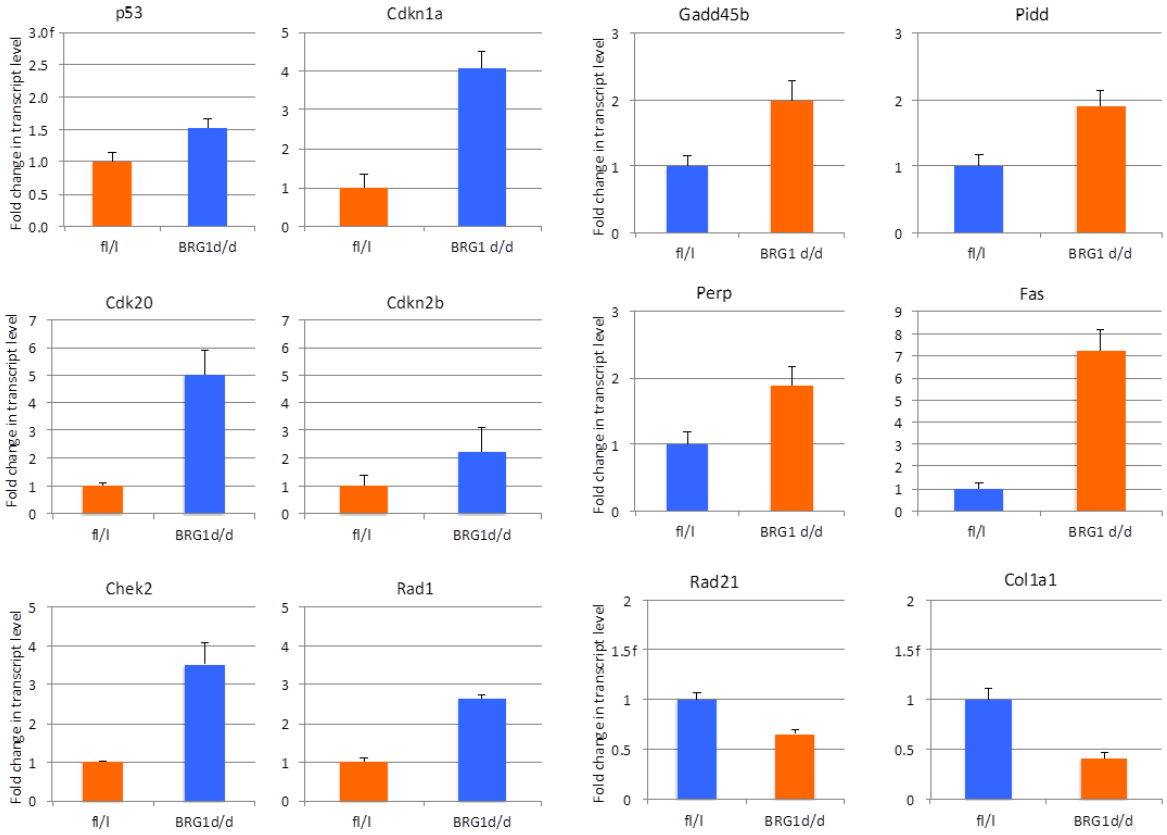

Figure 2.12: **Quantitative PCR analysis of mRNA expression of the indicated genes in Cre-BRG1 fl/fl and BRG1$^{d/d}$ embryos at E8.5.** mRNA levels normalized to GAPDH; data expressed as mean ± SD.

Discussion:

In this study we have used the cre-lox inducible gene knockout system to demonstrate BRG1 is required for early post-implantation development, particularly for normal cell cycle progression and proliferation during the perigastrulation period. BRG1 elimination during gastrulation (E6.5) results in developmental growth arrest and embryonic mortality by E9.5. BRG1 mutant embryos exhibit several gross morphological defects and are smaller in size compared to control littermates. Histologic analysis of *BRG1*$^{d/d}$ embryos revealed a variety of anatomical abnormalities. Subsequent quantitative rt-PCR and immunohistochemistry revealed changes in expression patterns of several genes related to proliferation and apoptosis, both critical processes in development.

BRG1 is expressed uniformly throughout the whole embryo and in extra-embryonic tissues. This suggests that BRG1 is globally required during development. It has been demonstrated that complete germline deletion of BRG1 results preimplantation lethality (9). Blastocysts progressing to the stage displaying inner cell mass (ICM) and trophoectoderm (TE) do not survive in vitro under conditions of BRG1 deletion (9). Cre-loxP approaches have shown the involvement of the BRG1 complex and its subunits in organogenesis and heart formation during mouse development (8, 10, 11, 34, 35). However, early embryonic mortality due to germ line deletion of BRG1 hindered the analysis of global gene function at later developmental time points. This study sought to bridge this gap by analyzing BRG1 expression and loss of function in the later perigastrulation developmental period. We have recently demonstrated quantitative mRNA expression levels of BRG1 in the early post-implantation embryos and in the heart, head and trunk of the E8.5, 9.5 and 10.5 embryos,

demonstrating uniform levels in early embryos; levels are higher in the embryonic head and trunk compared to the heart in early organogenesis (data not shown). Consistent with mRNA expression patterns, here BRG1 protein expression patterns are evenly distributed in the whole embryo and extraembryonic tissues. The previously described early embryonic death was overcome by utilizing the tamoxifen inducible *Cre*-loxP system to globally ablate BRG1 function beyond preimplantation development. The inducible system allowed us to elucidate novel BRG1-null associated effects in early post-implantation development, including several defects and retarded growth resulting in complete developmental arrest by E9.5.

The data included herein suggest several pathways for the observed developmental arrest at E9.5. The epiblast of the $BRG1^{d/d}$ embryos develops normally and the formation of three germ layers proceeded through gastrulation. However, postgastrulation $BRG1^{d/d}$ embryos were smaller in size and there was a decrease of cell proliferation and cell viability. Deletion of BRG1 does not affect survival or proliferation of fibroblast cells (9), suggesting that BRG1 plays a more complex role than that of a simple, general cell viability factor. BRG1 mutants display increased cell death in the embryonic tissue. Cellular proliferation rates are not compensatory and consequently, embryos are growth retarded. At their most advanced state, early organogenesis stage BRG1 mutant are morphologically anomalous and degenerating. Despite the growth deficiency and abnormal level of programmed cell death at E8.5, BRG1 mutants proceeded to improper organogenesis. Attachment of the allantois to the chorion was observed and extraembryonic mesoderm structures, including proamniotic fold, chorion and allantois, develop. However, the observed development of these tissues was suboptimal grossly.

The extra-embryonic tissue and endoderm serve a number of functions critical for the proper development of the conceptus. They play roles in embryonic patterning (36, 37) and supplying nutrients to the embryonic tissue by synthesizing serum components and endocytosing maternal macromolecules that have passed through Reichert's membrane into the parietal yolk sac cavity (38). Adjacent the extraembryonic ectoderm, polarization of the columnar visceral endoderm cells allows the activity of the many lysosomes and microvilli at the cells' apices. The anomalies observed in the extraembryonic and visceral endoderm of the BRG1 mutants suggest a requirement of BRG1 in extraembryonic tissue and visceral endoderm differentiation and function. Defects in extraembryonic tissue and visceral endoderm of the BRG1 mutants may interrupt the nutritional link between the visceral endoderm and the adjacent ectoderm, resulting in proliferation defects in the embryonic ectoderm. The combination of ectodermal cell death and histological defects in visceral endoderm at gastrulation stages previously have been reported in various mouse mutants including the *huntingtin*, *hnf4* and *Zfr* mutants (2, 39, 40). Inactivation of BRG1 results in several embryonic histological defects suggests that BRG1 absolutely required for embryonic growth and survival. The combination of defects in the neural fold and heart highlight the broader function of BRG1 in differentiation of various cell types consistent with the previous reports showing BRG1 is required for vertebrate neurogenesis and heart formation (41) (8). BRG1 protein is highly expressed and ubiquitously distributed in extra embryonic and embryonic tissue, suggesting BRG1's involvement in embryonic growth and development (34). The increased cell death and proliferation defects may be responsible for the developmental course seen in BRG1 mutants. The developmental arrest shown by BRG1

mutant embryos may be eventuated by the abnormal cell proliferation and DNA damage, and subsequent enhanced apoptotic cell death detected in gene expression assay. Data from the TUNEL assay showed that BRG1 deletion was associated with programmed cell death. These data suggest that apoptosis induced by lost expression of BRG1 may have been triggered by activation of the p53 pathway, which overcomes the anti-apoptotic action of Rb. Investigation of global gene expression analysis by microarrays identified several genes involved in cell cycle control and DNA surveillance, *p21* (+4.04) and *TP53* (+2.01), whose expression significantly changed in BRG1 mutants (Fig 2.12). Growth arrest is likely associated with increased expression of p53 and Rb, known effectors of Brg1 biological activity. Additionally, genes related to p53 and Rb pathways such as Rb2/p130 and the CDK inhibitors p21cip and p27kip1, play a role in cell cycle arrest (42). Complementing microarray analysis, quantitative RT-PCR showed many genes misregulated in BRG1 mutants, suggesting the BRG1 mutant phenotype is the result of disruption in the transcriptional network regulating genomic integrity during development. Corroborating changes in RNA expression, immunohistochemistry of marker genes of apoptosis, and DNA damage and proliferation showed different patterns of expression. Numerous roles for ATP-dependent chromatin remodeling complexes in almost every cellular differentiation event have been reported (15). Thus, homogeneous expression of the BRG1 in early development suggests that BRG1 is essential for multicellular differentiation and likely regulates genes of varying molecular pathways.

Cardiovascular circulation is critically required for embryonic growth, which is initially formed in *BRG1*$^{d/d}$ embryos but aberrant in later development. Although

vasculogenesis occurred, we observed cardiovascular defects in *BRG1*$^{d/d}$ embryos. The exponential embryonic growth requires continuous nutritional supply from mother to fetus through circulation. Vascular abnormalities were observed in BRG1 mutants, which were followed by embryonic mortality (34). Normal PECAM staining of individual vessel in *BRG1*$^{d/d}$ embryos suggests normal formation of vessels initially, however, the decreased number in the embryos further suggests a proliferation defect. The numerous phenotypic changes related to neural tube defects, cardiac structure malformation and ectopic cell proliferation observed in the BRG1 mutant are consistent with previous findings describing BRG1 function in neural development, heart development, ES cell self-renewal, primitive erythropoiesis, and vascular development (8, 10, 11, 41, 43, 44). Results of ubiquitous deletion of BRG1 suggest that BRG1 is universally required for complex processes of early embryogenesis. Loss of BRG1 results in multiple defects, leading to embryonic death. Using a tamoxifen-inducible cre-lox system, a temporal and global BRG1 functional requirement in perigastrulation period was observed, revealing BRG1 as a key regulator simultaneously involved in multiple development programs required for proper embryogenesis.

Chapter 2 References:

1. **H. SM.** 1977. Gastrulation in the mouse: growth and regionalization of the epiblast. . J Embryol Exp Morphol. **42:**293–303.
2. **Meagher MJ, Braun RE.** 2001. Requirement for the murine zinc finger protein ZFR in perigastrulation growth and survival. Molecular and cellular biology **21:**2880-2890.
3. **Lim DS, Hasty P.** 1996. A mutation in mouse rad51 results in an early embryonic lethal that is suppressed by a mutation in p53. Molecular and cellular biology **16:**7133-7143.
4. **Stefanovic S, Abboud N, Desilets S, Nury D, Cowan C, Puceat M.** 2009. Interplay of Oct4 with Sox2 and Sox17: a molecular switch from stem cell pluripotency to specifying a cardiac fate. The Journal of cell biology **186:**665-673.
5. **Eberharter A, Becker PB.** 2004. ATP-dependent nucleosome remodelling: factors and functions. J Cell Sci **117:**3707-3711.
6. **Wilson BG, Roberts CW.** 2011. SWI/SNF nucleosome remodellers and cancer. Nat Rev Cancer **11:**481-492.
7. **Trotter KW, Archer TK.** 2007. Nuclear receptors and chromatin remodeling machinery. Molecular and cellular endocrinology **265-266:**162-167.
8. **Hang CT, Yang J, Han P, Cheng HL, Shang C, Ashley E, Zhou B, Chang CP.** 2010. Chromatin regulation by Brg1 underlies heart muscle development and disease. Nature **466:**62-67.

9. **Bultman S, Gebuhr T, Yee D, La Mantia C, Nicholson J, Gilliam A, Randazzo F, Metzger D, Chambon P, Crabtree G, Magnuson T.** 2000. A Brg1 null mutation in the mouse reveals functional differences among mammalian SWI/SNF complexes. Molecular cell **6:**1287-1295.

10. **Griffin CT, Brennan J, Magnuson T.** 2008. The chromatin-remodeling enzyme BRG1 plays an essential role in primitive erythropoiesis and vascular development. Development (Cambridge, England) **135:**493-500.

11. **Stankunas K, Hang CT, Tsun ZY, Chen H, Lee NV, Wu JI, Shang C, Bayle JH, Shou W, Iruela-Arispe ML, Chang CP.** 2008. Endocardial Brg1 represses ADAMTS1 to maintain the microenvironment for myocardial morphogenesis. Developmental cell **14:**298-311.

12. **Takeuchi JK, Lou X, Alexander JM, Sugizaki H, Delgado-Olguin P, Holloway AK, Mori AD, Wylie JN, Munson C, Zhu Y, Zhou YQ, Yeh RF, Henkelman RM, Harvey RP, Metzger D, Chambon P, Stainier DY, Pollard KS, Scott IC, Bruneau BG.** 2011. Chromatin remodelling complex dosage modulates transcription factor function in heart development. Nat Commun **2:**187.

13. **Trotter KW, Fan HY, Ivey ML, Kingston RE, Archer TK.** 2008. The HSA domain of BRG1 mediates critical interactions required for glucocorticoid receptor-dependent transcriptional activation in vivo. Molecular and cellular biology **28:**1413-1426.

14. **Fryer CJ, Archer TK.** 1998. Chromatin remodelling by the glucocorticoid receptor requires the BRG1 complex. Nature **393:**88-91.

15. **de la Serna IL, Ohkawa Y, Imbalzano AN.** 2006. Chromatin remodelling in mammalian differentiation: lessons from ATP-dependent remodellers. Nat Rev Genet **7:**461-473.

16. **Dunaief JL, Strober BE, Guha S, Khavari PA, Alin K, Luban J, Begemann M, Crabtree GR, Goff SP.** 1994. The retinoblastoma protein and BRG1 form a complex and cooperate to induce cell cycle arrest. Cell **79:**119-130.

17. **Hendricks KB, Shanahan F, Lees E.** 2004. Role for BRG1 in cell cycle control and tumor suppression. Molecular and cellular biology **24:**362-376.

18. **Martens JA, Winston F.** 2003. Recent advances in understanding chromatin remodeling by Swi/Snf complexes. Curr Opin Genet Dev **13:**136-142.

19. **Murphy DJ, Hardy S, Engel DA.** 1999. Human SWI-SNF component BRG1 represses transcription of the c-fos gene. Molecular and cellular biology **19:**2724-2733.

20. **Reisman DN, Strobeck MW, Betz BL, Sciariotta J, Funkhouser W, Jr., Murchardt C, Yaniv M, Sherman LS, Knudsen ES, Weissman BE.** 2002. Concomitant down-regulation of BRM and BRG1 in human tumor cell lines: differential effects on RB-mediated growth arrest vs CD44 expression. Oncogene **21:**1196-1207.

21. **de la Serna IL, Ohkawa Y, Higashi C, Dutta C, Osias J, Kommajosyula N, Tachibana T, Imbalzano AN.** 2006. The microphthalmia-associated transcription factor requires SWI/SNF enzymes to activate melanocyte-specific genes. The Journal of biological chemistry **281:**20233-20241.

22. **Saha A, Wittmeyer J, Cairns BR.** 2006. Chromatin remodelling: the industrial revolution of DNA around histones. Nature reviews. Molecular cell biology **7:**437-447.

23. **Sumi-Ichinose C, Ichinose H, Metzger D, Chambon P.** 1997. SNF2beta-BRG1 is essential for the viability of F9 murine embryonal carcinoma cells. Molecular and cellular biology **17:**5976-5986.

24. **Indra AK, Dupe V, Bornert JM, Messaddeq N, Yaniv M, Mark M, Chambon P, Metzger D.** 2005. Temporally controlled targeted somatic mutagenesis in embryonic surface ectoderm and fetal epidermal keratinocytes unveils two distinct developmental functions of BRG1 in limb morphogenesis and skin barrier formation. Development (Cambridge, England) **132:**4533-4544.

25. **Kishigami S, Komatsu Y, Takeda H, Nomura-Kitabayashi A, Yamauchi Y, Abe K, Yamamura K, Mishina Y.** 2006. Optimized beta-galactosidase staining method for simultaneous detection of endogenous gene expression in early mouse embryos. Genesis **44:**57-65.

26. **Geijtenbeek TB, Engering A, Van Kooyk Y.** 2002. DC-SIGN, a C-type lectin on dendritic cells that unveils many aspects of dendritic cell biology. Journal of leukocyte biology **71:**921-931.

27. **Manova K, Tomihara-Newberger C, Wang S, Godelman A, Kalantry S, Witty-Blease K, De Leon V, Chen WS, Lacy E, Bachvarova RF.** 1998. Apoptosis in mouse embryos: elevated levels in pregastrulae and in the distal anterior region of gastrulae of normal and mutant mice. Dev Dyn **213:**293-308.

28. **Malumbres M, Barbacid M.** 2009. Cell cycle, CDKs and cancer: a changing paradigm. Nat Rev Cancer **9:**153-166.

29. **Sherr CJ, Roberts JM.** 1999. CDK inhibitors: positive and negative regulators of G1-phase progression. Genes & development **13:**1501-1512.

30. **Wang TC CR, Zukerberg L, Lees E, Arnold A, Schmidt EV.** 1994. Mammary hyperplasia and carcinoma in MMTV-cyclin D1 transgenic mice. Nature. **369:**669-671.

31. **Zhou P JW, Weghorst CM, et al:.** 1996. Over- expression of cyclin D1 enhances gene amplifica- tion. . Cancer Res **56:**36-39.

32. **Nelsen CJ, Kuriyama R, Hirsch B, Negron VC, Lingle WL, Goggin MM, Stanley MW, Albrecht JH.** 2005. Short term cyclin D1 overexpression induces centrosome amplification, mitotic spindle abnormalities, and aneuploidy. The Journal of biological chemistry **280:**768-776.

33. **Dzierzak E, Speck NA.** 2008. Of lineage and legacy: the development of mammalian hematopoietic stem cells. Nat Immunol **9:**129-136.

34. **Curtis CD, Griffin CT.** 2012. The chromatin-remodeling enzymes BRG1 and CHD4 antagonistically regulate vascular Wnt signaling. Molecular and cellular biology **32:**1312-1320.

35. **Griffin CT, Curtis CD, Davis RB, Muthukumar V, Magnuson T.** 2011. The chromatin-remodeling enzyme BRG1 modulates vascular Wnt signaling at two levels. Proceedings of the National Academy of Sciences of the United States of America **108:**2282-2287.

36. **Beddington RS, Robertson EJ.** 1998. Anterior patterning in mouse. Trends in genetics : TIG **14:**277-284.

37. **Miura S, Singh AP, Mishina Y.** 2010. Bmpr1a is required for proper migration of the AVE through regulation of Dkk1 expression in the pre-streak mouse embryo. Developmental biology **341:**246-254.

38. **Bielinska M, Narita N, Wilson DB.** 1999. Distinct roles for visceral endoderm during embryonic mouse development. The International journal of developmental biology **43:**183-205.

39. **Duyao MP, Auerbach AB, Ryan A, Persichetti F, Barnes GT, McNeil SM, Ge P, Vonsattel JP, Gusella JF, Joyner AL, et al.** 1995. Inactivation of the mouse Huntington's disease gene homolog Hdh. Science (New York, N.Y **269:**407-410.

40. **Zeitlin S, Liu JP, Chapman DL, Papaioannou VE, Efstratiadis A.** 1995. Increased apoptosis and early embryonic lethality in mice nullizygous for the Huntington's disease gene homologue. Nature genetics **11:**155-163.

41. **Seo S, Richardson GA, Kroll KL.** 2005. The SWI/SNF chromatin remodeling protein Brg1 is required for vertebrate neurogenesis and mediates transactivation of Ngn and NeuroD. Development (Cambridge, England) **132:**105-115.

42. **Galderisi U, Jori FP, Giordano A.** 2003. Cell cycle regulation and neural differentiation. Oncogene **22:**5208-5219.

43. **Yoo AS, Crabtree GR.** 2009. ATP-dependent chromatin remodeling in neural development. Current opinion in neurobiology **19:**120-126.

44. **Ho L, Ronan JL, Wu J, Staahl BT, Chen L, Kuo A, Lessard J, Nesvizhskii AI, Ranish J, Crabtree GR.** 2009. An embryonic stem cell chromatin remodeling complex, esBAF, is essential for embryonic stem cell self-renewal and pluripotency. Proceedings of the National Academy of Sciences of the United States of America **106:**5181-5186.

45. **Nishiyama A, Xin L, Sharov AA, Thomas M, Mowrer G, Meyers E, Piao Y, Mehta S, Yee S, Nakatake Y, Stagg C, Sharova L, Correa-Cerro LS, Bassey U, Hoang H, Kim E, Tapnio R, Qian Y, Dudekula D, Zalzman M, Li M, Falco G, Yang HT, Lee SL, Monti M, Stanghellini I, Islam MN, Nagaraja R, Goldberg I, Wang W, Longo DL, Schlessinger D, Ko MS.** 2009. Uncovering early response of gene regulatory networks in ESCs by systematic induction of transcription factors. Cell stem cell **5:**420-433.

CHAPTER 3: Deletion of the Brg1 Chromatin remodeling Factor Confers Sensitivity to Doxorubicin Cardiotoxicity in Mice

This content of this chapter is in the form required by the Society of Toxicologic Pathology for submission to their peer-reviewed publication *Toxicologic Pathology*. The research concept was devised by Michael C. Boyle. The animal experiments were designed by Michael C. Boyle, David E. Malarkey, and Trevor K. Archer. The molecular biology experiments were performed by Michael C. Boyle and Jackson A. Hoffman. The microarray analysis was performed by James P. Ward, Jackson A. Hoffman, and Michael C. Boyle. The manuscript was written by Michael C. Boyle.

Deletion of the Brg1 Chromatin Remodeling Factor Confers Sensitivity to Doxorubicin Cardiotoxicity in Mice

Abstract

Doxorubicin is one of the most effective anticancer medicines currently available, however, chronic use may cause cardiomyocyte damage leading to heart failure. The precise mechanisms responsible for cardiotoxicity are still unknown, and preventative adjuvant therapies and alternative formulations are limited both in number and efficacy. The chromatin remodeling factor Brg1, a known required factor in cardiovascular development and disease, may play a role in doxorubicin cardiotoxicity.

In this study, we utilized a tamoxifen-inducible transgenic mouse model to knock out the ATPase domain of Brg1 in adult male mice. Brg1 WT and Brg1 KO mice were then subjected to a ten-week repeat-dose doxorubicin cardiotoxicity study to emulate that used in the clinical setting. Microscopic analyses confirmed the presence of doxorubicin-associated lesions in treated mice, including cardiomyocyte degeneration, vacuolation, and mitochondrial degeneration and cristolysis; lesions were also observed to a lesser degree in untreated Brg1 KO mice. Analysis of serum biomarkers of cardiac injury Myl3 and FABP3 correlated with the degree of Brg1 deletion in Brg1 KO mice.

This study elucidated a protective effect of Brg1 in normal cardiac homeostasis. It also revealed a potentiation effect of Brg1 deletion in doxorubicin cardiotoxicity in a repeat-dose toxicity mouse model.

Introduction:

Heart disease is the number one killer of Americans, even more so than cancers; combined they contribute to 50% of the mortality in the United States (Seigel et al. 2013). The cardiotoxicity suffered by those requiring doxorubicin chemotheraphy for cancer ironically bridges the most common morbidities in America (Sawyer 2013). Anthracyclines are not the only successful and important chemotherapeutic class to have cardiotoxic side effects; indeed the tyrosine kinase inhibitors have been implicated as well (Slordal and Spigset 2006, Laverty *et al*. 2011, Cheng and Force 2010). There are multiple agents causing cardiotoxicity, and multiple molecular mechanisms described contributing to the myocardium's deleterious response to these agents, yet this broad field of research leaves gaps in our understanding. For instance, investigation into the roles of chromatin remodeling enzymes in doxorubicin cardiotoxicity, such as the master regulator Brg1, have not been described despite their critical roles in cardiovascular development and homeostasis, and therefore, disease (Hang et al. 2010).

Doxorubicin (trade name Adriamycin) is an anthracycline antibiotic isolated from the bacterium *Streptomyces peucetius caesius* (Roca-Alonso et al 2012, Carvalho et al 2013). It is used as a cancer therapeutic for a wide range of epithelial, mesenchymal, and round cell neoplasms, including breast cancer, Kaposi sarcoma, and Hodgkin's lymphoma (Volkova and Russell 2011). Its efficacy against tumor cells is mostly attributed to its ability to intercalate DNA, however, induction of ROS, DNA strand breaks, apoptosis, growth arrest, and DNA helicase disruption are also potential contributors (Carvalho et al 2013, Octavia et al 2013a, Tacar et al 2013). These mechanisms have also been implicated in the toxicity of

doxorubicin in the heart, which has been reported to cause heart failure in approximately 5-55% of patients receiving clinically relevant doses within months, years, or decades of cessation of therapy (Octavia et al 2012b, Shi et al 2011, Singal and Iliskovic 1998).

Doxorubicin chemotherapy is indicated for a variety of tumors from lymphoid tumors in adolescents to epithelial tumors that develop in the middle-aged and elderly. Dexrazoxane and other adjuvants have been investigated for their ability to reduce the toxicity of doxorubicin when administered to this large and variable patient population (Gharib and Burnett 2002, Schunke et al 2013, Jin et al 2013, Chen et al 2007, Wang et al 2013). This research into alternative or adjuvant therapies or paradigms is necessary due to the cardiotoxicity that is a risk factor with doxorubicin administration, including when administered in treatment protocols using therapies of other modalities, such as trastuzumab in HER2 positive breast cancer patients (Cheng and Force 2013, Klein and Dybdal 2003). Currently, mechanism-based solutions are the most promising hope for decreasing morbidity in a population that is continually gaining remission time and therefore more susceptible to the hazardous sequela of some of the most effective chemotherapies. In fact, the discipline of cardio-oncology is partly the result of unmet needs in this investigative area (Moslehi et al. 2013).

Brg1, or SMARCA4, ATPase is an essential subunit of the SWI/SNF (isotype-SWItching/Sucrose Non-Fermenting) transcriptional coregulator (Trotter and Archer 2008). Brg1 has myriad roles in cardiovascular development and disease (Hang et al. 2010, Ho and Crabtree 2010). A “return to the fetal transcriptome” is a common paradigm in cardiovascular research as the de facto response to injury (Oka et al. 2007, Rajabi et al.

2007). In a variety of test systems, Brg1 has been shown to be involved in the regulation of numerous genes and pathways evident in models of doxorubicin toxicity (Li et al. 2013, Xu et al. 2013, Sena et al. 2013, Kang et al 2004, Leung and Nevins 2012, Du et al. 2012). However, previous reports indicated that Brg1 is not required for adult tissue homeostasis (Hang et al. 2010, Bultman et al. 2008). Investigations into Brg1's contribution or prevention of doxorubicin cardiotoxicity may elucidate additional roles of Brg1 in gene regulation and open the door to a novel mechanism of toxicity prevention.

The current study was an investigation to find novel links amongst the various pathogeneses of doxorubicin cardiotoxicity involving the Brg1 chromatin-remodeling complex. These studies have the potential to reveal mechanistic information regarding new targets for decreasing the toxicity of a widely-used cancer therapy that causes significant morbidity under its current uses.

Materials and Methods:

Institutional Compliance Statement:

All animals were housed in AAALAC-accredited animal facilities. All animal procedures were conducted in compliance with the Animal Welfare Act Regulations, 9 CFR 1-4. All animals were handled and treated according to the *Guide for the Care and Use of Laboratory Animals, 8th ed*. (ILAR). Animals were multi-housed (breeding pairs or trios, up to 5 weanlings housed by sex) in 17 cm wide by 28 cm long and 13 cm high (476 cm^2 area) polycarbonate cages with microisolator tops. Cages were supplied with absorbent heat-

treated hardwood bedding (Northeastern Products Corp., Warrensburg, NY), which were changed twice weekly. Animals were fed Purina Rodent Diet No. 5001 *ad libitum* (Breeding). The diet was routinely analyzed for nutritional components. Reverse osmosis treated tap water was supplied *ad libitum* in polycarbonate water bottles with stainless steel sipper tubes, which was changed once weekly.

Animal room temperature ranges was kept between 20 and 25°C, with a relative humidity of 30-70%. . Animals were exposed to a 12-hour light cycle followed by a 12-hour dark cycle. For enrichment, cotton fiber nestlets (Ancare Corp., Bellmore, NY) was supplied to the animals *ad libitum*.

The NIH's ARAC Guidelines for Endpoints in Animal Study Protocols, Morbidity section was followed for all animals. Any test animals experiencing minimal or transient pain or distress were evaluated and/or euthanized.

Drug formulations and administration:

Tamoxifen citrate (Sigma-Aldrich) will be dissolved in corn oil for dosing at 75 or 100mg/kg; total dose volume is 60-100 uL in corn oil. Pharmaceutical grade doxorubicin hydrochloride (Sigma-Aldrich; 98-102% by HPLC) was dissolved in 0.9% sterile saline for dosing at 4mg/kg; total dose volume was 100 uL.

Selection of Animals:

Tamoxifen toxicity testing:

B6.129-*Gt(ROSA)26Sor*$^{tm1(cre/ERT2)Tyj}$/J mice containing a Cre-ER^{T2} cassette (shorthand:

ROSA-cre/ERT2) were crossed with B6.129S4-Gt(ROSA)26Sor^{tm1Sor}/J mice containing a polyA sequence (STOP sequence) flanked by *loxP* sites (shorthand: ROSA-stop) (Soriano 1999, Ventura et al 2007). Tamoxifen toxicity testing was performed in unmated mice, beginning with a tamoxifen citrate (Sigma-Aldrich) intraperitoneal (IP) dose level of 225-mg/kg body weight. To distinguish potential Cre toxicity from possible tamoxifen toxicity, and to establish a lowest observed adverse effects level (LOAEL) and a no observed adverse effect level (NOAEL), unmated adult ROSA-stop animals (without Cre) were dosed IP with 225, 150 and 100 mg/kg of body weight tamoxifen (10 ml/kg dosing volume). Animals received a total of two injections over two consecutive days. Body weights were collected prior to dosing and weekly for a total of 3 weeks (the length of time needed for a mother to raise a litter). Animals were observed daily for health effects. Mice receiving the 225 and 150 mg/kg dose levels were either found dead or were euthanized as moribund. Mice tolerated the tamoxifen dose level of 100 mg/kg for two consecutive days without evidence of tamoxifen toxicity on weight gain or tissue morphology. Having determined the LOAEL to be 150 mg/kg, and the NOAEL to be 100mg/kg in this study, 100 mg/kg of body weight tamoxifen citrate was selected as the maximum dose to be used in future studies.

Cre recombination evaluation:

ROSA-cre/ERT2 mice (B6.129-Gt(ROSA)26Sor$^{tm1(cre/ERT2)Tyj}$/J) were bred with ROSA-stop reporter mice (B6.129S4-Gt(ROSA)26Sor^{tm1Sor}/J). Pregnant females were dosed with 100 mg/kg tamoxifen on different embryonic days and fetuses were collected for measuring B-galactosidase activity in the double transgenic embryos (B6.129S4-Gt(ROSA)26Sor^{tm1Sor}/J Tg(B6.129-Gt(ROSA)26Sor$^{tm1(cre/ERT2)Tyj}$)) as a measure of Cre recombinase activity as

previously described (Loughna and Henderson 2007). ROSA-cre/ERT2 x ROSA-stop double transgenic embryos exhibited ubiquitous strong positive *lacZ* staining while their ROSA-stop embryo littermates showed negative staining at various developmental stages (data not shown). Significant Cre activity was absent in adults in crossings of B6;128S2-Smarca4^{tm1Pcn}/Mmnc mice (shorthand Brg1 fl/fl) with B6.129-*Gt(ROSA)26Sor*$^{tm1(cre/ERT2)Tyj}$/J mice (data not shown). The B6.Cg-Tg(CAG-cre/Esr1*)5Amc/J mouse (shorthand: CAG-Cre/Esr1*) contains a Cre-ER^{TM} cassette system driven by a CMV immediate-early enhancer coupled with a chicken a-actin/rabbit B-globulin hybrid promoter was selected for adult cre recombinetic studies (Hayashi and McMahon 2002). For re-evaluation of Cre recombinetics and comparison to concurrent Cre studies, Male CAG-Cre/Esr1* mice were crossed with female B6.129S4-Gt(ROSA)26Sor^{tm1Sor}/J mice; two pregnant females were administered a single IP 100 mg/kg tamoxifen citrate dose on embryonic day 6.5 (E6.5) for collection at E9.5. Two pregnant females were administered IP tamoxifen citrate doses of 100mg/kg once daily on E12.5 and E13.5 for collection at E15.5. Two additional pregnant females were allowed to pup; at seven weeks of age F1 pups were administered 75mg/kg tamoxifen citrate IP once daily for five consecutive days. F1 offspring of the Male CAG-Cre/Esr1* mice crossed with female B6.129S4-Gt(ROSA)26Sor^{tm1Sor}/J mice dosed at 7 weeks of age were euthanized at 9 weeks of age. Hearts from these mice were frozen in Tissue-Tek® OCT media (Electron Microscopy Services, Inc.), sectioned at 5um, and mounted on positively-charged glass slides for evaluating B-galactosidase activity as a measure of Cre recombinase activity as previously described (Loughna and Henderson 2007). B6.129S4-Gt(ROSA)26Sor^{tm1Sor}/J Tg B6.129-Gt(ROSA)26Sor$^{tm1(cre/ERT2)Tyj}$ fetuses treated in utero were

collected for evaluating B-galactosidase activity in whole mounts as a measure of Cre recombinase activity as previously described (Loughna and Henderson 2007).

Genotyping:

For BRG1 genotyping, three primers were used to amplify wild type (241bp PCR product), floxed (387bp PCR product) and deleted (313bp PCR product) BRG1 alleles; P1-GTCATACTTATGTCATAGCC, P2- GCCTTGTCTCAAACTGATAAG, P3-GATCAGCTCATGCCCTAAGG (REF). For Cre genotyping, the forward (5'-GCGGTCTGGCAGTAAAAACTATC-3') and the reverse (5'-GTGAAACAGCATTGCTGTCACTT-3') primer were used for PCR amplification (Sumi-Ichinose et al 1997). Genomic DNA was obtained by phenol extraction of DNA from tail tips obtained postmortem as previously described (Koh 2013).

Doxorubicin dose level justification:

Conversion of dose levels reported by Friedman *et al.* (JAMA 1976) to cause cardiomyocyte vacuolation, t-tubule dilatation, and intrasarcoplasmic swelling using the Center for Drug Evaluation and Research's guide *Estimating the maximum safe starting dose in initial clinical trials for therapeutics in adult healthy volunteers* (CDER 2005), allowing for construction of a repeat-dose toxicity paradigm, yielded a five-week protocol with twice-weekly 4mg/kg IP doses of doxorubicin hydrochloride. In a pilot study, 3 Adult male Cre-Brg1 floxed mice (B6.Cg-Tg(CAG-cre/Esr1*)5Amc/J Tg B6;128S2-Smarca4^{tm1Pcn}/Mmnc) and 3 adult male Brg1 floxed mice (B6;128S2-Smarca4^{tm1Pcn}/Mmnc) were given 75 mg/mL

tamoxifen citrate IP once daily for 5 consecutive days. Following a two week recovery period to allow for recombination, mice were administered 4mg/kg doxorubicin IP twice weekly for 5 weeks (cumulative dose: 40mg/kg; ~180mg/m^2) (CDER 2005, Desai et al. 2013). Bright field and electron microscopic examination of myocardial tissue from treated animals revealed more widespread and severe lesions in Cre-Brg1 floxed mice than Brg1 floxed mice, including cardiomyocyte vacuolation, t-tubule dilatation, and intrasarcoplasmic swelling (data not shown), similar to that described by Friedman et al. and reported herein and by other groups (Friedman et al. 1978, Desai et al. 2013).

Experimental design:

To detect a 2-fold increase or decrease in RNA expression with at least a 90% power assuming expression is log-normal distribution, 5 animals per group were required for biochemical analyses (Table 3.1). Five animals per group were also required for similar histopathologic and protein analyses, respectively; a total of 15 animals per treatment group were utilized for this study.

Table 3.1: Treatment Group Designations and Dosage Levels

Group #	Shorthand	Genotype	No. of Animals	Tamoxifen Dose Level	Tamoxifen Doses	Doxorubicin Dose Level	Doxorubicin Doses
1	Brg1 WT	B6;128S2-Smarca4^{tm1Pcn}/Mmnc	15	75 mg/kg	5		
2	Brg1 KO	B6.Cg-Tg(CAG-cre/Esr1*)5Amc/J Tg B6;128S2-Smarca4^{tm1Pcn}/Mmnc	15	75 mg/kg	5		
3	Brg1 WT + Dox	B6.Cg-Tg(CAG-cre/Esr1*)5Amc/J Tg B6;128S2-Smarca4^{tm1Pcn}/Mmnc	15			4 mg/kg	10
4	Brg1 KO + Dox	B6.Cg-Tg(CAG-cre/Esr1*)5Amc/J Tg B6;128S2-Smarca4^{tm1Pcn}/Mmnc	15	75 mg/kg	5	4 mg/kg	10

Thirty adult male Cre-Brg1 floxed mice (B6.Cg-Tg(CAG-cre/Esr1*)5Amc/J Tg B6;128S2-Smarca4^{tm1Pcn}/Mmnc) (Groups 2 and 4) and 15 adult male Brg1 floxed mice (B6;128S2-Smarca4^{tm1Pcn}/Mmnc) (Group 1) were given 75 mg/mL tamoxifen citrate IP once daily for 5 consecutive days; 15 Cre-Brg1 floxed mice (B6.Cg-Tg(CAG-cre/Esr1*)5Amc/J Tg B6;128S2-Smarca4^{tm1Pcn}/Mmnc) (Group 3) received an equal volume of sterile saline (~60-100 uL) as a vehicle control. Following a two week recovery period to allow for recombination, Group 3 and Group 4 mice were administered 4mg/kg doxorubicin hydrochloride IP twice weekly for 5 weeks; Groups 1 and 2 received an equal volume of IP sterile saline (100 uL) as a vehicle control (Figure 3.1).

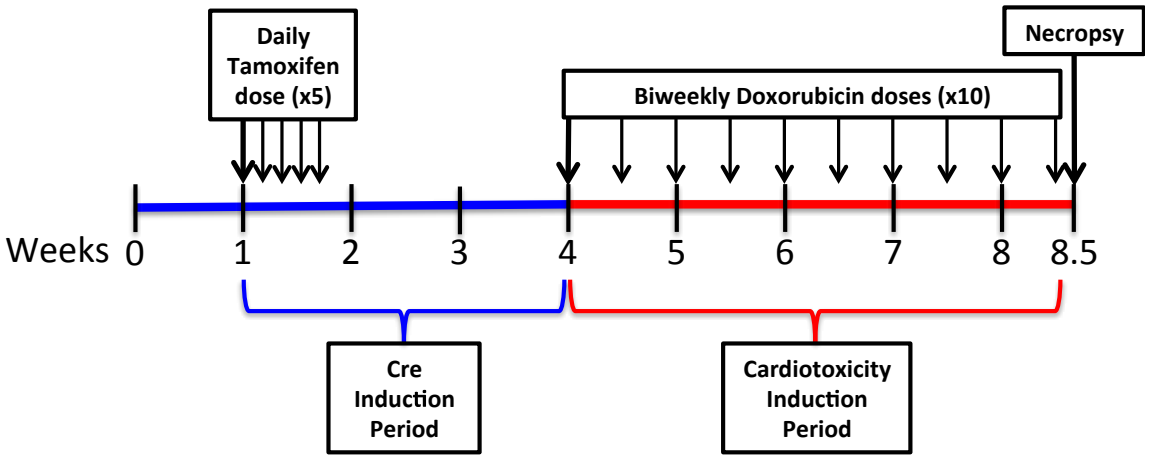

Figure 3.1: Brg1 KO repeat-dose doxorubicin cardiotoxicity study design. Animals receive five 75mg/kg tamoxifen doses for cre induction. After recombination, animals receive 4mg/kg doxorubicin twice weekly for 5 weeks.

In-life observations: Mice were weighed before injections, every 24 hours during treatment periods, and at the time of euthanasia. The ARAC Guidelines for Endpoints, Morbidity section were followed, including, but not limited to, the clinical signs described in section 1b (i.e. Rapid or progressive weight loss, edema, sizable abdominal enlargement or ascites, progressive dermatitis, lethargy or persistent recumbency, coughing, labored breathing, nasal discharge, jaundice, cyanosis, and/or pallor/anemia, neurological signs, bleeding from any orifice, self-induced trauma, any condition interfering with eating or drinking, ambulation, or elimination, excessive or prolonged hyperthermia or hypothermia).

Euthanasia and Blood collection:

Euthanasia was accomplished using CO_2 asphyxiation followed by decapitation according to the NIEHS "Guidelines for Euthanasia" and using a metered CO_2 line. The abdominal aorta was revealed via midline thoracoperitoneotomy, and blood removed from the abdominal aorta using a 3-5cc syringe with a 23-gauge needle.

Necropsy and Heart Weights:

Upon termination of aortic exsanguination, the heart was quickly excised and weighed. From all groups (1-4), 5 animals were designated for histopathology, 5 for protein analyses, and 5 for RNA analyses. For histopathology animals, at necropsy hearts were fixed in 10% neutral-buffered formalin. For the protein animals, at necropsy hearts were snap frozen in cryovials in liquid nitrogen and stored at -80 degrees Celsius. For the RNA animals, at necropsy a 1mm thick section of myocardium including atrium, valve, and ventricle was

removed from each heart and fixed in a modified Karnosky's fixative (2% glutaraldehyde, 2.5% paraformaldehyde in 0.1M PBS). The remaining RNA heart tissue was minced and snap-frozen in approximately 1700 uL RNALater (Qiagen).

Histopathology and electron microscopy:

Histopathology:

For histopathology animals, hearts were fixed in 10% neutral-buffered formalin for 24 hours, dehydrated, embedded in paraffin, sectioned at 5um, and mounted on positive-charged glass slides for hematoxylin and eosin (H&E) staining. H&E stained slides were independently and blindly examined by a pathologist for the diagnosis and severity of "Degeneration/necrosis, Cardiomyocyte" using the following severity grading criteria:

- Grade 0: Lesions absent
- Grade 1: >0-10% of the tissue section affected.
- Grade 2: >10-25% of the tissue section affected.
- Grade 3: >20-40% of the tissue section affected.
- Grade 4: >40% of the tissue section affected.

Electron microscopy:

From RNA animals, a 1mm thick section of myocardium including atrium, valve, and ventricle was fixed in a modified Karnosky's fixative (2% glutaraldehyde, 2.5% paraformaldehyde in 0.1M PBS) for 24-72 hours at 4 degrees Celsius before being rinsed in buffer, post-fixed in cacodylate-buffered 1% osmium tetroxide, stained in 2% aqueous uranyl

lead acetate, dehydrated, and embedded in Polybed 812 (Polysciences, Inc.). Thick sections (0.5um) were stained with 1% toluidine blue in 1% sodium borate. A subset of ultrathin (180nm) sections cut from a subset of thick section traps were placed on mesh copper grids, stained with 5% uranyl acetate and Reynolds lead citrate, and examined using a Tecnai 12 transmission electron microscope (FEI). Approximately 10 grids per animal were examined and photographed. Images were analyzed for lesions typical of doxorubicin cardiotoxicity and correlative to clinical outcome in humans as previously described (Berry et al. 1998, Bristow et al. 1981, Billingham et al. 1978).

Cardiac biomarker analysis:

Approximately 70 μL of serum from all RNA designated animals was collected and stored at -80 degrees Celsius until time of measurement. Serum levels of fatty acid binding protein 3 (FABP3), myosin light chain 3 (Myl3), cardiac troponin I (cTnI), and cardiac troponin T (cTnT), were measured using the Meso Scale Discovery (MSD) Cardiac Injury Panel 3 kit (Meso Scale Discovery) and SECTORTM Imager 2400 electrochemiluminescence detection platform [Meso Scale Discovery (MSDTM), Gaithersburg, MD]. This kit has been optimized in our laboratory for the analysis of both rat and mouse sera (data not shown). As per manufacturer's specifications, the limits of quantification were set as percent recovery at 100+/-25% and the & coefficient of variation (CoV) of the calculated concentration was <20% (mesoscalediscovery.com datasheet). Individual measurements, group, or assay results outside this range and/or below the limit of detection set by the standard curve were excluded from these analyses.

Protein analysis:

Hearts frozen at -80 degrees Celsius at necropsy were processed for nuclear and cytoplasmic protein extracts using the Pierce NE-PER kit (Thermo Scientific) following the manufacturer's instructions by thawing in 1x phosphate-buffered saline with 1x Phenylmethanesulfonyl fluoride (PMSF, Sigma-Aldrich) and 1x HALT protease inhibitor (Thermo Scientific). Nuclear protein isolates were prepared following the manufacturer's instructions for nuclear protein isolates from whole mammalian tissue. Gel electrophoresis was performed using an 4-12% tris-glycine gel (Novex). Protein was transferred to a PVDF membrane (BioRad Immunoblot). Western blotting was performed using a lab-raised rabbit anti-mouse Brg1 polyclonal antibody directed at the HSA and BRK domains at a concentration of 1:5000 and a rabbit anti-mouse Lamin A and C monoclonal antibody (Santa Cruz Biotechnology, H-110, sc-20681) at a concentration of 1:1000.

RNA analysis:

Hearts minced and frozen in RNALater (Qiagen) at -80 degrees Celsius at necropsy were thawed on ice and homogenized in Trizol (Invitrogen) using a Tissue Tearor Homogenizer (Biospec Products, Inc.). Homogenates were then processed with the Qiagen RNeasy Mini kit following the manufacturer's instructions. RNA was isolated from whole hearts in Trizol (Invitrogen) using a Superscript III Reverse Transcriptase (Invitrogen) to synthesize cDNA from 2 ug of RNA, and real-time PCR was performed with Brilliant III SYBR Green Master Mix (Agilent) on a Stratagene Mx3000P for evaluation of Brg1 expression levels.

Statistical evaluation:

Statistical analyses were performed using Microsoft Excel and VassarStats software (Excel 2008; Lowry 2013).

Results:

Genotyping and Protein Analysis:

In order to minimize variability in the experiment due to the relative contribution of gene deletion group animals not undergoing a deletional event, genotyping and protein analysis of representative tissues from experimental animals must be performed. Additionally, expression or lost expression of the gene(s) of interest in the tissue(s) of interest must be demonstrated to additionally decrease the concern of variability between animals within a particular group.

Two pregnant females were administered IP tamoxifen citrate doses of 100mg/kg once daily on E12.5 and E13.5 for collection at E15.5. Two additional pregnant females were allowed to pup; at seven weeks of age F1 pups were administered 75mg/kg tamoxifen citrate IP once daily for five consecutive days. F1 offspring of the Male CAG-Cre/Esr1* mice crossed with female B6.129S4-Gt(ROSA)26Sor^{tm1Sor}/J mice dosed at 7 weeks of age were euthanized at 9 weeks of age. Hearts from these mice were frozen in Tissue-Tek® OCT media (Electron Microscopy Services, Inc.). B6.129S4-Gt(ROSA)26Sor^{tm1Sor}/J Tg B6.129-Gt(ROSA)26Sor$^{tm1(cre/ERT2)Tyj}$ fetuses treated in utero and F1 adult hearts treated at 7 weeks of age were collected for measuring β-galactosidase activity using whole mount X-gal staining as a measure of Cre recombinase activity as previously described (Loughna and Henderson 2007). Strong Cre activity was present at all stages examined (Figure 3.2A-G).

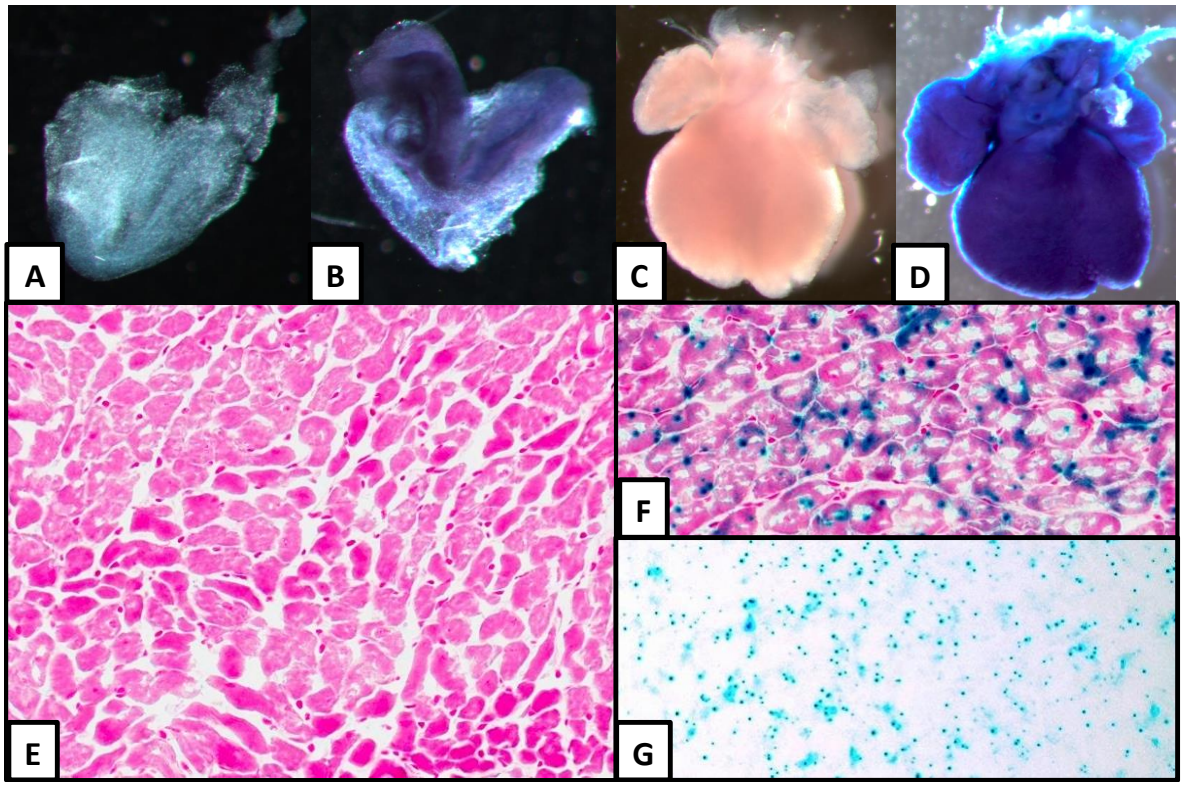

Figure 3.2: X-gal staining of induced embryos and adults. Lack of staining is present in control embryonic day 9.5 (E9.5) whole embryos (3.2A), E15.5 heart (3.2C) whole mounts, and 9 week-old mouse heart frozen sections (3.2E). Positive indigo staining is present in Cre-ROSA E9.5 whole embryo (3.2B), E15.5 heart (3.2D) whole mounts, and 9 week-old mouse heart frozen sections (3.2F). X-gal stained section without nuclear fast counterstain (3.2G). Nuclear fast red counterstain (3.2E, 3.2F). 3.2A-D, original dissecting microscope magnification objective 5x. 3.2E-G, original brighfield microscope magnification objective 20x.

Results of genomic PCR of hearts from B6.Cg-Tg(CAG-cre/Esr1*)5Amc/J Tg B6;128S2-Smarca4^{tm1Pcn}/Mmnc (Cre-Brg1 floxed) mice revealed a >60% recombination efficiency in Cre-Brg1 floxed mice with induced Cre recombination (Figure 3.3A). Real-time PCR of samples from Groups 1-4 revealed an approximately two-fold decrease in Brg1 mRNA expression relative to GAPDH in Brg1 KO animals (Figure 3.3B). Brg1 mRNA expression decreases translated to protein expression decreases in Brg1 KO animals (Figure 3.3C).

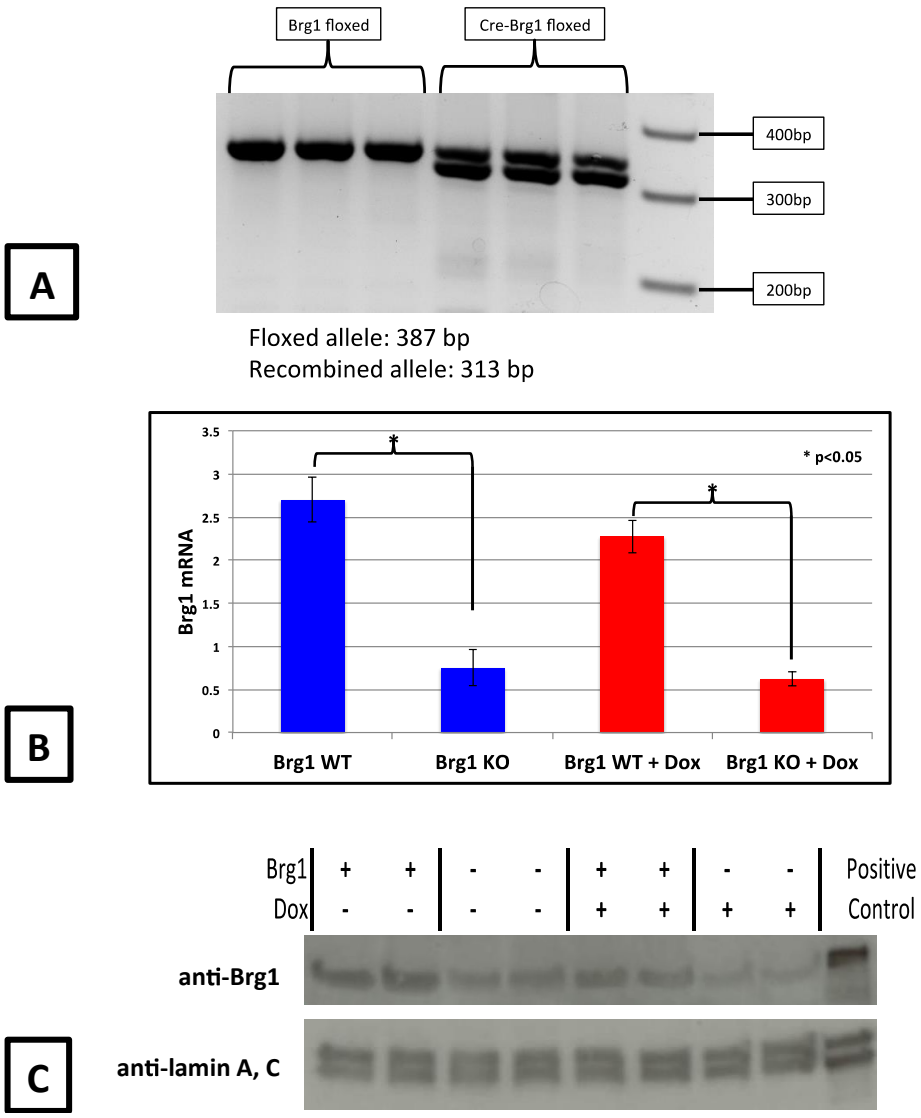

Figure 3.3: Brg1 knockout evaluation. Genomic PCR revealed a >60% recombination efficiency (3.3A). rt-PCR of Brg1 mRNA revealed a significant decrease in Brg1 mRNA expression in Brg1 KO mice with or without doxorubicin treatment (3.3B). Western blotting for Brg1 protein revealed a decreased protein expression in Brg1 KO mice with or without doxorubicin treatment (3.3C).

Necropsy, Body and Organ Weights:

Gross analysis of experimental animals is necessary to identify abnormalities representative of potential effects not anticipated at the time of experimental design, in addition to the expected effects of the treatment. This is includes visual inspection of the carcass at necropsy, and careful examination of all organs not limited to those with expected effects. Body weight measurements may be used to identify differences between groups due to treatment(s) in the experiment, and may identify individual animals within a treatment group more severely or less severely affected than others in the group which may lead to difficulties in statistical analysis. Organ weights may also be used to identify differences between groups or within groups. However, some organ weights may have change concomitant to body weight changes. For example, an animal may have a decreased liver weight without a direct toxic effect damaging hepatocytes demonstrated; this liver weight change may simply be due to inanition and decreased organ weights from decreased growth associated with less nutrient intake. For these circumstances, organ weight to body weight ratios are used to show a relative status of the organ weight. Less biased methods of evaluating organ weights include performing organ weight to brain weight ratios, as brain weight is thought to be relatively insensitive to the decreased growth of organs that accompanies inanition and many toxicities.

No significant gross cardiovascular abnormalities were observed upon necropsy. Brg1 WT animals consistently gained weight throughout the study; Brg1 KO animals gained weight poorly upon Brg1 deletion; Brg1 KO animals continued to gain weight poorly whereas Brg1 KO + Dox animals began losing weight upon institution of the doxorubicin cardiotoxicity

protocol. Brg1 WT animals continued to gain weight throughout the study whereas Brg1 WT + Dox animals began losing weight upon institution of the doxorubicin cardiotoxicity protocol (Figure 3.4A). Overall percent body weight gain progressively decreased across groups with Brg1 WT animals exhibiting the greatest percent body weight gain throughout the study, Brg1 KO animals having no net percent body weight gain, and both Brg1 WT and Brg1 KO animals treated with doxorubicin exhibiting loss from the study start (Figure 3.4B). heart to body weight ratios were not significantly different between Brg1 WT animals with or without doxorubicin treatment, or between Brg1 KO animals with or without doxorubicin treatment. However, Brg1 KO animals had significantly increased heart/body weight ratios over Brg1 WT animals (Figure 3.4C).

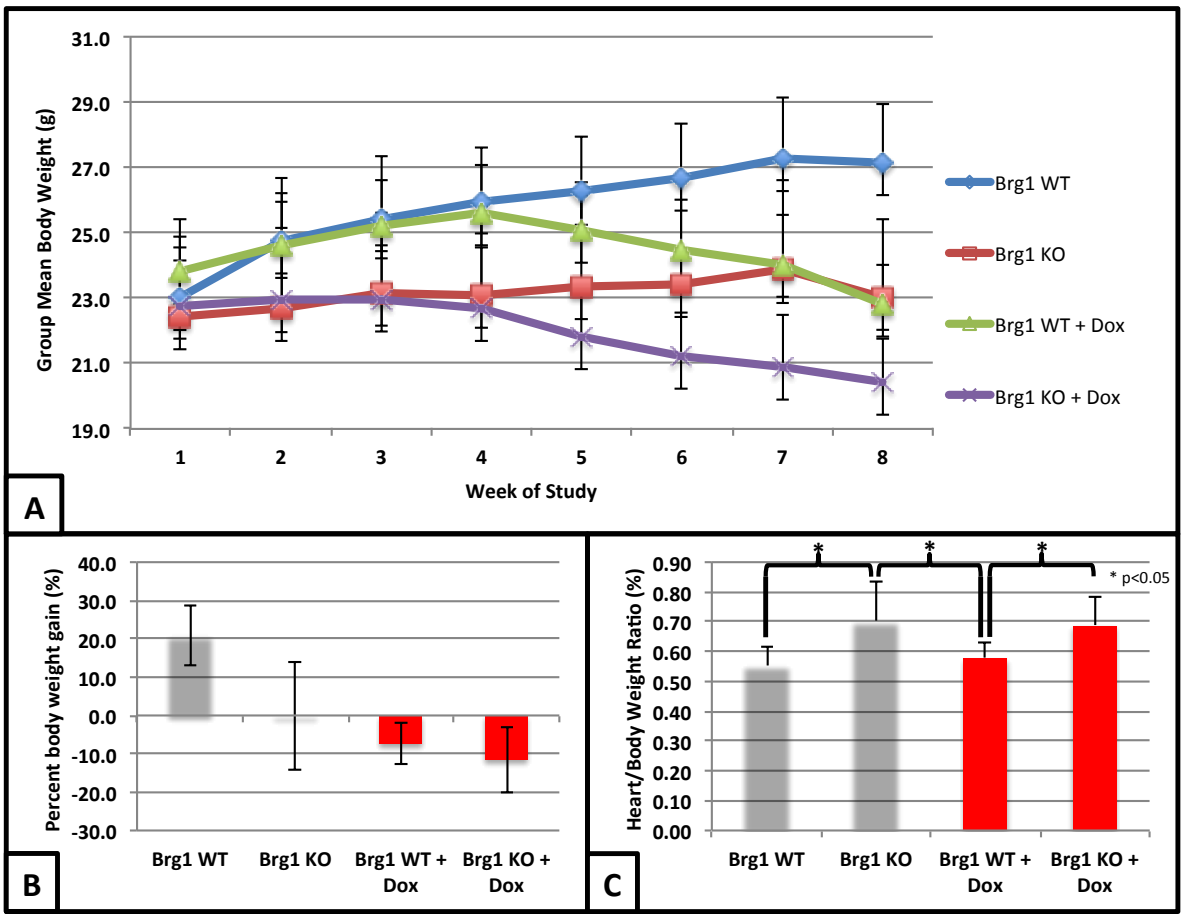

Figure 3.4: Body and heart weights. Brg1 KO is related to stunted weight gain upon recombination (1-2 weeks); doxorubicin treatment accelerated weight loss (4 weeks) (3.4A). Percent body weight gains were negligible with Brg1 KO, but decreased with doxorubicin treatment with or without Brg1 KO (3.4B). Heart weights were significantly increased in Brg1 KO mice, with or without doxorubicin treatment (3.4C).

Microscopy:

Microscopic examination of experimental animal tissues by an expert trained in comparative animal histopathology is a common method of investigating the pathophysiology of experimental treatments on the subject animals. This survey often provides critical information diagnostic for a disease or toxic process in that organ or animal, which can be used to help explain abnormalities or confirm lack of abnormalities in other laboratory tests.

Critical to this examination is knowledge of "background" findings in the experimental species, which may confound experimental results. Several publications describing background findings in experimental animal species may aid the pathologist in making the determination of whether a finding is due to "background" changes inherent in the organ or system of that particular animal strain and species or whether it may be due to the experimental treatment. In the case of the present experiment, a strong working knowledge of the background heart lesions in rodents is necessary in order to differentiate the changes likely due to the gene deletion event and/or treatment with doxorubicin, and the lesions associated with Murine Progressive Cardiomyopathy. Lesions of the latter include cardiomyocyte necrosis, inflammatory cell infiltrates that are predominantly mononuclear in nature, and fibrosis. These changes have a predilection for certain areas of the heart, and presence and severity of these lesions is generally related to the age of the animal. Hearts were examined with no threshold for morphologic changes. A single diagnosis of "Degeneration/necrosis, cardiomyocyte" was used to encompass the following changes: shrunken, hypereosinophilic myofibers, sarcoplasmic fragmentation, sarcoplasmic vacuolization, nuclear pyknosis, and/or shrunken myofibers. Heart sections were peer reviewed by a second pathologist. No disputes of severity between the two pathologists were greater than a single grade; in the case of disputes the peer review pathologist's severity grade was used. Using the grading scheme described in materials and methods, lesion incidence within groups, average severities, and standard deviations were calculated (Figure 3.5A). Lesions were present in Groups 2-4 (Brg1 KO, Brg1 WT+Dox, and Brg1 KO+Dox). However, average severity grade of degeneration/necrosis, cardiomyocyte was significantly

different between Brg1 WT and KO animals, and Brg1 WT and KO animals treated with doxorubicin, respectively (Figure 3.5B).

A

	WT	KO	WT + Dox	KO + Dox	
Animals in study	5	4	5	5	
Degeneration/Necrosis, Cardiomyocyte	0 (0%) [0]	4 (100%) [1.75] c	3 (60%) [1.6]	5 (100%) [3.7]	(% affeted) [av. sev. grade]

B

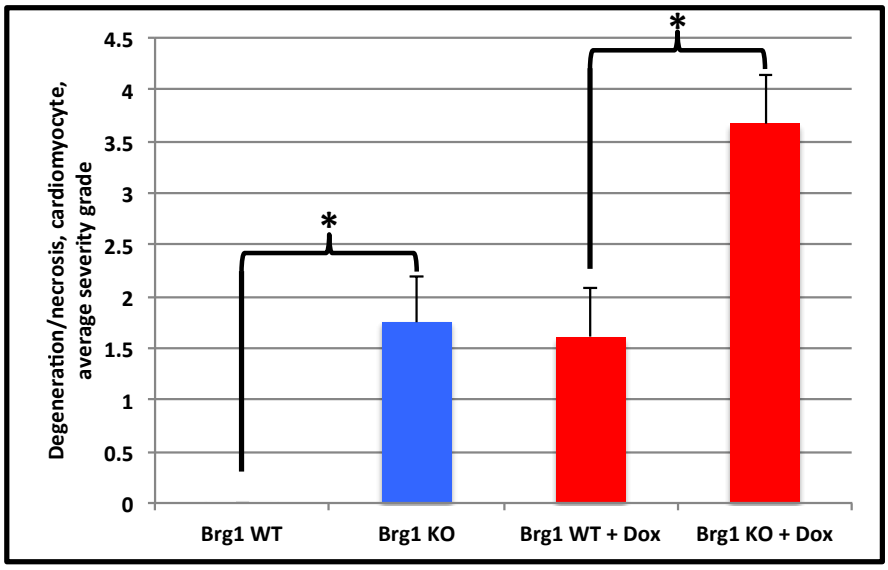

* p<0.05

Figure 3.5: Incidence of degeneration/necrosis, cardiomyocyte (3.5A). Brg1 knockout and doxorubicin treatment significantly increased lesion severity grade relative to respective controls (3.5B).

Lesion character (i.e. type, cells affected) was similar between animals and between groups, and consisted of primarily vacuolization with fewer shrunken myofibers (Figure 3.6). No significant lesions were observed in sections of liver, lung, kidney, or skeletal muscles examined from animals of all dose groups.

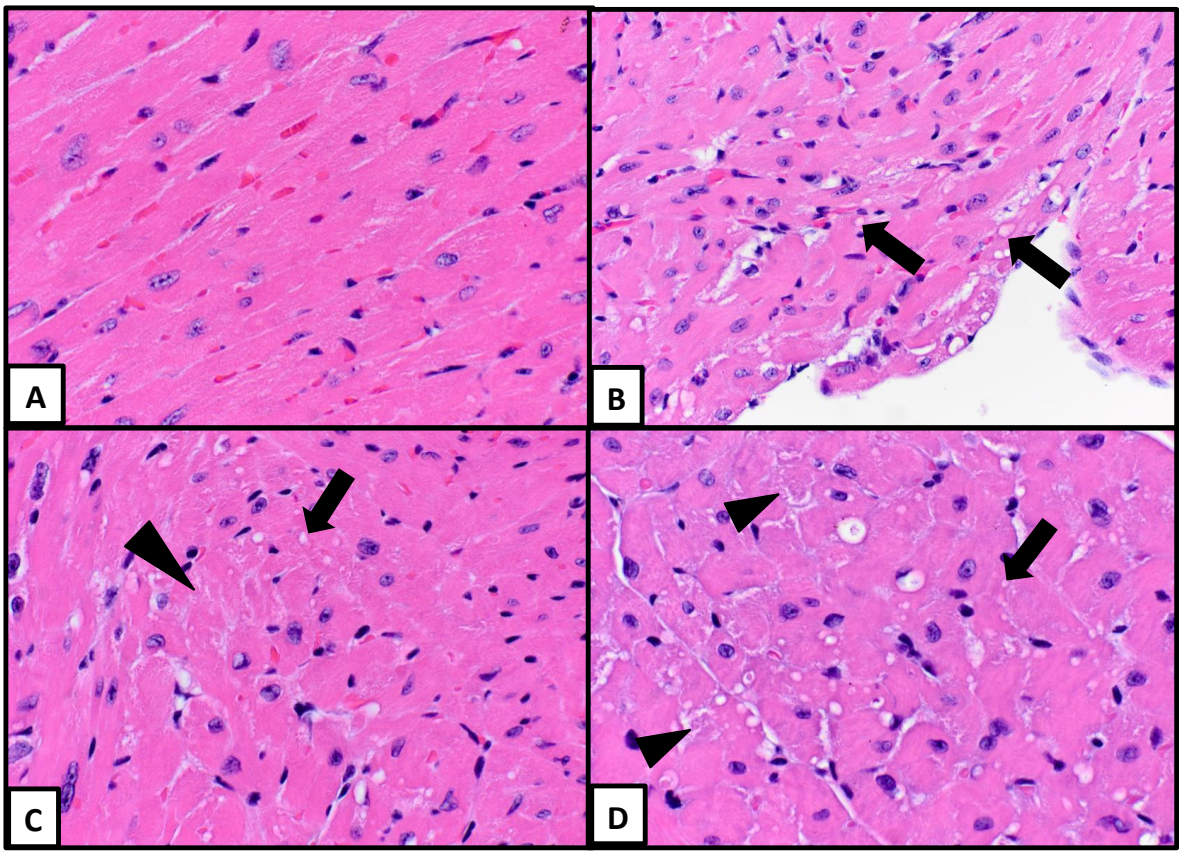

Figure 3.6: Cardiac histology of Brg1 WT (A), Brg1 KO (B), Brg1 WT+Dox (C), and Brg1 KO+Dox (D) mice. Sarcoplasmic vacuolation (arrows) and fragmentation/degeneration was observed (arrowheads).

Transmission electron microscopy of myocardium of Group 1 did not reveal abnormalities. Sections from Groups 2-4 revealed an increasingly prominent and severe constellation of lesions consisting of increased mitochondrial fission/fusion events, varying stages of mitochondrial degeneration, and t-tubule dilatation and degeneration (Figure 3.7).

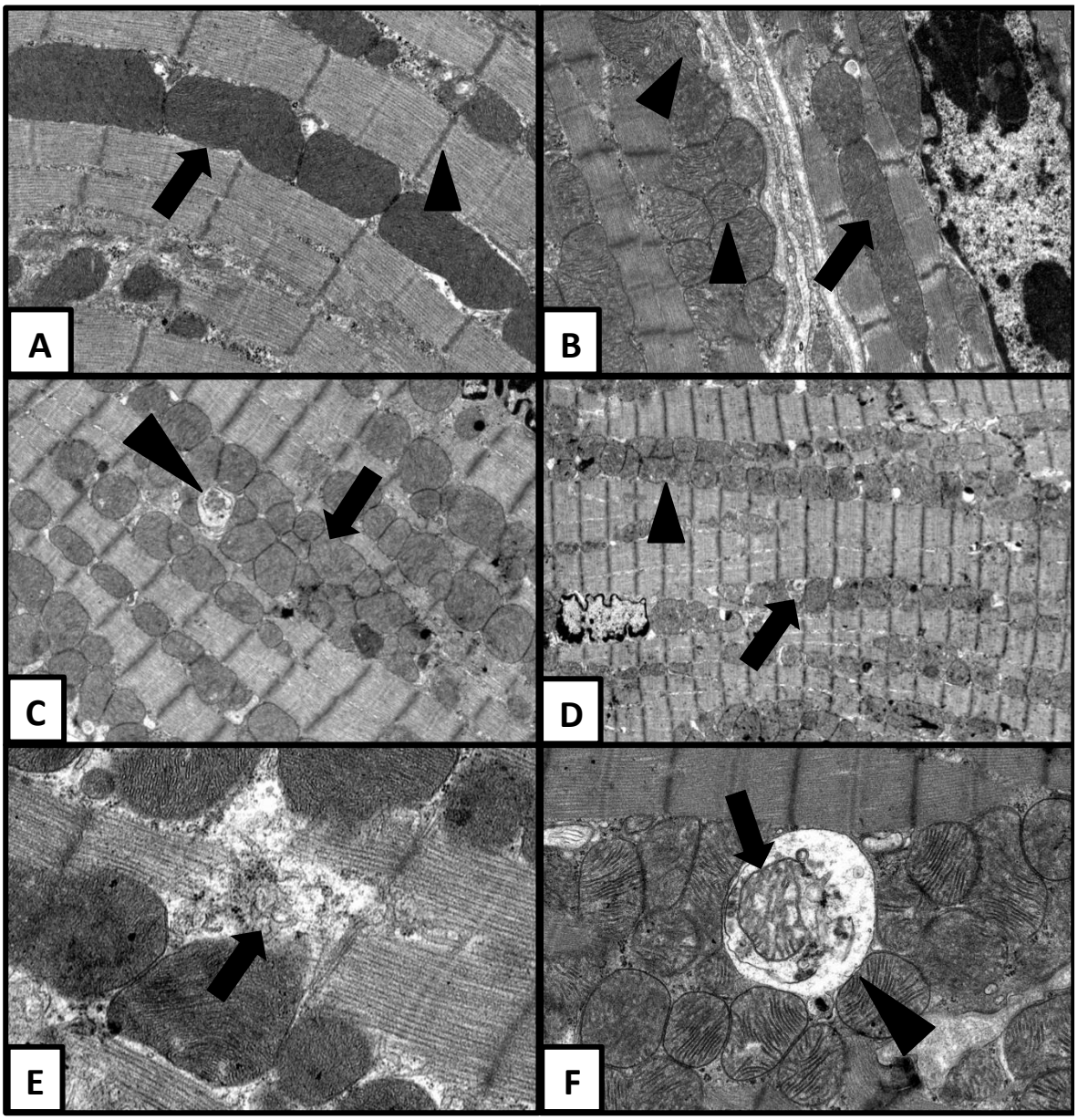

Figure 3.7: Cardiac electron microscopy. Brg1 KO+Dox animals (D-F). Normal mitochondrial morphology (arrow) and Z bands in register (arrowhead) in a Brg1 WT+Dox mouse (A). Increased size (arrow) and presence of numerous fission/fusion events (arrowhead) in Brg1 KO mice (B). Mitochondrial myelin figures (arrow) and T-tubule dilation (arrowhead) in a Brg1 WT+Dox mice (C). T-tubule dilation and disruption (arrow) in a Brg1 KO+Dox mouse (E). Mitochondrial degeneration and christolysis (arrowhead) and variable morphology (arrow) in a Brg1 KO+Dox mouse (F). Magnification of 7A-F: 11,500x, 13,000x, 9,300x, 4,800x, 30,000x, and 18,500x, respectively.

Cardiac biomarker analysis:

There was a statistically significant difference ($p<0.05$) in serum fatty acid binding protein 3 (FABP3) between the Brg1 KO+Dox animals and the remaining treatment groups, which were not significantly different than each other, respectively (Figure 3.8A). There was a statistically significant difference ($p<0.05$) in serum myosin light chain 3 (Myl3) between all treatment groups (Figure 3.8B). There was a weak correlation between the levels of serum FABP3 and Myl3 in Brg1 WT+Dox animals (Figures 3.8C and 3.8D). There was a strong correlation between the levels of serum FABP3 and Myl3 in Brg1 KO+Dox animals (Figures 3.8E and 3.8F). The levels of serum cTnI and cTnT were below the limit of detection of the assay used, and as such, had no correlation with other cardiac biomarkers.

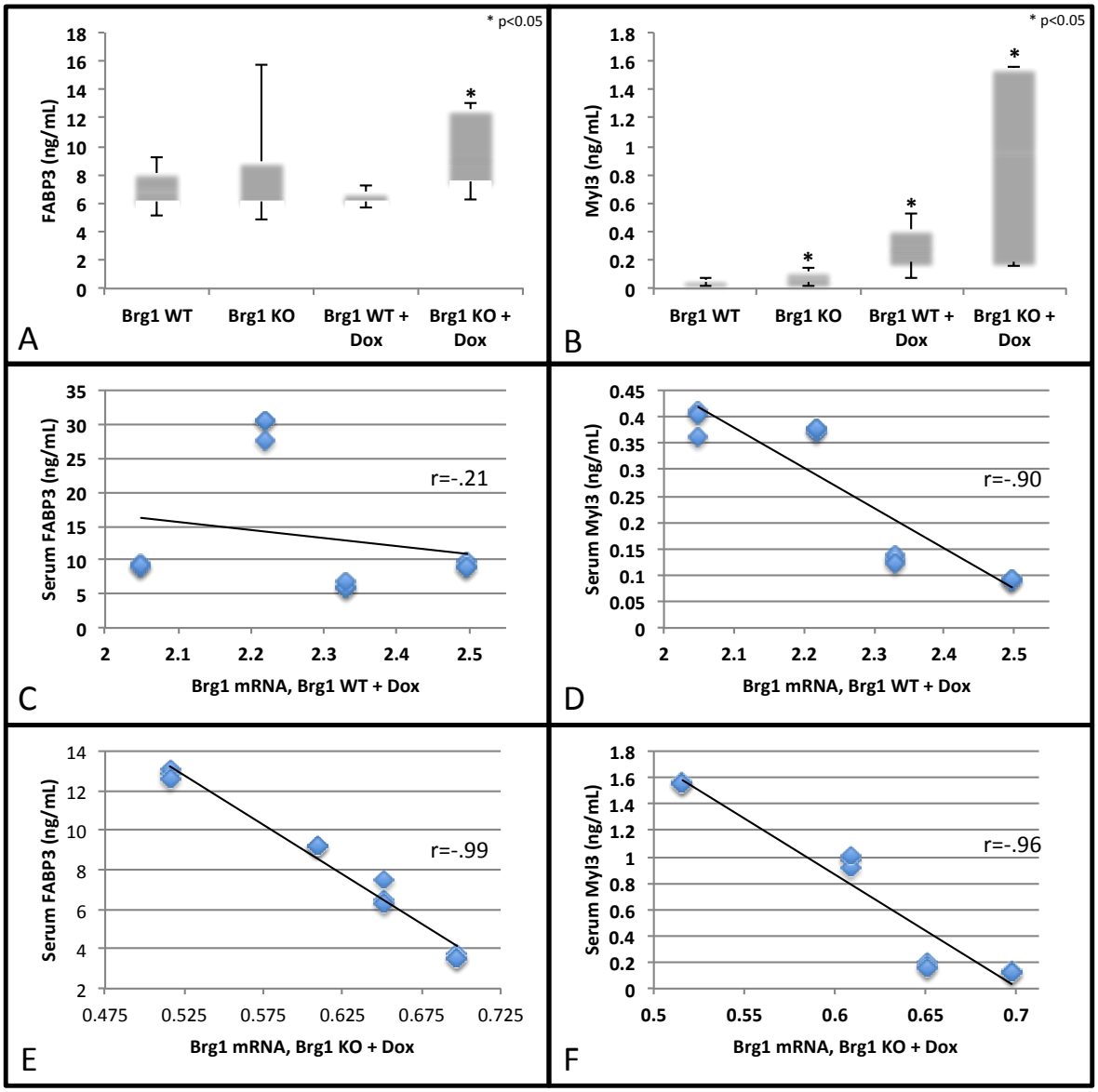

Figure 3.8: Cardiac biomarker analysis. Serum fatty acid binding protein 3 (FABP3) (A) and myosin light chain 3 (Myl3) (B) levels. Weak correlation is observed between relative Brg1 mRNA and FABP3 (C) or Myl3 (D), respectively, in Brg1 WT+Dox animals. Strong correlation was observed between relative Brg1 mRNA and FABP3 (E) or Myl3 (F), respectively, in Brg1 KO+Dox animals.

Discussion:

Heart failure is a global pandemic that is particularly associated with comorbidities such as diabetes and hypertension. Approximately 1 million people are hospitalized for heart failure ever year in the United States (Kazi and Mark 2013). A fraction of those patients are suffering from heart failure due to successful or ongoing treatment of cancer. Drug-induced cardiotoxicity is a well-known phenomenon in the safety assessment space; numerous medicines are known to cause or worsen cardiomyopathies and heart failure (Slordal and Spigset 2006, Pai and Nahata 2000). However, doxorubicin cardiotoxicity is currently the most widely studied of this phenomenon's causes. Doxorubicin's designation as one of the most potent anticancer drugs on the market warrants investigation into potential adjuvant palliative therapies or treatment modifications that would increase the maximum tolerated cumulative dose (Octavia et al. 2012a). Although the maximum cumulative dose recommended is reported as approximately 550mg/m^2 body surface area, patients have been reported to develop cardiotoxicity with a dose as low as 200mg/m^2 (Chatterjee et al. 2010, Friedman et al. 1978). Novel formulations of doxorubicin and adjuvant therapies have yet to sufficiently address cardiotoxicity concerns, which demand further investigation (Tacar et al. 2013). Despite these drawbacks, doxorubicin remains the first line of treatment, and in the case of some soft-tissue sarcomas including GISTs, liposarcomas, and dermatofibrosarcomas, one of the only lines of treatment in hopes of remission (Ray-Coquard and Le Cesne 2012).

Our study revealed the role of the Brg1 chromatin remodeling complex as a cardioprotective agent, which is not only required for normal cardiac homeostasis, but in the

protective response against doxorubicin cardiotoxicity. Previous groups have shown that Brg1 is not required for normal adult cardiac homeostasis in the mouse (Hang et al. 2010, Bultman et al. 2008). However, our data show that Brg1 knockout alone may be sufficient to impart decreased body weight gain, increased heart to body weight ratio, and an incidence and severity of lesions that is significantly above the wild-type control group (Figures 3.4-7). Furthermore, these data from the Brg1 knockout animals not treated with doxorubicin are on a scale in the incidence and severity of deleterious changes comparable to that of wild-type animals treated with doxorubicin, suggesting the absence of Brg1 and the treatment with doxorubicin induce similar changes within the cardiomyocyte.

Returning to the fetal paradigm, integrating the data from the Hang et al study of Brg1 in development and hypertrophy, it becomes clear that Brg1's function in cardiovascular development and disease is specific to the developmental paradigm or disease pathway (Hang et al. 2010). Indeed, it is shown here that Brg1 deletion increases the pathologic response to a stimulus (doxorubicin), whereas it is required to increase the pathologic response to a different stimulus (increased afterload). This paradox becomes even more interesting in light of data by De Angelis et al., who discovered that maintenance of stemness is protective in cardiac progenitor cells stressed with doxorubicin, though that program is precisely to be avoided according to the Hang et al. study (De Angelis et al. 2010, Hang et al. 2010). The data from De Angelis et al. suggests that Brg1, which was shown in the Hang et al. study to maintain the "fetal genome", is protective in cardiac progenitor cells as well as in the myocardium as a whole, as shown in the current work.

The results of the present study reveal a novel regulator in the pathogenesis of

doxorubicin cardiotoxicity. The graded response to the deletion of Brg1 also suggests the tamoxifen-inducible knockout mouse is a suitably sensitive model for the detection of cardiomyocyte toxicities. The necessity to minimize animal use and sample sufficient numbers for biomarker analysis prevented the evaluation of chronicity in this study, which may have significantly added value had there been an increased or decreased response based on Brg1 deletion. Future studies should attempt to address the translational aspect of the chronicity of the disease in human patients, which is not well modeled with this repeat-dose toxicity paradigm of short duration. Perhaps addition of study groups given extended recovery periods may elucidate other aspects of the doxorubicin cardiotoxicity phenomenon.

Chapter 3 References:

Berry, G., Billingham, M., Alderman, E., Richardson, P., Torti, F., Lum, B., Patek, A., and Martin, F. J. (1998). The use of cardiac biopsy to demonstrate reduced cardiotoxicity in AIDS Kaposi's sarcoma patients treated with pegylated liposomal doxorubicin. *Annals of oncology : official journal of the European Society for Medical Oncology / ESMO* 9(7), 711-6.

Billingham, M. E., Mason, J. W., Bristow, M. R., and Daniels, J. R. (1978). Anthracycline cardiomyopathy monitored by morphologic changes. *Cancer treatment reports* 62(6), 865-72.

Bristow, M. R., Mason, J. W., Billingham, M. E., and Daniels, J. R. (1981). Dose-effect and structure-function relationships in doxorubicin cardiomyopathy. *American heart journal* 102(4), 709-18.

Bultman, S. J., Herschkowitz, J. I., Godfrey, V., Gebuhr, T. C., Yaniv, M., Perou, C. M., and Magnuson, T. (2008). Characterization of mammary tumors from Brg1 heterozygous mice. *Oncogene* 27(4), 460-8, 10.1038/sj.onc.1210664.

Carvalho, F. S., Burgeiro, A., Garcia, R., Moreno, A. J., Carvalho, R. A., and Oliveira, P. J. (2013). Doxorubicin-Induced Cardiotoxicity: From Bioenergetic Failure and Cell Death to Cardiomyopathy. *Medicinal research reviews*, 10.1002/med.21280.

Chatterjee, K., Zhang, J., Honbo, N., and Karliner, J. S. (2010). Doxorubicin cardiomyopathy. *Cardiology* 115(2), 155-62, 10.1159/000265166.

Chen, B., Peng, X., Pentassuglia, L., Lim, C. C., and Sawyer, D. B. (2007). Molecular and cellular mechanisms of anthracycline cardiotoxicity. *Cardiovascular toxicology* 7(2), 114-21, 10.1007/s12012-007-0005-5.

Cheng, H., and Force, T. (2010). Molecular mechanisms of cardiovascular toxicity of targeted cancer therapeutics. *Circulation research* 106(1), 21-34, 10.1161/CIRCRESAHA.109.206920.

De Angelis, A., Piegari, E., Cappetta, D., Marino, L., Filippelli, A., Berrino, L., Ferreira-Martins, J., Zheng, H., Hosoda, T., Rota, M., Urbanek, K., Kajstura, J., Leri, A., Rossi, F., and Anversa, P. (2010). Anthracycline cardiomyopathy is mediated by depletion of the cardiac stem cell pool and is rescued by restoration of progenitor cell function. *Circulation* 121(2), 276-92, 10.1161/CIRCULATIONAHA.109.895771.

Desai, V. G., Herman, E. H., Moland, C. L., Branham, W. S., Lewis, S. M., Davis, K. J., George, N. I., Lee, T., Kerr, S., and Fuscoe, J. C. (2013). Development of doxorubicin-

induced chronic cardiotoxicity in the B6C3F1 mouse model. *Toxicology and applied pharmacology* 266(1), 109-21, 10.1016/j.taap.2012.10.025.

Du, W., Rani, R., Sipple, J., Schick, J., Myers, K. C., Mehta, P., Andreassen, P. R., Davies, S. M., and Pang, Q. (2012). The FA pathway counteracts oxidative stress through selective protection of antioxidant defense gene promoters. *Blood* 119(18), 4142-51, 10.1182/blood-2011-09-381970.

Friedman, M. A., Bozdech, M. J., Billingham, M. E., and Rider, A. K. (1978). Doxorubicin cardiotoxicity. Serial endomyocardial biopsies and systolic time intervals. *JAMA : the journal of the American Medical Association* 240(15), 1603-6.

Gharib, M. I., and Burnett, A. K. (2002). Chemotherapy-induced cardiotoxicity: current practice and prospects of prophylaxis. *European journal of heart failure* 4(3), 235-42.

Hang, C. T., Yang, J., Han, P., Cheng, H. L., Shang, C., Ashley, E., Zhou, B., and Chang, C. P. (2010). Chromatin regulation by Brg1 underlies heart muscle development and disease. *Nature* 466(7302), 62-7, 10.1038/nature09130.

Hayashi, S., and McMahon, A. P. (2002). Efficient recombination in diverse tissues by a tamoxifen-inducible form of Cre: a tool for temporally regulated gene activation/inactivation in the mouse. *Developmental biology* 244(2), 305-18, 10.1006/dbio.2002.0597.

Ho, L., and Crabtree, G. R. (2010). Chromatin remodelling during development. *Nature* 463(7280), 474-84, 10.1038/nature08911.

Jin, Z., Zhang, J., Zhi, H., Hong, B., Zhang, S., Guo, H., and Li, L. (2013). The beneficial effects of tadalafil on left ventricular dysfunction in doxorubicin-induced cardiomyopathy. *Journal of cardiology* 62(2), 110-6, 10.1016/j.jjcc.2013.03.018.

Kang, H., Cui, K., and Zhao, K. (2004). BRG1 controls the activity of the retinoblastoma protein via regulation of p21CIP1/WAF1/SDI. *Molecular and cellular biology* 24(3), 1188-99.

Kazi, D. S., and Mark, D. B. (2013). The economics of heart failure. *Heart failure clinics* 9(1), 93-106, 10.1016/j.hfc.2012.09.005.

Klein, P. M., and Dybdal, N. (2003). Trastuzumab and cardiac dysfunction: update on preclinical studies. *Seminars in oncology* 30(5 Suppl 16), 49-53.

Koh, C. M. (2013). Isolation of genomic DNA from mammalian cells. *Methods in enzymology* 529, 161-9, 10.1016/B978-0-12-418687-3.00013-6.

Laverty, H., Benson, C., Cartwright, E., Cross, M., Garland, C., Hammond, T., Holloway, C., McMahon, N., Milligan, J., Park, B., Pirmohamed, M., Pollard, C., Radford, J., Roome, N., Sager, P., Singh, S., Suter, T., Suter, W., Trafford, A., Volders, P., Wallis, R., Weaver, R.,

York, M., and Valentin, J. (2011). How can we improve our understanding of cardiovascular safety liabilities to develop safer medicines? *British journal of pharmacology* 163(4), 675-93, 10.1111/j.1476-5381.2011.01255.x.

Leung, J. Y., and Nevins, J. R. (2012). E2F6 associates with BRG1 in transcriptional regulation. *PloS one* 7(10), e47967, 10.1371/journal.pone.0047967.

Li, L., Liu, D., Bu, D., Chen, S., Wu, J., Tang, C., Du, J., and Jin, H. (2013). Brg1-dependent epigenetic control of vascular smooth muscle cell proliferation by hydrogen sulfide. *Biochimica et biophysica acta* 1833(6), 1347-55, 10.1016/j.bbamcr.2013.03.002.

Loughna, S., and Henderson, D. (2007). Methodologies for staining and visualisation of beta-galactosidase in mouse embryos and tissues. *Methods Mol Biol* 411, 1-11.

Moslehi, J., and Cheng, S. (2013). Cardio-oncology: it takes two to translate. *Science translational medicine* 5(187), 187fs20, 10.1126/scitranslmed.3006490.

Octavia, Y., Brunner-La Rocca, H. P., and Moens, A. L. (2012). NADPH oxidase-dependent oxidative stress in the failing heart: From pathogenic roles to therapeutic approach. *Free radical biology & medicine* 52(2), 291-7, 10.1016/j.freeradbiomed.2011.10.482.

Octavia, Y., Tocchetti, C. G., Gabrielson, K. L., Janssens, S., Crijns, H. J., and Moens, A. L. (2012). Doxorubicin-induced cardiomyopathy: from molecular mechanisms to therapeutic strategies. *Journal of molecular and cellular cardiology* 52(6), 1213-25, 10.1016/j.yjmcc.2012.03.006.

Oka, T., Xu, J., and Molkentin, J. D. (2007). Re-employment of developmental transcription factors in adult heart disease. *Seminars in cell & developmental biology* 18(1), 117-31, 10.1016/j.semcdb.2006.11.012.

Pai, V. B., and Nahata, M. C. (2000). Cardiotoxicity of chemotherapeutic agents: incidence, treatment and prevention. *Drug safety : an international journal of medical toxicology and drug experience* 22(4), 263-302.

Rajabi, M., Kassiotis, C., Razeghi, P., and Taegtmeyer, H. (2007). Return to the fetal gene program protects the stressed heart: a strong hypothesis. *Heart failure reviews* 12(3-4), 331-43, 10.1007/s10741-007-9034-1.

Ray-Coquard, I., and Le Cesne, A. (2012). A role for maintenance therapy in managing sarcoma. *Cancer treatment reviews* 38(5), 368-78, 10.1016/j.ctrv.2011.07.003.

Roca-Alonso, L., Pellegrino, L., Castellano, L., and Stebbing, J. (2012). Breast cancer treatment and adverse cardiac events: what are the molecular mechanisms? *Cardiology* 122(4), 253-9, 10.1159/000339858.

Schunke, K. J., Coyle, L., Merrill, G. F., and Denhardt, D. T. (2013). Acetaminophen attenuates doxorubicin-induced cardiac fibrosis via osteopontin and GATA4 regulation: Reduction of oxidant levels. *Journal of cellular physiology*, 10.1002/jcp.24367.

Sena, J. A., Wang, L., and Hu, C. J. (2013). BRG1 and BRM chromatin remodeling complexes regulate the hypoxia response by acting as a co-activator for a subset of HIF target genes. *Molecular and cellular biology*, 10.1128/MCB.00731-13.

Shi, Y., Moon, M., Dawood, S., McManus, B., and Liu, P. P. (2011). Mechanisms and management of doxorubicin cardiotoxicity. *Herz* 36(4), 296-305, 10.1007/s00059-011-3470-3.

Siegel, R., Naishadham, D., and Jemal, A. (2013). Cancer statistics, 2013. *CA: a cancer journal for clinicians* 63(1), 11-30, 10.3322/caac.21166.

Singal, P. K., and Iliskovic, N. (1998). Doxorubicin-induced cardiomyopathy. *The New England journal of medicine* 339(13), 900-5, 10.1056/NEJM199809243391307.

Slordal, L., and Spigset, O. (2006). Heart failure induced by non-cardiac drugs. *Drug safety : an international journal of medical toxicology and drug experience* 29(7), 567-86.

Soriano, P. (1999). Generalized lacZ expression with the ROSA26 Cre reporter strain. *Nature genetics* 21(1), 70-1, 10.1038/5007.

Sumi-Ichinose, C., Ichinose, H., Metzger, D., and Chambon, P. (1997). SNF2beta-BRG1 is essential for the viability of F9 murine embryonal carcinoma cells. *Molecular and cellular biology* 17(10), 5976-86.

Tacar, O., Sriamornsak, P., and Dass, C. R. (2013). Doxorubicin: an update on anticancer molecular action, toxicity and novel drug delivery systems. *The Journal of pharmacy and pharmacology* 65(2), 157-70, 10.1111/j.2042-7158.2012.01567.x.

Trotter, K. W., and Archer, T. K. (2008). The BRG1 transcriptional coregulator. *Nuclear receptor signaling* 6, e004, 10.1621/nrs.06004.

Ventura, A., Kirsch, D. G., McLaughlin, M. E., Tuveson, D. A., Grimm, J., Lintault, L., Newman, J., Reczek, E. E., Weissleder, R., and Jacks, T. (2007). Restoration of p53 function leads to tumour regression in vivo. *Nature* 445(7128), 661-5, 10.1038/nature05541.

Volkova, M., and Russell, R., 3rd (2011). Anthracycline cardiotoxicity: prevalence, pathogenesis and treatment. *Current cardiology reviews* 7(4), 214-20.

Wang, Y., Zheng, D., Wei, M., Ma, J., Yu, Y., Chen, R., Lacefield, J. C., Xu, H., and Peng, T. (2013). Over-expression of calpastatin aggravates cardiotoxicity induced by doxorubicin. *Cardiovascular research* 98(3), 381-90, 10.1093/cvr/cvt048.

Xu, J., Lei, S., Liu, Y., Gao, X., Irwin, M. G., Xia, Z. Y., Hei, Z., Gan, X., Wang, T., and Xia, Z. (2013). Antioxidant N-acetylcysteine attenuates the reduction of brg1 protein expression in the myocardium of type 1 diabetic rats. *Journal of diabetes research* 2013, 716219, 10.1155/2013/716219.

Chapter 4

Detection of Unique Transcriptional Pathways Associated with the Interplay Between Doxorubicin Cardiotoxicity and Brg1 Deletion in Mice

Abstract:

Cardiotoxicity is an important and poorly-understood side effect of doxorubicin chemotherapy; its predictable toxicity limits the use of the efficacious anthracycline drug and others in its class. A role for Brg1 in adult cardiac homeostasis and doxorubicin cardiotoxicity is not well-investigated, and may be a drug discovery avenue for toxicity prevention or amelioration. A mouse model of repeat-dose doxorubicin-induced cardiac toxicity was employed to initiate cardiomyocyte damage. Wild-type and Brg1 deleted mice were subjected to the repeat-dose cardiotoxicity protocol, and cardiac tissue was harvested for gene expression analysis. Agilent mouse whole genome arrays representing 43,379 genes were used to identify differentially expressed genes (DEGs) in groupwise comparisons with doxorubicin treatment and/or Brg1 deletion as variables; 1501 genes unique to the groupwise comparisons were identified. Network enrichment yielded canonical and novel aspects of heart disease, muscle phenotype, and ubiquitin-mediated proteolysis responses. Of the novel genes previously unidentified in relation to doxorubicin cardiotoxicity, Brg1 lowered expression of Sin3β and Alox12 which function in cellular stability but have not previously been shown to be regulated by Brg1. Brg1 also blunted the differential expression of Dnmt3a and Cdkn1b; these genes were not significantly differentially expressed in groupwise comparisons with Brg1 expression intact. These novel gene associations may be

important in discovering new targets for abrogating doxorubicin cardiotoxicity.

Introduction:

Cardiotoxicity is a devastating side effect to those administered doxorubicin for the treatment of a variety of different cancers (Slordal and Spigset 2006, Laverty *et al*. 2011, Cheng and Force 2010). The exact mechanisms of doxorubicin cardiotoxicity have not been elucidated to date; reactive oxygen species generation, DNA intercalation and helicase disruption, and triggering of apoptosis are among several mechanisms implicated (Carvalho et al 2013, Octavia et al 2013a, Tacar et al 2013).

The previous work (Chapter 3) has emulated this toxicity in a mouse model of repeat-dose doxorubicin toxicity. Interestingly, it also elucidated the necessity of Brg1 for normal adult cardiac homeostasis, and demonstrated the cardiac lesions resulting from Brg1 deletion. Furthermore, these lesions were not dissimilar from lesions induced by repeat-dose doxorubicin treatment. Previous work from other laboratories has stated Brg1 is not required for adult cardiomyocyte homeostasis; the current work has shed light on new findings regarding this assumption (Bultman et al. 2000). There is no current published work detailing the interplay, if any exists, between doxorubicin cardiotoxicity and the presence or deletion of Brg1. Previous work (Chapter 2) demonstrated Brg1 is required for genome stability during the middle stages of development, and disruption of genome surveillance during this period leads to the lethal phenotypes observed. Later work demonstrated this deletion in adulthood lead to cardiomyocyte degeneration, with morphology akin to that observed due to doxorubicin toxicity in the same experiment (Chapter 3). Examination of

the gene expression similarities and dissimilarities between all these seemingly disparate events may suggest common mechanisms between development and cardiotoxicity. Additionally, this type of investigation may elucidate as yet undescribed causal or protective links between Brg1 expression and doxorubicin cardiotoxicity.

The current study seeks to examine the tissues from animals that have been subjected to an experiment in which both Brg1 deletion and repeat-dose doxorubicin cardiotoxicity have been implemented and controlled for, in order to elucidate genes identified through this unique experimental paradigm (see Chapter 3). Groupwise comparisons between the four different experimental groups made by combinations of doxorubicin or vehicle treatment with and without Brg1 deletion will enable comparison of confirmatory gene expression signals (i.e. lower expression of Brg1 in the Brg1 deletion animals) in concert with differentially expressed gene sets not previously examined (i.e. doxorubicin treatment of Brg1 deletion animals).

Materials and Methods:

Institutional Compliance Statement:

All animals were housed in AAALAC-accredited animal facilities. All animal procedures were conducted in compliance with the Animal Welfare Act Regulations, 9 CFR 1-4. All animals were handled and treated according to the *Guide for the Care and Use of Laboratory Animals, 8th ed*. (ILAR). Animals were multi-housed (breeding pairs or trios, up to 5 weanlings housed by sex) in 17 cm wide by 28 cm long and 13 cm high (476 cm^2 area)

polycarbonate cages with microisolator tops. Cages were supplied with absorbent heat-treated hardwood bedding (Northeastern Products Corp., Warrensburg, NY), which were changed twice weekly. Animals were fed Purina Rodent Diet No. 5001 *ad libitum* (Breeding). The diet was routinely analyzed for nutritional components. Reverse osmosis treated tap water was supplied *ad libitum* in polycarbonate water bottles with stainless steel sipper tubes, which was changed once weekly.

Animal room temperature ranges was kept between 20 and 25°C, with a relative humidity of 30-70%. . Animals were exposed to a 12-hour light cycle followed by a 12-hour dark cycle. For enrichment, cotton fiber nestlets (Ancare Corp., Bellmore, NY) was supplied to the animals *ad libitum*.

The NIH's ARAC Guidelines for Endpoints in Animal Study Protocols, Morbidity section was followed for all animals. Any test animals experiencing minimal or transient pain or distress were evaluated and/or euthanized.

Drug formulations and administration:

Tamoxifen citrate (Sigma-Aldrich) will be dissolved in corn oil for dosing at 75 or 100mg/kg; total dose volume is 60-100 uL in corn oil. Pharmaceutical grade doxorubicin hydrochloride (Sigma-Aldrich; 98-102% by HPLC) was dissolved in 0.9% sterile saline for dosing at 4mg/kg; total dose volume was 100 uL.

Selection of Animals:

Tamoxifen toxicity testing:

B6.129-*Gt(ROSA)26Sor*$^{tm1(cre/ERT2)Tyj}$/J mice containing a Cre-ER^{T2} cassette (shorthand: ROSA-cre/ERT2) were crossed with B6.129S4-Gt(ROSA)26Sor^{tm1Sor}/J mice containing a polyA sequence (STOP sequence) flanked by *loxP* sites (shorthand: ROSA-stop) (Soriano 1999, Ventura et al 2007). Tamoxifen toxicity testing was performed in unmated mice, beginning with a tamoxifen citrate (Sigma-Aldrich) intraperitoneal (IP) dose level of 225-mg/kg body weight. To distinguish potential Cre toxicity from possible tamoxifen toxicity, and to establish a lowest observed adverse effects level (LOAEL) and a no observed adverse effect level (NOAEL), unmated adult ROSA-stop animals (without Cre) were dosed IP with 225, 150 and 100 mg/kg of body weight tamoxifen (10 ml/kg dosing volume). Animals received a total of two injections over two consecutive days. Body weights were collected prior to dosing and weekly for a total of 3 weeks (the length of time needed for a mother to raise a litter). Animals were observed daily for health effects. Mice receiving the 225 and 150 mg/kg dose levels were either found dead or were euthanized as moribund. Mice tolerated the tamoxifen dose level of 100 mg/kg for two consecutive days without evidence of tamoxifen toxicity on weight gain or tissue morphology. Having determined the LOAEL to be 150 mg/kg, and the NOAEL to be 100mg/kg in this study, 100 mg/kg of body weight tamoxifen citrate was selected as the maximum dose to be used in future studies.

Cre recombination evaluation:

ROSA-cre/ERT2 mice (B6.129-Gt(ROSA)26Sor$^{tm1(cre/ERT2)Tyj}$/J) were bred with ROSA-stop reporter mice (B6.129S4-Gt(ROSA)26Sor^{tm1Sor}/J). Pregnant females were dosed with 100

mg/kg tamoxifen on different embryonic days and fetuses were collected for measuring B-galactosidase activity in the double transgenic embryos (B6.129S4-Gt(ROSA)26Sor^{tm1Sor}/J Tg(B6.129-Gt(ROSA)26Sor$^{tm1(cre/ERT2)Tyj}$)) as a measure of Cre recombinase activity as previously described (Loughna and Henderson 2007). ROSA-cre/ERT2 x ROSA-stop double transgenic embryos exhibited ubiquitous strong positive *lacZ* staining while their ROSA-stop embryo littermates showed negative staining at various developmental stages (data not shown). Significant Cre activity was absent in adults in crossings of B6;128S2-Smarca4^{tm1Pcn}/Mmnc mice (shorthand Brg1 fl/fl) with B6.129-*Gt(ROSA)26Sor$^{tm1(cre/ERT2)Tyj}$*/J mice (data not shown). The B6.Cg-Tg(CAG-cre/Esr1*)5Amc/J mouse (shorthand: CAG-Cre/Esr1*) contains a Cre-ER^{TM} cassette system driven by a CMV immediate-early enhancer coupled with a chicken a-actin/rabbit B-globulin hybrid promoter was selected for adult cre recombinetic studies (Hayashi and McMahon 2002). For re-evaluation of Cre recombinetics and comparison to concurrent Cre studies, Male CAG-Cre/Esr1* mice were crossed with female B6.129S4-Gt(ROSA)26Sor^{tm1Sor}/J mice; two pregnant females were administered a single IP 100 mg/kg tamoxifen citrate dose on embryonic day 6.5 (E6.5) for collection at E9.5. Two pregnant females were administered IP tamoxifen citrate doses of 100mg/kg once daily on E12.5 and E13.5 for collection at E15.5. Two additional pregnant females were allowed to pup; at seven weeks of age F1 pups were administered 75mg/kg tamoxifen citrate IP once daily for five consecutive days. F1 offspring of the Male CAG-Cre/Esr1* mice crossed with female B6.129S4-Gt(ROSA)26Sor^{tm1Sor}/J mice dosed at 7 weeks of age were euthanized at 9 weeks of age. Hearts from these mice were frozen in Tissue-Tek® OCT media (Electron Microscopy Services, Inc.), sectioned at 5um, and mounted on positively-

charged glass slides for evaluating B-galactosidase activity as a measure of Cre recombinase activity as previously described (Loughna and Henderson 2007). B6.129S4-Gt(ROSA)26Sor^{tm1Sor}/J Tg B6.129-Gt(ROSA)26Sor$^{tm1(cre/ERT2)Tyj}$ fetuses treated in utero were collected for evaluating B-galactosidase activity in whole mounts as a measure of Cre recombinase activity as previously described (Loughna and Henderson 2007).

Genotyping:

For BRG1 genotyping, three primers were used to amplify wild type (241bp PCR product), floxed (387bp PCR product) and deleted (313bp PCR product) BRG1 alleles; P1-GTCATACTTATGTCATAGCC, P2- GCCTTGTCTCAAACTGATAAG, P3-GATCAGCTCATGCCCTAAGG (REF). For Cre genotyping, the forward (5'-GCGGTCTGGCAGTAAAAACTATC-3') and the reverse (5'-GTGAAACAGCATTGCTGTCACTT-3') primer were used for PCR amplification (Sumi-Ichinose et al 1997). Genomic DNA was obtained by phenol extraction of DNA from tail tips obtained postmortem as previously described (Koh 2013).

Doxorubicin dose level justification:

Conversion of dose levels reported by Friedman *et al.* (JAMA 1976) to cause cardiomyocyte vacuolation, t-tubule dilatation, and intrasarcoplasmic swelling using the Center for Drug Evaluation and Research's guide *Estimating the maximum safe starting dose in initial clinical trials for therapeutics in adult healthy volunteers* (CDER 2005), allowing for construction of a repeat-dose toxicity paradigm, yielded a five-week protocol with twice-

weekly 4mg/kg IP doses of doxorubicin hydrochloride. In a pilot study, 3 Adult male Cre-Brg1 floxed mice (B6.Cg-Tg(CAG-cre/Esr1*)5Amc/J Tg B6;128S2-Smarca4^{tm1Pcn}/Mmnc) and 3 adult male Brg1 floxed mice (B6;128S2-Smarca4^{tm1Pcn}/Mmnc) were given 75 mg/mL tamoxifen citrate IP once daily for 5 consecutive days. Following a two week recovery period to allow for recombination, mice were administered 4mg/kg doxorubicin IP twice weekly for 5 weeks (cumulative dose: 40mg/kg; ~180mg/m^2) (CDER 2005, Desai et al. 2013). Bright field and electron microscopic examination of myocardial tissue from treated animals revealed more widespread and severe lesions in Cre-Brg1 floxed mice than Brg1 floxed mice, including cardiomyocyte vacuolation, t-tubule dilatation, and intrasarcoplasmic swelling (data not shown), similar to that described by Friedman et al. and reported herein and by other groups (Friedman et al. 1978, Desai et al. 2013).

Experimental design:

To detect a 2-fold increase or decrease in RNA expression with at least a 90% power assuming expression is log-normal distribution, 5 animals per group were required for biochemical analyses (Table 3.1). Five animals per group were also required for similar histopathologic and protein analyses, respectively; a total of 15 animals per treatment group were utilized for this study.

Table 4.1: Treatment Group Designations and Dosage Levels

Group #	Shorthand	Genotype	No. of Animals	Tamoxifen Dose Level	Tamoxifen Doses	Doxorubicin Dose Level	Doxorubicin Doses
1	Brg1 WT	B6;128S2-Smarca4^{tm1Pcn}/Mmnc	15	75 mg/kg	5		
2	Brg1 KO	B6.Cg-Tg(CAG-cre/Esr1*)5Amc/J Tg B6;128S2-Smarca4^{tm1Pcn}/Mmnc	15	75 mg/kg	5		
3	Brg1 WT + Dox	B6.Cg-Tg(CAG-cre/Esr1*)5Amc/J Tg B6;128S2-Smarca4^{tm1Pcn}/Mmnc	15			4 mg/kg	10
4	Brg1 KO + Dox	B6.Cg-Tg(CAG-cre/Esr1*)5Amc/J Tg B6;128S2-Smarca4^{tm1Pcn}/Mmnc	15	75 mg/kg	5	4 mg/kg	10

Thirty adult male Cre-Brg1 floxed mice (B6.Cg-Tg(CAG-cre/Esr1*)5Amc/J Tg B6;128S2-Smarca4^{tm1Pcn}/Mmnc) (Groups 2 and 4) and 15 adult male Brg1 floxed mice (B6;128S2-Smarca4^{tm1Pcn}/Mmnc) (Group 1) were given 75 mg/mL tamoxifen citrate IP once daily for 5 consecutive days; 15 Cre-Brg1 floxed mice (B6.Cg-Tg(CAG-cre/Esr1*)5Amc/J Tg B6;128S2-Smarca4^{tm1Pcn}/Mmnc) (Group 3) received an equal volume of sterile saline (~60-100 uL) as a vehicle control. Following a two week recovery period to allow for recombination, Group 3 and Group 4 mice were administered 4mg/kg doxorubicin hydrochloride IP twice weekly for 5 weeks; Groups 1 and 2 received an equal volume of IP sterile saline (100 uL) as a vehicle control (Figure 3.1).

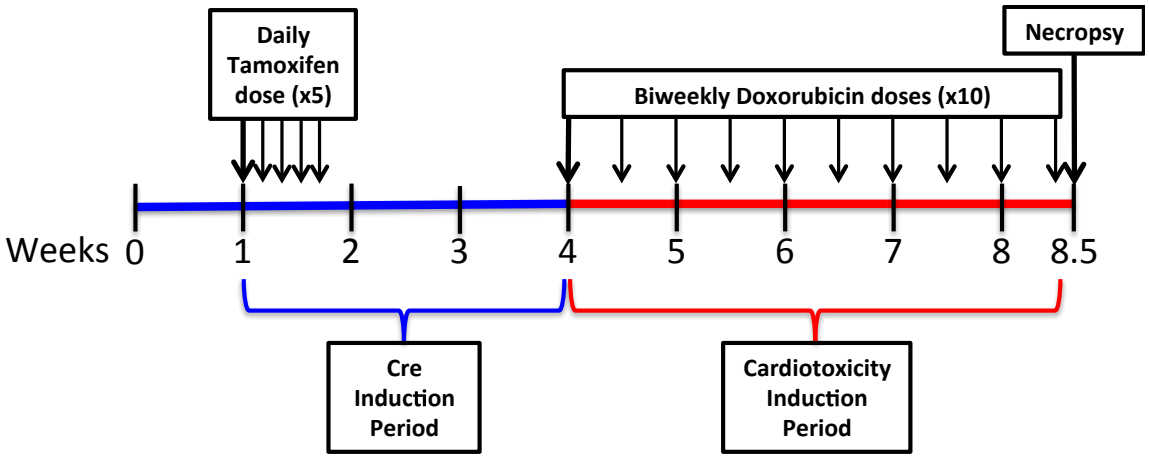

Figure 3.1: Brg1 KO repeat-dose doxorubicin cardiotoxicity study design. Animals receive five 75mg/kg tamoxifen doses for cre induction. After recombination, animals receive 4mg/kg doxorubicin twice weekly for 5 weeks.

In-life observations: Mice were weighed before injections, every 24 hours during treatment periods, and at the time of euthanasia. The ARAC Guidelines for Endpoints, Morbidity section were followed, including, but not limited to, the clinical signs described in section 1b (i.e. Rapid or progressive weight loss, edema, sizable abdominal enlargement or ascites, progressive dermatitis, lethargy or persistent recumbency, coughing, labored breathing, nasal discharge, jaundice, cyanosis, and/or pallor/anemia, neurological signs, bleeding from any orifice, self-induced trauma, any condition interfering with eating or drinking, ambulation, or elimination, excessive or prolonged hyperthermia or hypothermia).

Euthanasia and Blood collection:

Euthanasia was accomplished using CO_2 asphyxiation followed by decapitation according to the NIEHS "Guidelines for Euthanasia" and using a metered CO_2 line. The abdominal aorta was revealed via midline thoracoperitoneotomy, and blood removed from the abdominal aorta using a 3-5cc syringe with a 23-gauge needle.

RNA analysis:

Hearts minced and frozen in RNALater (Qiagen) at -80 degrees Celsius at necropsy were thawed on ice and homogenized in Trizol (Invitrogen) using a Tissue Tearor Homogenizer (Biospec Products, Inc.). Homogenates were then processed with the Qiagen RNeasy Mini kit following the manufacturer's instructions. RNA was isolated from whole hearts in Trizol (Invitrogen) using a Superscript III Reverse Transcriptase (Invitrogen) to synthesize cDNA from 2 ug of RNA, and real-time PCR was performed with Brilliant III SYBR Green Master Mix (Agilent) on a Stratagene Mx3000P for evaluation of Brg1 expression levels and validation of targets elucidated through microarray analysis including Acta2, Cacna1g, Casq1, Cdkn1b, Ceacam1, Col6a2, Hist1h1c, Il1b, Itga3, Kit, Nes, Nr1d1, Plekhn1, S100a8, S100a9, Slc25a35, Slc35a4, Smarca4, Tecr, Tgfb1, and Ttn (Appendix 1).

Microarray analysis:

For microarray analysis, Trizol-isolated RNA was cleaned-up using the RNeasy Midi kit (Qiagen) and submitted to the Microarray Group of the NIEHS Molecular Genomics Core. Gene expression analysis was conducted using Agilent Whole Mouse Genome 4x44

multiplex format oligo arrays (014868) (Agilent) following the Agilent 1-color microarray-based gene expression analysis protocol. Starting with 500ng of total RNA, Cy3 labeled cRNA was produced according to manufacturer's protocol. Samples were staggered across Agilent chips to control for chip to chip variation. For each sample, 1.65ug of Cy3 labeled cRNAs were fragmented and hybridized for 17 hours in a rotating hybridization oven. Slides were washed and then scanned with an Agilent Scanner. Data was obtained using the Agilent Feature Extraction software (v9.5), using the 1-color defaults for all parameters. The Agilent Feature Extraction Software performed error modeling, adjusting for additive and multiplicative noise. The resulting data were processed using OmicSoft Array Studio (Version 6.0) software.

Results:

Microarray analysis of heart tissue was used in this experiment to rapidly assess expression levels of 43,379 genes to determine if expression changed due to gene manipulation and/or treatment with a cardiotoxin. Raw Agilent data was quantile corrected for pairwise comparisons (Figure 4.1A). Differentially expressed genes and groupwise commonalities were investigated for ≥1.5 fold-change at $p<0.01$ to yield 1501 significant differentially expressed genes (DEGs) (Figure 4.1B). Cluster analysis revealed patterns of DEGs in a similar trend under the conditions of Brg1 knockout or doxorubicin treatment (Figure 4.1C). Clusters of genes appeared to change in expression directionally, with an increased effect of this expression as first Brg1 is deleted, followed by treatment with doxorubicin, and finally, both deletion of Brg1 and treatment with doxorubicin (Figure 4.1C). Analysis also revealed three distinct DEG groups: doxorubicin-induced DEGs that require Brg1 ("A not C"), doxorubicin-induced DEGs blocked by Brg1 ("C not A"), and doxorubicin-induced DEGs independent of Brg1 ("A and C") (Figure 4.1D).

Among the genes implicated in doxorubicin toxicity that are Brg1 dependent ("A not C"), changes in expression included increases in Casq1, S100a9, and Il-1β, and decreases in Kit. A full complement of Brg1 blocked doxorubicin-induced increases in Sin3β and Alox12, as well as decreases in Dnmt3a and Cdnk1b ("C not A"). Increases in Dusp4 expression and decreases in Gata4 expression due to doxorubicin administration appeared independent of Brg1 expression ("A and C"). Expectedly, changes in Brg1 expression were only observed in groupwise comparisons where Brg1 was deleted in one comparison ("B and D"; Figure 4.1B); indeed it was the single DEG in that group.

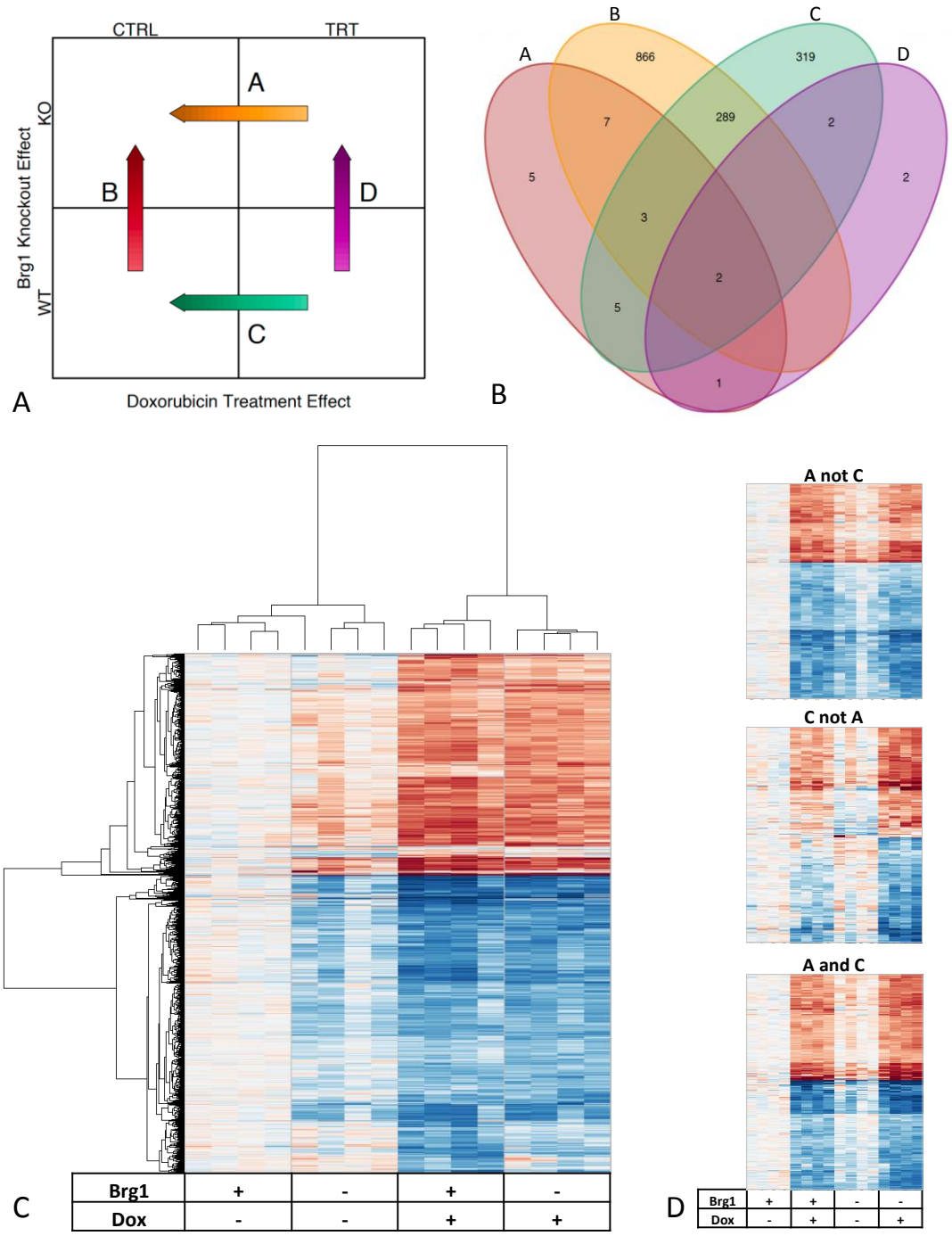

Figure 4.1: Microarray analysis. Pairwise comparisons (A) and the genes sets yielded based on comparisons (B). Gene signature gradation correlation from loss of Brg1 to treatment with doxorubicin (C). Doxorubicin-induced changes that require Brg1 ("A not C"), doxorubicin-induced changes blocked by Brg1 ("C not A"), and doxorubicin-induced changes independent of Brg1 ("A and C") (D).

For microarray validation, rt-PCR results from select genes differentially expressed in the array were analyzed, and the groupwise comparisons of the rt-PCR data were plotted against the array results (Figure 4.2A). This took into account magnitude of change both of the treatment and corresponding comparator group; the genes analyzed for this validation appeared correlative (Figures 4.2B, C).

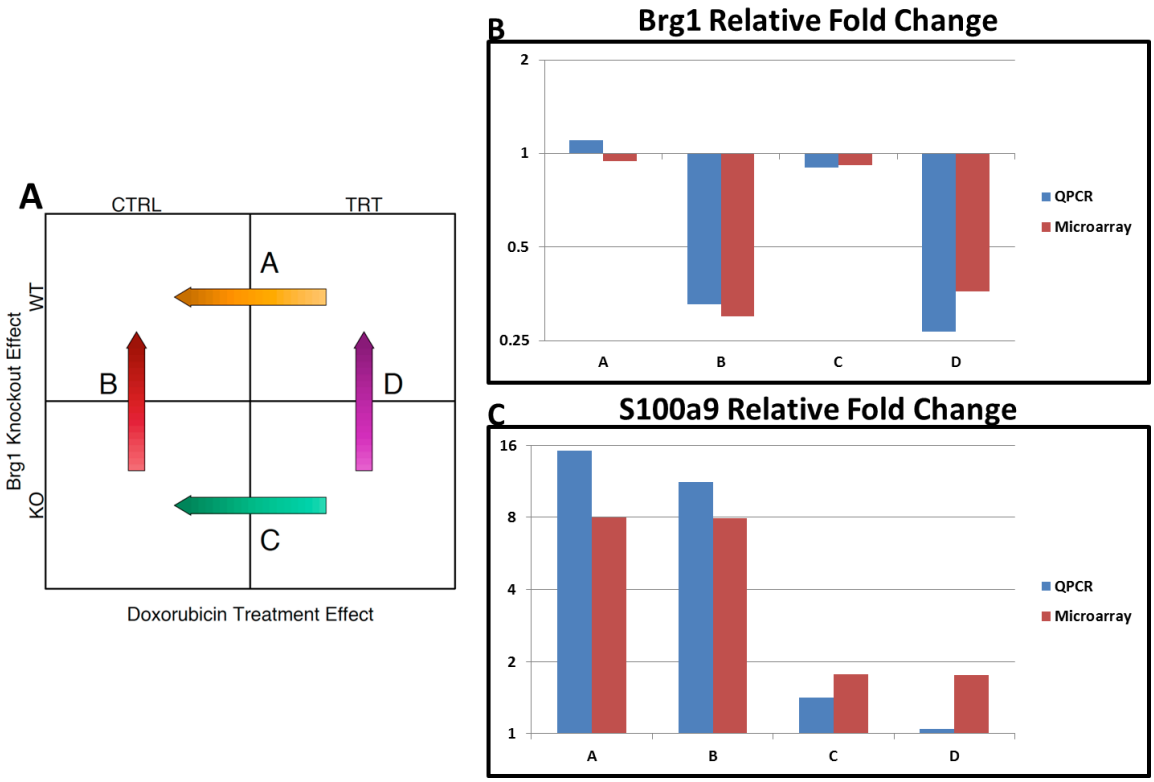

Figure 4.2: rt-PCR of select validation genes. Pairwise comparisons (A) and comparative validation of the relative fold change of Brg1 (B) and S100a9 (C) in those comparisons by rt-PCR and microarray analysis.

Network analysis using Ingenuity Pathway Analysis tools was performed for various groupwise comparisons across the experiments. Common DEG pathways in doxorubicin administration in both groupwise comparisons of wild-type mice and knockout mice ("A and

C") included those associated with inflammation, apoptosis, proliferation, oxidative stress, drug response, cell adhesion, and metabolism (Figure 4.3).

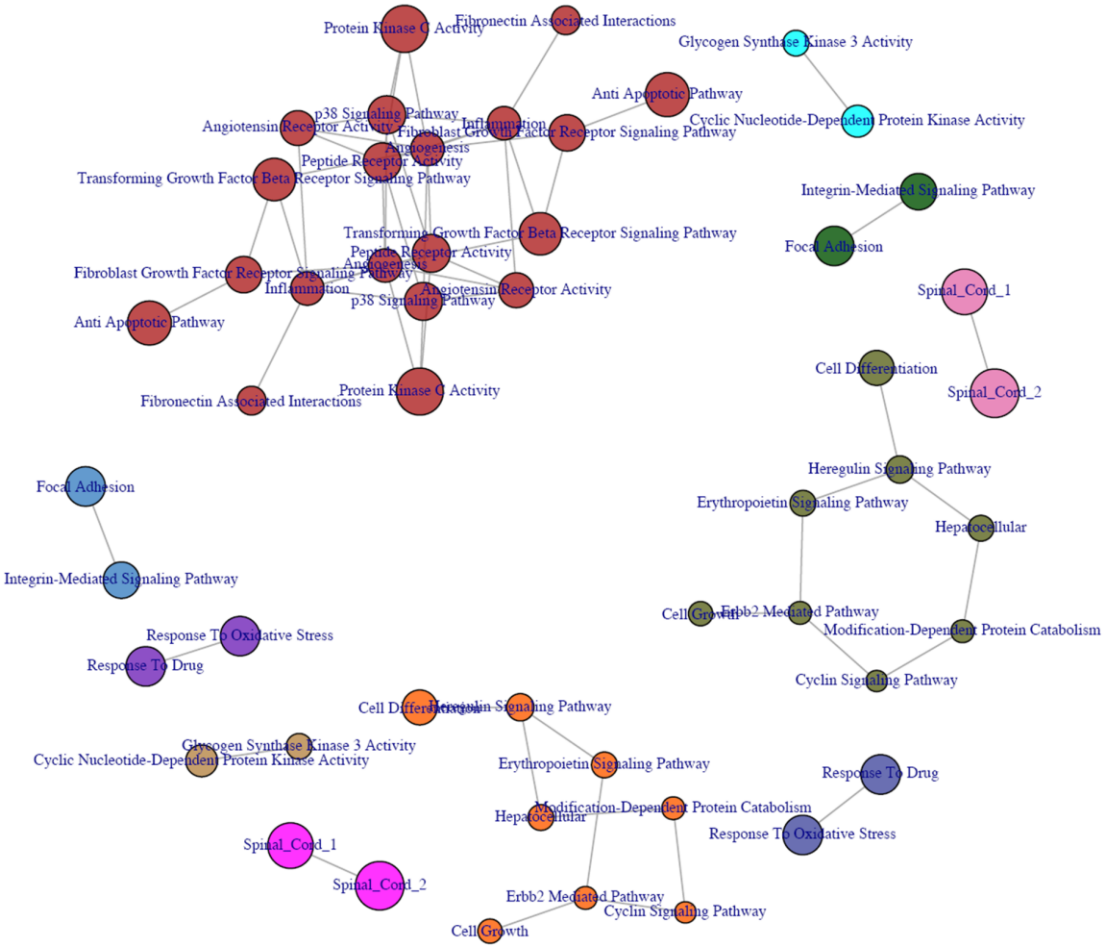

Figure 4.3: Enriched networks for doxorubicin-induced gene expression changes in both wild-type and Brg1 deletion mice. Cardiac gene expression changes induced by doxorubicin treatment independent of Brg1 gene deletion.

Common DEG pathways in groupwise comparisons of the effect of Brg1 deletion or doxorubicin administration ("A and B") included canonical and nonspecific pathways such as the JAK-Stat signaling cascade, and MAP kinase signaling and its upstream regulators

including TGF-β (Figure 4.4). This network was also enriched for inflammatory pathways through receptors lacking intrinsic tyrosine kinase activity, such as Il-1β.

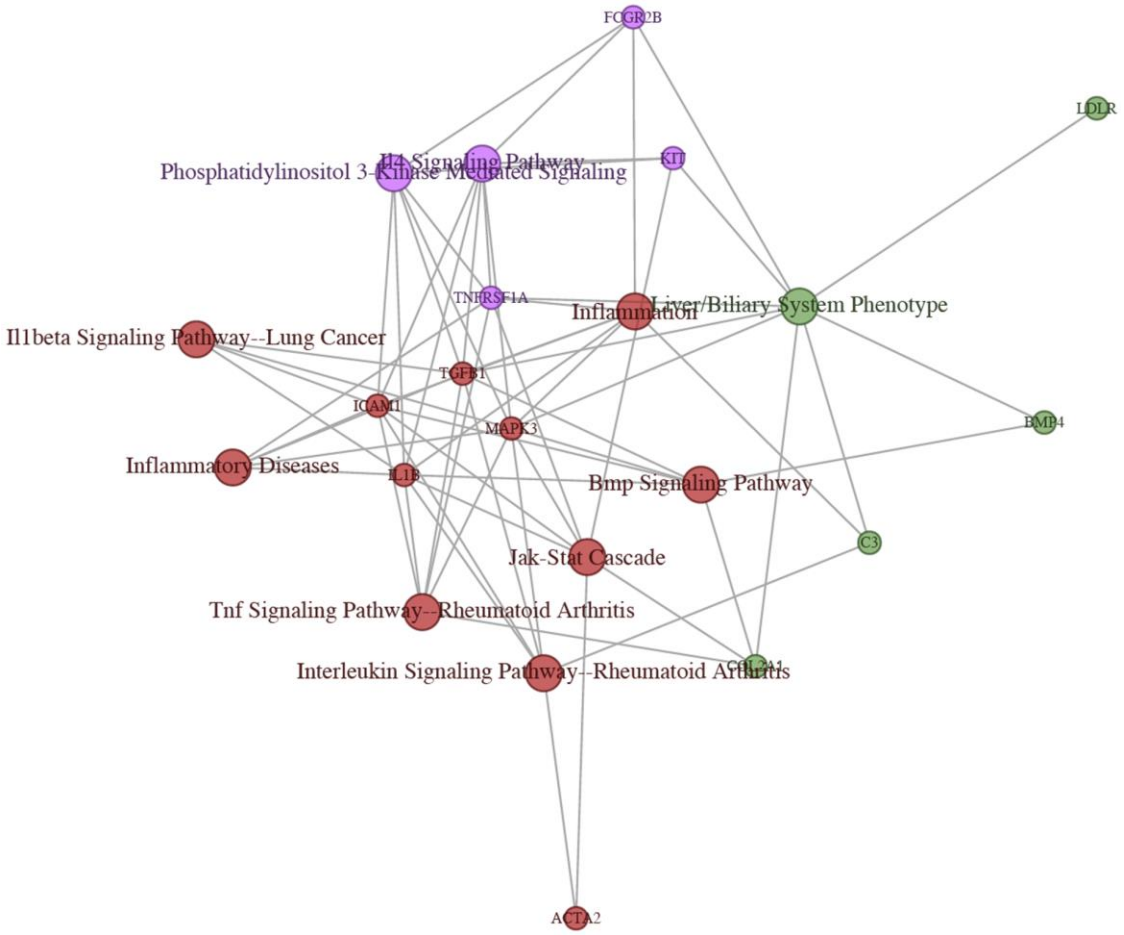

Figure 4.4: Enriched networks for doxorubicin-induced or Brg1 deletion-induced gene expression changes. Canonical cell-signaling pathways are enriched either by doxorubicin treatment or by Brg1 deletion.

Network analysis of pathways enriched in the groupwise comparison of DEGs due to doxorubicin treatment, which were significant only when Brg1 deletion animals were treated with doxorubicin ("C not A"), revealed highly-enriched networks in, the heart and muscle,

the systems of primary interest in this experiment (Figure 4.5A). Additional enriched networks regarding ubiquitin-mediated proteolysis events were revealed (Figure 4.5B).

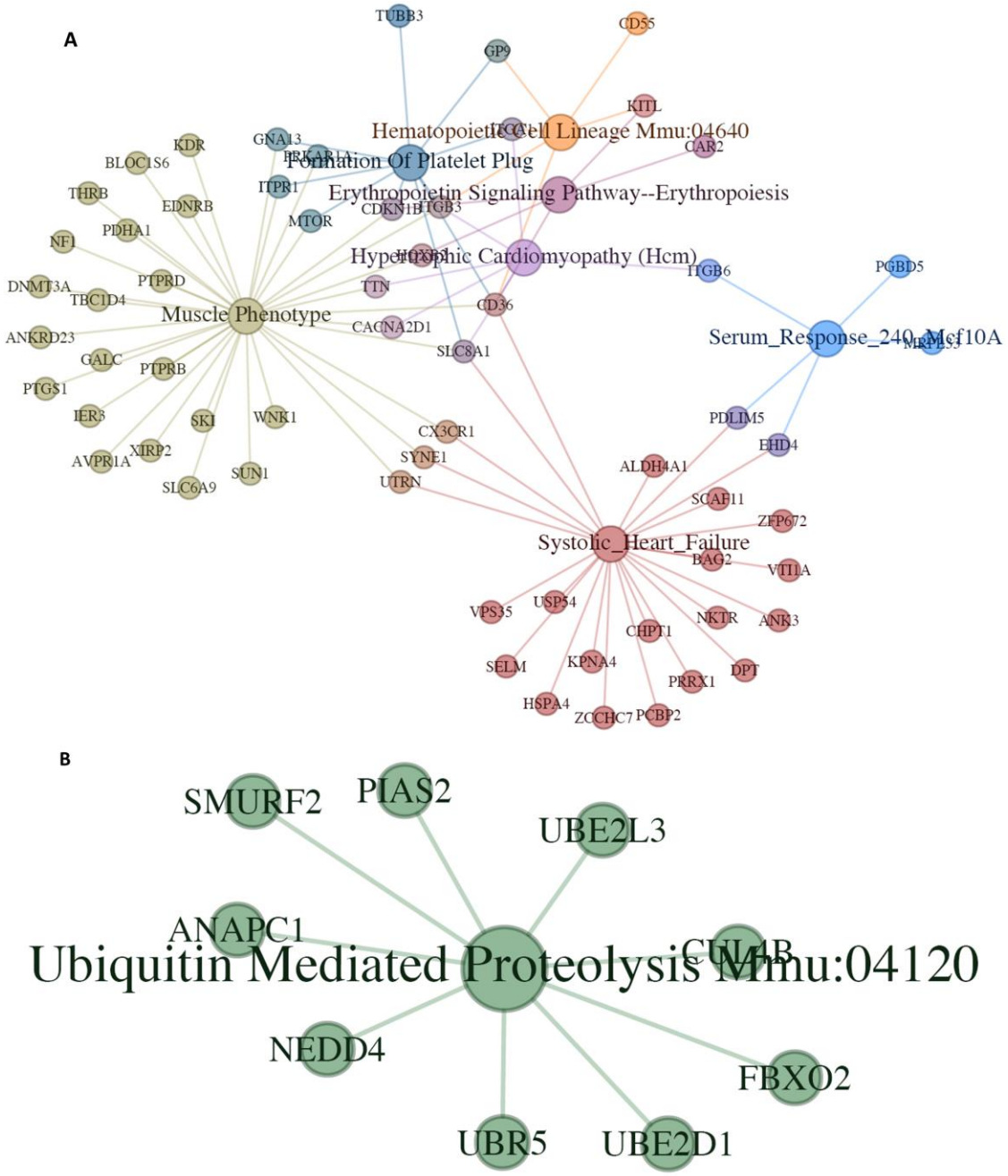

Figure 4.5: Enriched networks for doxorubicin-induced gene expression changes blocked by Brg1 expression. Brg1 expression prevents differential expression of pathways associated with heart disease (A), and ubiquitin-mediated proteolysis (B).

Discussion

Gene expression analysis yields layers of information supplemental to morphology data obtained from histopathologic studies, information which may bring confirmatory or novel insight into the changes observed microscopically. Mapping of differentially expressed genes (DEGs) from all groups of animals (Figure 4.1) reveals genome-wide differences, which are demonstrated when comparing the clustering of genes in Brg1 WT versus Brg1 KO animals. As the animals used in the experiment were inbred and controlled for age and sex, these changes were most likely due to the experimental design, which controlled the treatment conditions. An internal control for the conduct of the study in the groupwise comparison of the differences in DEGs between groups A-D (Figure 4.1A) was the yield of just one gene differentially expressed in the comparison where the treatment of doxorubicin is comparatively removed from comparison leaving only the effect of Brg1 deletion, and indeed that single gene was Brg1. Further rt-PCR analysis of select genes validated the array results (Figure 4.2). DEGs from comparisons of treated animals reveal a pattern of degree of expression within similar gene sets, rather than expression of different gene paradigms. When observing the results of all four comparisons (Figure 4.1C), it becomes evident that the pattern of degree of DEGs begins not with treatment of the WT mice, but with knockout of Brg1 in untreated mice. This further supports the microscopic data suggesting the constellation of changes (lesions, DEGs) seen in the group comparisons are similar between groups whether the variable is treatment with doxorubicin or knockout of Brg1. Upon further analysis, it becomes clear that this is not necessarily the case, and that there are DEGs common to groups of mice treated with doxorubicin, regardless of Brg1

status, and vice versa, as well as DEGs only in each comparison (Figure 4.1D). This analysis has elucidated there are doxorubicin-induced DEGs that require Brg1 ("A not C"), doxorubicin-induced DEGs that are blocked by Brg1 ("C not A"), and doxorubicin induced DEGs that were independent of Brg1 ("A and C"), or present in all treated animals. Additionally, there were DEGs that are common to both the pathology caused by doxorubicin treatment in the absence of Brg1 as well as due to Brg1 deletion alone ("A and B") (Figure 4.1).

Network enrichment using Ingenuity Pathway Analysis yielded some expected and unexpected findings. As doxorubicin has known cytotoxicity, pathways associated with cell death and nonspecific responses to cell injury and/or stimulation are expected to be differentially expressed upon treatment, demonstrated in Figure 4.3. Interestingly, there were several enriched pathways associated with cell responses not associated with doxorubicin treatment alone, but commonly differentially expressed whether the cardiotoxic insult was a result of doxorubicin treatment or Brg1 deletion (Figure 4.4). This result further strengthens the hypothesis previously proposed that Brg1 deletion and doxorubicin treatment share common pathways as evidenced by damage morphology (Chapter 3) and DEG patterns by group (Figure 4.1C). To further investigate this relationship between Brg1 deletion response and doxorubicin treatment response, network enrichment was analyzed for those genes that were differentially expressed in Brg1 deletion animals treated with doxorubicin but not in wild-type animals treated with doxorubicin ("C not A") (Figure 4.1). This analysis revealed that pathways involved in heart disease and damage response, such as the ubiquitin proteasome system were involved, which may be expected with a cardiomyocyte damage

phenotype (Figure 4.5). This last analysis, however, had the greatest possibility of elucidating genes heretofore unknown to be involved in the deleterious cardiomyocyte response to doxorubicin treatment, but are related to the stabile expression of Brg1 for its protective effect.

To determine whether the genes differentially expressed are representative of the responses indicated, one must look at individual genes in the various groupwise comparisons. Among the genes implicated in doxorubicin toxicity that were Brg1 dependent ("A not C"), changes in expression included increases in Casq1, S100a9, and Il-1β, and decreases in Kit. Calsequestrins are well known calcium-handling genes involved in a variety of cardiovascular homeostatic processes, as well as being involved in doxorubicin-induced heart disease (Olson et al 2005). S100a9 has recently been implicated as a doxorubicin response gene in breast cancer patients, and indeed may have potential as a biomarker (Yang et al 2012). Il-1β signaling is important in doxorubicin cardiotoxicity and also may have potential as a biomarker in treated individuals (Zhu et al 2011). Kit expression decreases, as well as other indicators of cellular senescence, have been demonstrated in cardiac progenitor cells upon doxorubicin treatment (Piegari et al 2013).

A full complement of Brg1 blocked doxorubicin-induced increases in Sin3β and Alox12, as well as decreases in Dnmt3a and Cdnk1b ("C not A"). These are a few genes of interest due to their previously unreported role in doxorubicin cardiotoxicity. Furthermore, the protective effect of Brg1 prevents their differential expression, which may part of the pathogenesis in the greater than additive damage observed in the Brg1 deletion animals treated with doxorubicin than in animals with either Brg1 or doxorubicin treatment alone.

Alox12 has been described as an important pro-inflammatory component in atherosclerosis as a function of the lipoxygenase pathway, and indeed it is upregulated in ischemia/reperfusion injury, though its role in doxorubicin cardiotoxicity has not been described (Burdon et al 2010, Lemaitre et al 2009). Sin3β expression was shown in the present study to be differentially expressed in the absence of Brg1 in the repeat-dose cardiotoxicity mouse model. It was previously shown to interact directly with p53 in cell lines under stress of doxorubicin treatment (Bansal et al 2011), but has not been shown in the context of cardiotoxicity; neither Sin3β nor Alox12 have been described in reference to Brg1. DNA methyltransferases 3A was previously shown to interact directly with Brg1, and function in a repressive manner in P1798 cells (Datta et al 2005). Dnmt3a was also shown to be a primary factor in determining progression to apoptosis in a p53-dependent manner in a human cancer cell line (Zhang et al 2011). It is not surprising that cyclin-dependent kinases are involved in doxorubicin cardiotoxicity, but interestingly Cdnk1b was only involved in the response when the protective effect of Brg1 was diminished through gene deletion. Neither the Dnmt3a response nor the Cdnk1b response has been described in reference to Brg1 and doxorubicin cardiotoxicity.

Network enrichment for those DEGs from groupwise comparisons where Brg1 blocked the doxorubicin response ("C not A") revealed a cluster involved in ubiquitin-mediated proteolysis (Figure 4.5B). Several of the genes elucidated in this analysis, including F-box only protein 2 (FbxO2), Ube2l3, and Smurf2 have not been described in the Brg1 literature (Mallinger et al 2012, Weissman 2001). Ube2l3, a ubiquitin enzyme, has been shown to interact with ligases present in heart tissue, but has not previously been

described in the context of Brg1 or doxorubicin treatment (Larsen et al 2012). Smurf2 is an E3 ligase previously reported to play critical roles in carcinogenesis and susceptibility to chemotherapy, and has been shown to inhibit TGF-β signaling in cardiac fibrosis. (Ramkumar et al 2013, Smith et al 2013, Cunnington et al 2009). Though there are intuitive mechanistic links (cardiac fibrosis, MEK inhibitor chemotherapy, targeted receptor destruction), these networks have not been described in the context of doxorubicin treatment.

Lastly, increases in Dusp4 expression and decreases in Gata4 expression due to doxorubicin administration appeared independent of Brg1 expression ("A and C"). Dusp4 has recently been identified as a target for doxorubicin resistance, and unsurprisingly was revealed to be Brg1-independent in its expression under the condition of doxorubicin treatment in these experiments (Liu et al 2013). Gata4 downregulation in response to doxorubicin toxicity has been well-described, and in the current work was shown to be Brg1-independent as well.

The strategy of groupwise comparison analysis of differential gene expression under the conditions of Brg1 gene deletion and repeat-dose doxorubicin treatment revealed expected as well as novel responses in network enrichment and gene expression. The current work was controlled through group comparisons to yield so called "control genes", such as the gene being deleted and those known to be involved in doxorubicin administration. Additionally, expected network enrichments were observed, such as those involve in cardiac disease, muscle disease processes, as well as those involved in cell signaling, apoptosis, and inflammation. Several as-yet unpublished gene responses were observed, the most interesting being those related to the suggested protective response of Brg1 in the face of

doxorubicin treatment, including Sin3β and Alox12. Further analysis of these genes and others elucidated through future microarray experiments may uncover new important regulators of the heart's response to doxorubicin chemotherapy, and bring promising treatments or palliations for the cardiotoxicity observed in that patient population.

Chapter 4 References:

Bansal, N., Kadamb, R., Mittal, S., Vig, L., Sharma, R., Dwarakanath, B. S., and Saluja, D. (2011). Tumor suppressor protein p53 recruits human Sin3B/HDAC1 complex for down-regulation of its target promoters in response to genotoxic stress. *PloS one* **6**(10), e26156, 10.1371/journal.pone.0026156.

Bultman, S., Gebuhr, T., Yee, D., La Mantia, C., Nicholson, J., Gilliam, A., Randazzo, F., Metzger, D., Chambon, P., Crabtree, G., and Magnuson, T. (2000). A Brg1 null mutation in the mouse reveals functional differences among mammalian SWI/SNF complexes. *Molecular cell* **6**(6), 1287-95.

Burdon, K. P., Rudock, M. E., Lehtinen, A. B., Langefeld, C. D., Bowden, D. W., Register, T. C., Liu, Y., Freedman, B. I., Carr, J. J., Hedrick, C. C., and Rich, S. S. (2010). Human lipoxygenase pathway gene variation and association with markers of subclinical atherosclerosis in the diabetes heart study. *Mediators of inflammation* **2010**, 170153, 10.1155/2010/170153.

Carvalho, F. S., Burgeiro, A., Garcia, R., Moreno, A. J., Carvalho, R. A., and Oliveira, P. J. (2013). Doxorubicin-Induced Cardiotoxicity: From Bioenergetic Failure and Cell Death to Cardiomyopathy. *Medicinal research reviews*, 10.1002/med.21280.

CDER (2005). Guidance for Industry. Estimating the maximum safe starting dose in initial clinical trials for therapeutics in adult healthy volunteers. In (

Cheng, H., and Force, T. (2010). Molecular mechanisms of cardiovascular toxicity of targeted cancer therapeutics. *Circulation research* **106**(1), 21-34, 10.1161/CIRCRESAHA.109.206920.

Cunnington, R. H., Nazari, M., and Dixon, I. M. (2009). c-Ski, Smurf2, and Arkadia as regulators of TGF-beta signaling: new targets for managing myofibroblast function and cardiac fibrosis. *Canadian journal of physiology and pharmacology* **87**(10), 764-72, 10.1139/y09-076.

Datta, J., Majumder, S., Bai, S., Ghoshal, K., Kutay, H., Smith, D. S., Crabb, J. W., and Jacob, S. T. (2005). Physical and functional interaction of DNA methyltransferase 3A with Mbd3 and Brg1 in mouse lymphosarcoma cells. *Cancer research* **65**(23), 10891-900, 10.1158/0008-5472.can-05-1455.

Desai, V. G., Herman, E. H., Moland, C. L., Branham, W. S., Lewis, S. M., Davis, K. J., George, N. I., Lee, T., Kerr, S., and Fuscoe, J. C. (2013). Development of doxorubicin-induced chronic cardiotoxicity in the B6C3F1 mouse model. *Toxicology and applied pharmacology* **266**(1), 109-21, 10.1016/j.taap.2012.10.025.

Friedman, M. A., Bozdech, M. J., Billingham, M. E., and Rider, A. K. (1978). Doxorubicin cardiotoxicity. Serial endomyocardial biopsies and systolic time intervals. *JAMA : the journal of the American Medical Association* **240**(15), 1603-6.

Hayashi, S., and McMahon, A. P. (2002). Efficient recombination in diverse tissues by a tamoxifen-inducible form of Cre: a tool for temporally regulated gene activation/inactivation in the mouse. *Developmental biology* **244**(2), 305-18, 10.1006/dbio.2002.0597.

Koh, C. M. (2013). Isolation of genomic DNA from mammalian cells. *Methods in enzymology* **529**, 161-9, 10.1016/B978-0-12-418687-3.00013-6.

Larsen, K., Madsen, L. B., and Bendixen, C. (2012). Porcine dorfin: molecular cloning of the RNF19 gene, sequence comparison, mapping and expression analysis. *Molecular biology reports* **39**(12), 10053-62, 10.1007/s11033-012-1874-7.

Laverty, H., Benson, C., Cartwright, E., Cross, M., Garland, C., Hammond, T., Holloway, C., McMahon, N., Milligan, J., Park, B., Pirmohamed, M., Pollard, C., Radford, J., Roome, N., Sager, P., Singh, S., Suter, T., Suter, W., Trafford, A., Volders, P., Wallis, R., Weaver, R., York, M., and Valentin, J. (2011). How can we improve our understanding of cardiovascular safety liabilities to develop safer medicines? *British journal of pharmacology* **163**(4), 675-93, 10.1111/j.1476-5381.2011.01255.x.

Lemaitre, R. N., Rice, K., Marciante, K., Bis, J. C., Lumley, T. S., Wiggins, K. L., Smith, N. L., Heckbert, S. R., and Psaty, B. M. (2009). Variation in eicosanoid genes, non-fatal myocardial infarction and ischemic stroke. *Atherosclerosis* **204**(2), e58-63, 10.1016/j.atherosclerosis.2008.10.011.

Liu, Y., Du, F., Chen, W., Yao, M., Lv, K., and Fu, P. (2013). Knockdown of dual specificity phosphatase 4 enhances the chemosensitivity of MCF-7 and MCF-7/ADR breast cancer cells to doxorubicin. *Experimental cell research* **319**(20), 3140-9, 10.1016/j.yexcr.2013.08.023.

Loughna, S., and Henderson, D. (2007). Methodologies for staining and visualisation of beta-galactosidase in mouse embryos and tissues. *Methods Mol Biol* **411**, 1-11.

Octavia, Y., Tocchetti, C. G., Gabrielson, K. L., Janssens, S., Crijns, H. J., and Moens, A. L. (2012). Doxorubicin-induced cardiomyopathy: from molecular mechanisms to therapeutic strategies. *Journal of molecular and cellular cardiology* **52**(6), 1213-25, 10.1016/j.yjmcc.2012.03.006.

Olson, R. D., Gambliel, H. A., Vestal, R. E., Shadle, S. E., Charlier, H. A., Jr., and Cusack, B. J. (2005). Doxorubicin cardiac dysfunction: effects on calcium regulatory proteins, sarcoplasmic reticulum, and triiodothyronine. *Cardiovascular toxicology* **5**(3), 269-83.

Piegari, E., De Angelis, A., Cappetta, D., Russo, R., Esposito, G., Costantino, S., Graiani, G., Frati, C., Prezioso, L., Berrino, L., Urbanek, K., Quaini, F., and Rossi, F. (2013). Doxorubicin induces senescence and impairs function of human cardiac progenitor cells. *Basic research in cardiology* **108**(2), 334, 10.1007/s00395-013-0334-4.

Ramkumar, C., Cui, H., Kong, Y., Jones, S. N., Gerstein, R. M., and Zhang, H. (2013). Smurf2 suppresses B-cell proliferation and lymphomagenesis by mediating ubiquitination and degradation of YY1. *Nature communications* **4**, 2598, 10.1038/ncomms3598.

Slordal, L., and Spigset, O. (2006). Heart failure induced by non-cardiac drugs. *Drug safety : an international journal of medical toxicology and drug experience* **29**(7), 567-86.

Smith, M. P., Ferguson, J., Arozarena, I., Hayward, R., Marais, R., Chapman, A., Hurlstone, A., and Wellbrock, C. (2013). Effect of SMURF2 targeting on susceptibility to MEK inhibitors in melanoma. *Journal of the National Cancer Institute* **105**(1), 33-46, 10.1093/jnci/djs471.

Sumi-Ichinose, C., Ichinose, H., Metzger, D., and Chambon, P. (1997). SNF2beta-BRG1 is essential for the viability of F9 murine embryonal carcinoma cells. *Molecular and cellular biology* **17**(10), 5976-86.

Tacar, O., Sriamornsak, P., and Dass, C. R. (2013). Doxorubicin: an update on anticancer molecular action, toxicity and novel drug delivery systems. *The Journal of pharmacy and pharmacology* **65**(2), 157-70, 10.1111/j.2042-7158.2012.01567.x.

Weissman, A. M. (2001). Themes and variations on ubiquitylation. *Nature reviews. Molecular cell biology* **2**(3), 169-78, 10.1038/35056563.

Yang, W. S., Moon, H. G., Kim, H. S., Choi, E. J., Yu, M. H., Noh, D. Y., and Lee, C. (2012). Proteomic approach reveals FKBP4 and S100A9 as potential prediction markers of therapeutic response to neoadjuvant chemotherapy in patients with breast cancer. *Journal of proteome research* **11**(2), 1078-88, 10.1021/pr2008187.

Zhang, Y., Gao, Y., Zhang, G., Huang, S., Dong, Z., Kong, C., Su, D., Du, J., Zhu, S., Liang, Q., Zhang, J., Lu, J., and Huang, B. (2011). DNMT3a plays a role in switches between doxorubicin-induced senescence and apoptosis of colorectal cancer cells. *International journal of cancer. Journal international du cancer* **128**(3), 551-61, 10.1002/ijc.25365.

Zhu, J., Zhang, J., Zhang, L., Du, R., Xiang, D., Wu, M., Zhang, R., and Han, W. (2011). Interleukin-1 signaling mediates acute doxorubicin-induced cardiotoxicity. *Biomedicine & pharmacotherapy = Biomedecine & pharmacotherapie* **65**(7), 481-5, 10.1016/j.biopha.2011.06.005.

Chapter 5

Discussion and Conclusions

It is known the chromatin remodeling factor Brg1, a catalytic subunit of the SWI/SNF ATPase chromatin remodeling complex, is required in cardiovascular development and pathologic cardiac hypertrophy. BRG1 ablation beginning at E6.5 results in arrested growth and embryonic death by E9.5 due to developmental defects. Microarray analysis revealed BRG1's role maintaining genomic integrity, without which there is aberrant expression of cell cycle, proliferation, and apoptosis pathways leading to the observed pathologic phenotype. This suggests BRG1's role in genomic surveillance is essential for survival after the pre-implantation period for normal cellular proliferation and differentiation. Adult Brg1 WT and Brg1 deletion mice were subjected to a doxorubicin regimen analogous to that used in the human clinical setting. Analyses of tissues including protein and RNA analyses, microarray analysis, serum biochemistry, and light and electronic microscopic analyses confirmed the presence of doxorubicin-associated lesions in treated mice; however, lesions were also observed to a lesser degree in untreated Brg1 deletion mice. The lesions observed with Brg1 deletion were similar in morphology to those observed in the repeat-dose doxorubicin cardiotoxicity model. Brg1 deletion appeared to have a potentiation effect on doxorubicin toxicity, as the animals subjected to the repeat-dose toxicity protocol with Brg1 deletion appeared to have greater cardiotoxicity than the combined effect of Brg1 deletion alone or doxorubicin administration. Microarray analysis revealed significant differentially expressed genes with common clustering between both the treated groups and the Brg1 KO

groups, suggesting both common and dissimilar molecular mechanisms between Brg1 KO-induced cardiomyocyte lesions and those induced by doxorubicin treatment. Groupwise analysis of differentially-expressed genes (DEGs) in the microarray studies revealed expected and unexpected results. As expected, canonical pathways one associates with doxorubicin toxicity and cell injury were enriched. Deletion of Brg1 had common and dissimilar mechanisms to that induced by treatment with doxorubicin, suggesting mechanisms unique to Brg1 knockout irrespective of treatment may reveal new therapeutic targeting pathways in patients at risk for doxorubicin cardiotoxicity. Interestingly, genes came to light that previously have not been associated with the doxorubicin cardiotoxicity paradigm, either with or without being Brg1-associated. These latter novel findings remain the most important aspects of the current work.

This work revealed that not only is Brg1 required for the maintenance of normal cardiomyocyte homeostasis during development, but that is required in adulthood as well, despite previous reports. The developmental biology work in Chapter 2 described portions of the foundation of Brg1's role in genome surveillance and stability. This effect was reflected in the microarray analysis results detailed in Chapter 4, which again highlighted Brg1's protective role in the adult under various stresses (normal cardiac homeostasis or doxorubicin toxicity). Indeed, the same pathways were enriched in both circumstances (p53, cyclin-dependent kinases, etc.).

At present, there are several chromatin modifying medicines in the clinic or in development, namely DNA methyltransferases and histone deacytylase inhibitors (Kwa et al. 2011). The possibility that the Brg1 chromatin remodeling factor, and potentially that of

other chromatin remodeling factors, is clinically relevant for therapeutic targets in the prevention of cardiotoxicity is very exciting. Recent work by Oike et al outlining the relationships of various Brg1-associated factors and cancers suggests that inhibition of SWI/SNF ATPases may have therapeutic potential in cancers already deficient in this ATPase family (Oike et al 2013). The possible clinical contraindications involved in manipulating these pathways are intuitive in these studies, and demand further mechanistic research.

The B6.Cg-Tg(CAG-cre/Esr1*)5Amc/J Tg B6;128S2-Smarca4^{tm1Pcn}/Mmnc mouse proved to be an adequate model to evaluate the deletion of Brg1 in a mammalian system and a sensitive test species to evaluate cardiotoxicity. The data in Figure 3.9 demonstrates DEGs related specifically to Brg1 deletion, doxorubicin treatment, or both. This suggests that the pathways unrelated to doxorubicin treatment or doxorubicin treatment and Brg1 deletion are the protective effects conferred by Brg1, and any potential test toxin or stressor operating by any of those mechanisms may have a stronger response in this mouse model. Although future mechanistic investigations will likely take place using in vitro systems, the use of the mammalian system is justified due to several confounding factors of translation with in vitro models (Branco et al. 2012).

Throughout the course of this research several study design flaws became evident. In the design of the cardiotoxicity study, based on an expectation of severity of degeneration and necrosis of cardiomyocytes, it was anticipated that troponin levels would still be elevated in the doxorubicin-treated mice at 24 hours post-dose based on an expectation of severity of degeneration and necrosis of cardiomyocytes. The latter expectation was not fulfilled,

therefore the former expectation could not be met. This factor was unfortunate as cardiac troponins are highly specific for non-adaptive cardiac damage, and stand alone as a diagnostic biomarker for cardiac injury, with the exception of extreme endurance athletic performances in humans (Shave and Oxborough 2012). Additionally, a significant correlation exists between troponin release following chemotherapy and heart failure (Kalam and Marwick 2013). Nevertheless, useful data resulted from the analysis of alternative cardiac biomarkers. In an extensive study of various biomarkers of cardiotoxicity involving several therapeutics, Tonomura et al. showed Myl3 and FABP3 to be the most responsive of the biomarkers to doxorubicin cardiotoxicity (Tonomura et al. 2012).

Developmental biology and pathology are quite complementary fields. Though not well known outside of those familiar with a pathology residency training program, a significant portion of the pathologist's training is being able to recognize normal from abnormal. Only then, and with relative ease, can the successful histopathologist recognize pathophysiology playing out in a moment in time on a thin slice of tissue. The developmental biologist's knowledge base stems from this as well: recognizing normal cell and organ processes from abnormal ones. The work in this dissertation attempted to access and bridge aspects of both disciplines in the investigation of an interesting chromatin remodeler, and its potential role(s) in a heart toxicity. The approach of identifying an adult disorder and searching for its cause or correlate in an organism's development is not a new one, though it is newly being applied to various conditions, including cancers, every day. This approach was taken with the work herein in an investigation into a developmental paradigm that, despite previous reports and popular opinion, indeed plays an important role

in adult homeostasis.

Although no curative breakthrough is claimed in these few chapters, novel avenues for analysis have been laid out. Future publications from these data will hopefully be used as background for the development of a new therapy to prevent or ameliorate cardiotoxicity suffered by some requiring doxorubicin chemotherapy. If singly referenced in any of that work, this effort becomes all the more worthwhile.

Chapter 5 References:

Branco, A. F., Sampaio, S. F., Moreira, A. C., Holy, J., Wallace, K. B., Baldeiras, I., Oliveira, P. J., and Sardao, V. A. (2012). Differentiation-dependent doxorubicin toxicity on H9c2 cardiomyoblasts. *Cardiovascular toxicology* **12**(4), 326-40, 10.1007/s12012-012-9177-8.

Tacar, O., Sriamornsak, P., and Dass, C. R. (2013). Doxorubicin: an update on anticancer molecular action, toxicity and novel drug delivery systems. *The Journal of pharmacy and pharmacology* **65**(2), 157-70, 10.1111/j.2042-7158.2012.01567.x.

Tonomura, Y., Matsushima, S., Kashiwagi, E., Fujisawa, K., Takagi, S., Nishimura, Y., Fukushima, R., Torii, M., and Matsubara, M. (2012). Biomarker panel of cardiac and skeletal muscle troponins, fatty acid binding protein 3 and myosin light chain 3 for the accurate diagnosis of cardiotoxicity and musculoskeletal toxicity in rats. *Toxicology* **302**(2-3), 179-89, 10.1016/j.tox.2012.07.012.

Shave, R., and Oxborough, D. (2012). Exercise-induced cardiac injury: evidence from novel imaging techniques and highly sensitive cardiac troponin assays. *Progress in cardiovascular diseases* **54**(5), 407-15, 10.1016/j.pcad.2012.01.007.

Oike, T., Ogiwara, H., Nakano, T., Yokota, J., and Kohno, T. (2013). Inactivating mutations in SWI/SNF chromatin remodeling genes in human cancer. *Japanese journal of clinical oncology* **43**(9), 849-55, 10.1093/jjco/hyt101.

Kwa, F. A., Balcerczyk, A., Licciardi, P., El-Osta, A., and Karagiannis, T. C. (2011). Chromatin modifying agents - the cutting edge of anticancer therapy. *Drug discovery today* **16**(13-14), 543-7, 10.1016/j.drudis.2011.05.012.

Kalam, K., and Marwick, T. H. (2013). Role of cardioprotective therapy for prevention of cardiotoxicity with chemotherapy: a systematic review and meta-analysis. *Eur J Cancer* **49**(13), 2900-9, 10.1016/j.ejca.2013.04.030.

APPENDICES

Appendix 1: rt-PCR Validation Gene Primers from Microarray Analysis

Gene	Primer construct	Gene	Primer construct
Acta2 ex8F	TTGCTGACAGGATGCAGAAG	Nr1d1 ex8R	CGGTTCTTCAGCACCAGAG
Acta2 ex9R	TGATCCACATCTGCTGGAAG	Plekhn1 ex13F	GGCTCAGGATCACTCTTTGG
Cacna1g ex33F	ACTCTCTGCCCAATGACAGC	Plekhn1 ex14R	GGTCCAGGCGATGTCTGTAT
Cacna1g ex34R	TAGGATGCAGCTGGTGTCTG	S100a8 ex2F	CCATGCCCTCTACAAGAATGA
Casq1 ex10F	CCCGTACTGGGAGAAGACCT	S100a8 ex3R	ATCACCATCGCAAGGAACTC
Casq1 ex11R	CAGGTCCTCCTCGTTATCCA	S100a9 ex2F	ACACCCTGAGCAAGAAGGAA
Cdkn1b ex1F	GGGTCTCAGGCAAACTCTGA	S100a9 ex3R	GTCCTGGTTTGTGTCCAGGT
Cdkn1b ex2R	TCTGTTGGCCCTTTTGTTTT	Slc25a35 ex4F	TGAGTGGTGTCGCCATAGTC
Ceacam1 ex4F	CGGAACCTATACCTGCTTCG	Slc25a35 ex5F	AAGATCCCCCGGTACATGAG
Ceacam1 ex5R	GAGGAAGGGCTGAGTCACTG	Slc35a4 ex2F	CGTGTGGAAGGTGAAGTCAA
Col6a2 ex25F	GTGGTCTTCGTCATCGACAG	Slc35a4 ex3R	ACTGCTGATGCCCTCAGTTT
Col6a2 ex26R	GTACTGCACCACACCCACAC	Smarca4 P1	GTCATACTTATGTCATAGCC
Hist1h1c F	CTTTTCAGAGCCACCACTCC	Smarca4 P2	GCCTTGTCTCAAACTGATAAG
Hist1h1c R	AGCCCAGCACAAACAAGTCT	Smarca4 P3	GATCAGCTCATGCCCTAAGG
Il1b ex5F	GCTGAAAGCTCTCCACCTCA	Tecr ex2F	CAAAGACGAGGGAGAAGCTG
Il1b ex6R	AGGCCACAGGTATTTTGTCG	Tecr ex3-4R	ATACCACTGCGGGTGTGTCT
Itga3 ex25F	AGGCAGAAGGCTGAGATGAA	Tgfb1 ex5F	GGAGAGCCCTGGATACCAAC
Itga3 ex26R	TGCATGGTACTTGGGCATAA	Tgfb1 ex6R	ACTTCCAACCCAGGTCCTTC
Kit ex20F	CCTTGAAAAGGCCAACATTC	Ttn ex311F	GCATGACACAACTGGAAAGC
Kit ex21R	GCAGTTTGCCAAGTTGGAGT	Ttn ex312R	CCCAGTAAAGGCACAGGCTA
Nes ex3F	GGAAGAAGTTCCCAGGCTTC	Wfdc1 ex6F	GGGACAACAGAGGCACTTTC
Nes ex4R	ATTAGGCAAGGGGGAAGAGA	Wfdc1 ex7R	TGCTGTTCTGTGGAATGGAG
Nr1d1 ex7F	CACTTACCGAGGAGGAGCTG		

Appendix 2: Publication References Within Scope

Jokinen MP, Lieuallen WG, **Boyle MC**, Johnson CL, Malarkey DE, Nyska A. **2011**. Morphologic Aspects of Rodent Cardiotoxicity in a Retrospective Evaluation of National Toxicology Program Studies. Toxicol Pathol 39(5):850-60.

The heart is increasingly recognized as a target for toxicity. As studies in laboratory rodents are commonly used to investigate the potential toxicity of various agents, the identification and characterization of lesions of cardiotoxicity is of utmost importance. Although morphologic criteria have been established for degenerative myocardial lesions in rats and mice, differentiation of spontaneously occurring lesions from toxin-induced or toxin-related lesions remains difficult. A retrospective light microscopic evaluation was performed on the hearts of F344 rats and B6C3F1 mice from National Toxicology Program (NTP) studies of six chemicals identified in the NTP database in which treatment-induced myocardial toxicity was present. Two previously defined myocardial lesions were observed: ‘‘cardiomyopathy’’ that occurred spontaneously or as a treatment-related effect and ‘‘myocardial degeneration’’ that occurred as a treatment-related effect. Both lesions consisted of the same basic elements, beginning with myofiber degeneration and necrosis, with varying amounts of inflammation, interstitial cell proliferation, and eventual fibrosis. This observation is indicative of the heart’s limited repertoire of responses to myocardial injury, regardless of the nature of the inciting agent. A prominent differentiating factor between spontaneous and treatment-induced lesions was distribution and lesion onset. Once the respective lesions had undergone fibrosis, however, they generally appeared morphologically indistinguishable.

Boyle MC, Crabbs TA, Wyde ME, Painter JT, Hill GA, Malarkey DE, Lieuallen WG, Nyska A. **2012.** Indole-3-carbinol Induced Lymphangiectasis in Fischer 344 Rats Following Subchronic Exposure via Oral Gavage. Toxicol Pathol 40(4):561-76.

To investigate the toxicity and carcinogenic potential of indole-3-carbinol (I3C), the National Toxicology Program has conducted 13-week subchronic studies in Fisher 344 rats and B6C3F1 mice, and chronic 2-year bioassays in Sprague-Dawley rats and B6C3F1 mice. While the chronic study results are not yet available, subchronic study results and short-term special evaluations of interim sacrifices in the 2-year rat bioassay are presented. F344 rats were orally gavaged 300 mg I3C/kg body weight 5 days a week for 13 weeks. Rats treated with 150 mg/kg demonstrated a dose-related dilation of lymphatics (lymphangiectasis) of the duodenum, jejunum, and mesenteric lymph nodes. Material within dilated lacteals stained positively for Oil Red O and Sudan Black, consistent with lipid. Electron microscopic evaluation confirmed extracellular lipid accumulation within the villar lamina propria, lacteals, and within villar macrophages. Analyses of hepatic and pulmonary CYP1A enzymes demonstrated dose-dependent I3C induction of CYP1A1 and 1A2. B6C3F1 mice orally gavaged 250 mg I3C/kg body weight did not demonstrate histopathological changes; however, hepatic CYP induction was similar to that in rats. The histopathologic changes of intestinal lymphangiectasis and lipidosis in this study share similarities with intestinal lymphangiectasia as observed in humans and dogs. However, the resultant clinical spectrum of protein-losing enteropathy was not present.

Kane AM, DeFrancesco TC, **Boyle MC**, Malarkey DE, Ritchey JW, Atkins CE, Cullen JM, Kornegay JN, Keene BW. **2013**. Cardiac Structure and Function in Female Carriers of a Canine Model of Duchenne Muscular Dystrophy. Res Vet Sci. 94(3):610-7.

This investigation tested the hypothesis that carriers of golden retriever muscular dystrophy (GRMD), a genetically homologous condition of Duchenne muscular dystrophy (DMD), have quantifiable abnormalities in myocardial function, structure, or cardiac rhythm. Eleven GRMD carriers and four matched controls had cardiac evaluations and postmortem examinations. 24-h ECG Holter monitoring disclosed ventricular ectopy in 10 of 11 carriers and 2 of 4 controls. Conventional echocardiography failed to demonstrate significant differences between carriers and controls in systolic function. All carriers had multifocal, minimal to marked myofiber necrosis, fibrosis, mineralization, inflammation, and/or fatty change in their hearts. Immunohistochemistry revealed a mosaic dystrophin deficiency in scattered cardiac myofibers in all carriers. No controls had cardiac histologic lesions; all had uniform dystrophin staining. Despite cardiac mosaic dystrophin expression and degenerative cardiac lesions, GRMD carriers at up to 3 years of age could not be distinguished statistically from normal controls by echocardiography or 24-h Holter monitoring.

Oakley RH, Ren R, Cruz-Topete D, Bird GS, Myers PS, **Boyle MC**, Schneider MD, Willis MS, Cidlowski JA. **2013**. Essential Role of Stress Hormone Signaling in Cardiomyocytes for the Prevention of Heart Disease. Proc Natl Acad Sci. Oct 15;110(42):17035-40.

Heart failure is a leading cause of death in humans, and stress is increasingly associated with adverse cardiac outcomes. Glucocorticoids are primary stress hormones, but their direct role in cardiovascular health and disease is poorly understood. To determine the in vivo function of glucocorticoid signaling in the heart, we generated mice with cardiomyocyte-specific deletion of the glucocorticoid receptor (GR). These mice are born at the expected Mendelian ratio, but die prematurely from spontaneous cardiovascular disease. By 3 mo of age, mice deficient in cardiomyocyte GR display a marked reduction in left ventricular systolic function, as evidenced by decreases in ejection fraction and fractional shortening. Heart weight and left ventricular mass are elevated, and histology revealed cardiac hypertrophy without fibrosis. Removal of endogenous glucocorticoids and mineralocorticoids neither augmented nor lessened the hypertrophic response. Global gene expression analysis of knockout hearts before pathology onset revealed aberrant regulation of a large cohort of genes associated with cardiovascular disease as well as unique disease genes associated with inflammatory processes. Genes important for maintaining cardiac contractility, repressing cardiac hypertrophy, promoting cardiomyocyte survival, and inhibiting inflammation had decreased expression in the GR-deficient hearts. These findings demonstrate that a deficiency in cardiomyocyte glucocorticoid signaling leads to spontaneous cardiac hypertrophy, heart failure, and death, revealing an obligate role for GR in maintaining normal cardiovascular

function. Moreover, our findings suggest that selective activation of cardiomyocyte GR may represent an approach for the prevention of heart disease.